

A Survey of mmWave Radar-Based Sensing in Autonomous Vehicles, Smart Homes and Industry

Hao Kong^{ID}, Member, IEEE, Cheng Huang^{ID}, Member, IEEE, Jiadi Yu^{ID}, Senior Member, IEEE,
and Xuemin Shen^{ID}, Fellow, IEEE

IT PARTIALLY ADDRESSES VITAL SIGNS DETECTION (PAGE 30)

Abstract—Sensing technology plays a crucial role in bridging the physical and digital worlds. By transforming a multitude of physical phenomena into digital data, it significantly enhances our understanding of the environment and is instrumental in a wide range of applications. Given the wide bandwidth and short wavelength characteristics, millimeter wave (mmWave) radar sensing is considered one of the most promising sensing techniques beyond mmWave communication. In this paper, we provide a comprehensive survey of mmWave radar-based sensing techniques and applications in autonomous vehicles, smart homes, and industry. Specifically, we first review widely exploited mmWave radar techniques and signal processing techniques from the perspective of dedicated radars and communication integration, which are the basis of mmWave radar sensing. Then, we introduce mainstream machine learning techniques, especially the latest deep learning techniques for designing applications with mmWave signals. Related hardware devices, available public datasets, and evaluation metrics are also presented. Afterward, we provide a taxonomy of emerging mmWave radar sensing applications, and review the developments in object detection, ego-motion estimation, simultaneous localization and mapping, activity recognition, pose estimation, gesture recognition, speech recognition, vital sign monitoring, user authentication, indoor positioning, industrial imaging, industrial measurement, environmental monitoring, etc. We conclude the paper by discussing challenges and potential future research directions.

Index Terms—Millimeter wave radar, wireless sensing, radar signal processing, deep learning, autonomous vehicle, smart home, industry.

I. INTRODUCTION

NOWADAYS, sensing technology has emerged for measuring various physical, environmental, or biological phenomena by specialized sensors. By analyzing the measured

Manuscript received 8 June 2023; revised 5 November 2023 and 16 April 2024; accepted 23 May 2024. Date of publication 11 June 2024; date of current version 17 February 2025. This work was supported in part by the National Natural Science Foundation of China under Grant 62172277; in part by the Artificial Intelligence Technology Support Special Project of Science and Technology Commission of Shanghai Municipality under Grant 22DZ1100103; and in part by the Fudan University Start-Up Funding under Grant JIH2301061Y. (*Corresponding author: Jiadi Yu*)

Hao Kong is with the School of Computer Engineering and Science, Shanghai University, Shanghai 200444, China (e-mail: haokong@shu.edu.cn).

Cheng Huang is with the School of Computer Science, Fudan University, Shanghai 200438, China (e-mail: chuang@fudan.edu.cn).

Jiadi Yu is with the Department of Computer Science and Engineering, Shanghai Jiao Tong University, Shanghai 200240, China (e-mail: jiadiyu@sjtu.edu.cn).

Xuemin Shen is with the Department of Electrical and Computer Engineering, University of Waterloo, Waterloo, ON N2L 3G1, Canada (e-mail: sshen@uwaterloo.ca).

Digital Object Identifier 10.1109/COMST.2024.3409556

phenomena, sensing technology provides the understanding, control and interaction with the real world. Many sensing technologies including vision, wearable devices and wireless signals have been extensively exploited in Internet of Things (IoT) scenarios, among which millimeter wave (mmWave) radar sensing is considered one of the most promising solutions.

A. Overview of mmWave Radar Sensing

Millimeter wave radar sensing technology leverages modulated signals to sense and reveal environmental information. The signals typically operate at the frequency range of 30 to 300 Gigahertz (GHz) and are originally exploited to enable high rate, ultra-reliable, and low latency wireless communications [1], [2], [3]. Along with its properties in wide bandwidth, millimeter wavelength, and small physical size antenna array, mmWave has brought new functions of sensing beyond wireless communications. A typical mmWave radar is built with a transmit antenna array and a receive antenna array. The transmit antenna array continuously emits modulated mmWave signals to the environment. The signals propagate through the environment and are then reflected by environmental objects, which are finally received by the receive antenna array. Through analyzing the reflected signals, the radar can reveal spatial and temporal information about the objects, enabling contactless and passive sensing for the environment. The sensing capability is mainly derived from frequency-modulated continuous-wave (FMCW) techniques, which has been a critical focus and supported several commodity mmWave radars (e.g., Texas Instruments (TI) mmWave radar sensors [4]).

Sensing with mmWave radars has many advantages. Compared to the attached or built-in sensors, the contactless sensing manner provides a nonintrusive user experience for humans and low deploying costs for devices. mmWave radars work in complex weather conditions and some none-line-of-sight (NLOS) scenarios with practicable sensing ranges, which releases the strict requirement of cameras and lidars in complicated situations. mmWave radars enable a higher spatial resolution compared to commodity WiFi, RFID and acoustic signals owing to small wavelengths. In addition, with the gradual attention to personal privacy, mmWave radars can alleviate privacy concerns that vision technologies could bring about. Given these properties, mmWave radars have become promising enablers for a variety of sensing applications far

beyond traditional radar scenarios, covering autonomous vehicles, smart homes, industry, etc. In autonomous vehicles, mmWave radars are one of the most common tools for obstacle detection and motion estimation, which contributes to the gradual maturity of autonomous driving. In smart homes, activity and gesture recognition based on mmWave radar can offer an “in-air” human-computer interaction for virtual reality (VR) applications. In manufacturing industry, mmWave radars act as important sensors that can measure physical phenomena with high resolution and low cost. The application scenarios have given rise to the surge of research studies in the recent decade.

B. Related Surveys of mmWave Radar Sensing

There have been several recent surveys related to mmWave radar sensing. Davoli et al. [5] provided an overview of machine learning and deep learning techniques in multi-input multi-output (MIMO) radar sensing. The survey first introduced colocated MIMO radar techniques. Then, it presented machine learning and deep learning techniques with case studies and technical details. The numerical results based on both synthetically generated and experimental datasets were also illustrated. Abdu et al. [6] studied deep learning approaches in mmWave radar-based detection and classification in autonomous driving. The survey first gave an overview of radar techniques and deep learning methods. Afterward, it focused on the detection and classification of radar signals using deep learning techniques. It also presented multi-sensor fusion technologies of radars and cameras. The related datasets are also introduced in the survey. Shastri et al. [7] gave a survey of device-based localization and device-free sensing using mmWave communications and radars. It reviewed mmWave signal propagation and system design, detailing approaches, algorithms, and applications for mmWave localization and sensing. The survey then introduced device-free human sensing using mmWave radars. Peng and Li [8] focused on radar-based localization and life-tracking works. The survey first briefly introduced FMCW radar techniques, and then paid attention to the emerging applications in human sensing and automobiles. Venon et al. [9] surveyed automotive applications of recognition and localization based on mmWave radars. The survey first described mmWave FMCW radars with working principles and challenges, and then presented data processing methods and learning techniques. Afterward, it reviewed the applications in perception, recognition and localization of automotive scenarios. Fan et al. [10] reviewed 4D mmWave radar techniques and presented the developments in target detection and tracking for autonomous driving with 4D mmWave radars. Wei et al. [11] presented a review of fusion technologies of mmWave radars and vision in objective detection. The paper first introduced the tasks, evaluation criteria, and datasets of object detection in autonomous driving. Then, it divided mmWave radar and vision fusion into three types, and introduced mainstream applications in object detection driven by sensor-fusion techniques. Pearce et al. [12] discussed multi-object detection works based on mmWave

radars. The survey first presented a typical tracking system architecture based on mmWave sensing. Then, it introduced technologies and methodologies in mmWave tracking systems. Afterward, multi-object tracking studies were reviewed in the paper. Coluccia et al. [13] presented a review on drone detection techniques and applications driven by radars. The survey first introduced the basic theory of radar signal processing. Then, it gave a lot of space to introduce FMCW radar-based drone detection, drone verification and drone classification. Patole et al. [14] surveyed signal processing techniques of automotive radars including mmWave radars. The surveys [15], [16], [17] reviewed vital sign monitoring works especially human respiration and heartbeat activities based on radars. The authors in [15] first introduced radar system topologies and architectures. Then, the effect of transmit power and operational frequency on radar design was studied. Afterward, practical non-contact vital sign monitoring was presented, especially in multi-resident scenarios. Similarly, the survey [16] introduced continuous wave Doppler radars and presented the principles that support vital sign monitoring. Then, it reviewed the technical advancements and emerging applications in radar-enabled healthcare monitoring and several other applications. Another recent survey [17] explores human anatomy and various measurement methods. Next, four mmWave-based vital sign sensing signal models are introduced, with deep learning technologies and related studies reviewed. The literature [18], [19] focused on a common daily human-centric application, i.e., gesture recognition, and presented surveys on radar-based gesture recognition works. The survey [18] first described hand gesture signal acquisition based on radars. Then, it reviewed the signal representation for hand gestures and presented hand gesture recognition algorithms, in which recent related studies were reviewed. The survey [19] of the same topic reviewed existing gesture recognition applications and focused on FMCW radar gesture recognition systems. It gave a general framework of gesture recognition, including gesture data acquisition, signal preprocessing, gesture recognition algorithm and classification results. The applications of coarse-grained and fine-grained granularity were analyzed. Another survey [20] presented human activity recognition techniques especially deep learning methods based on radars. It first introduced deep learning techniques and radar systems. Then, it gave a large space to present deep learning approaches for human activity recognition in radars. van Berlo et al. [21] reviewed application pipelines and building blocks of mmWave radar sensing. The survey first introduced its review methodology that shows how the related studies are surveyed. Next, the application pipelines for radar-enabled sensing systems were given, with an integration of recent applications in automobiles and human sensing. A more recent survey [22] studied mmWave-based human sensing, i.e., the technology and applications related to human tracking, recognition, measurement, and imaging. It first introduced the platforms of mmWave radar sensing. Then, it presented techniques in signal processing and feature extraction. Next, it reviewed the applications in human sensing scenarios.

TABLE I
COMPARISON AND SUMMARY OF RELATED SURVEYS ON MMWAVE RADAR SENSING

Topic	Machine Learning	Deep Learning	Devices	Datasets	Metrics	Application Taxonomy	Automobile	Smart Home	Industry	LLM-aided Sensing	YoP	Ref
ML & DL technique	✓	✓					✓	✓			2021	[5]
DL technique	✓	✓		✓			✓	✓			2021	[6]
Localization technique	✓	✓		✓			✓	✓			2022	[7]
Localization & tracking			✓				✓	✓			2019	[8]
Automotive application		✓			✓		✓				2022	[9]
Autonomous driving		✓		✓			✓				2024	[10]
Vision fusion		✓	✓	✓	✓		✓				2022	[11]
Object detection	✓	✓	✓		✓		✓				2023	[12]
Drone's detection	✓	✓							✓		2020	[13]
Signal processing	✓						✓				2017	[14]
Vital sign monitoring	✓							✓			2020	[15]
Vital sign monitoring	✓			✓				✓			2016	[16]
Vital sign monitoring	✓	✓			✓			✓			2023	[17]
Gesture recognition	✓	✓		✓				✓			2021	[18]
Gesture recognition	✓	✓			✓			✓			2022	[19]
Activity recognition	✓	✓	✓					✓			2019	[20]
Application pipeline	✓	✓		✓	✓	✓	✓	✓			2021	[21]
Human sensing	✓	✓	✓	✓				✓			2023	[22]
mmWave radar sensing techniques and applications	✓	✓	✓	✓	✓	✓	✓	✓	✓	✓		This survey

Different from existing literature, our focus is to present mmWave sensing techniques covering a wide range of different application scenarios, including autonomous driving, smart home, and industry. An in-depth analysis of techniques and the insightful relation between techniques and applications are given (the existing surveys focus on either specific techniques [5], [6], [7] or only technical pipelines [21]). Our survey elaborates on hardware devices, available public datasets, and common evaluation metrics, which guide the implementation of sensing systems. Our survey presents a taxonomy basis of emerging mmWave radar sensing applications and gives broad visions of current research works in autonomous vehicles, smart homes, and industry. This is different from existing surveys that cover specific application scenarios [5], [6], [7], [8], [9], [11], [12], [13], [14], [15], [16], [18], [19], [20], [21], [22], [17]. Our survey discusses several challenges and future tendencies. Especially, the large language model (LLM)-aided sensing with mmWave, is discussed with potential directions in data synthesizing and physical comprehension.

Particularly, compared to the work [21], our survey reviews mmWave radar-based industrial sensing scenarios, covering three fields of industrial imaging, industrial measurement, and environmental monitoring. Our survey reviews mmWave radar sensing techniques from the perspective of dedicated radars and communication integration. Our survey presents a thorough collection of mmWave radar devices and also gives our insights and solutions on LLM-aided sensing with mmWave. Compared to the recent survey [22], our survey covers more extensive application scenarios including not only human sensing but also automotive and industrial applications, which makes much of the content different. Our survey provides techniques from another perspective of communication integration. Our survey gives an application taxonomy for emerging applications to provide the basis for application classification. Our survey presents more details (e.g., evaluation metrics) in mmWave sensing design and gives our insights on LLM-aided sensing.

The comparison between this survey and recent related surveys is summarized in Table I.

C. Scope and Organization

The paper provides a comprehensive survey of mmWave radar sensing techniques and applications. It begins with the building blocks, which encompasses mmWave radar techniques, signal processing techniques, and machine learning techniques. Specifically, the widely exploited mmWave radar techniques and signal processing techniques that fundamentally support sensing capability are first introduced from the perspectives of dedicated radars and communication integration. Mainstream machine learning techniques, especially the latest deep learning approaches, are then presented for designing mmWave radar sensing applications, in which our understanding and insights are given. Afterward, this paper presents related hardware devices, available public datasets and evaluation metrics. Then, an elaborated taxonomy of the emerging mmWave radar sensing applications is introduced covering autonomous vehicles, smart homes and industry. Based on the application taxonomy, this paper reviews a multitude of studies for these applications: object detection, ego-motion estimation, simultaneous localization and mapping (SLAM), activity recognition, pose estimation, gesture recognition, speech recognition, vital sign monitoring, user authentication, indoor positioning, industrial imaging, industrial measurement, environmental monitoring, etc. Finally, this paper discusses the challenges of existing studies and prospects for potential future research directions in integrated sensing and communication (ISAC), LLM-aided sensing, environmental noise, and training efforts. The main contribution of the survey paper is summarized as follows.

- To bridge the physical and digital worlds, mmWave radar sensing technology comes into being to enable a nonintrusive and low-cost sensing mode, which has yielded a number of applications among different fields. In this survey, we provide a comprehensive review of mmWave radar sensing in autonomous vehicles, smart homes and industry.
- We study mmWave radar and signal processing techniques from the perspective of dedicated radars and communication integration. We review advanced machine learning techniques and elaborate on the insightful relation between techniques and applications.
- We conduct a comprehensive review of mmWave radar devices, datasets, and evaluation metrics. The introduction of the three aspects helps to select devices, utilize public datasets, and apply evaluation metrics for a convenient implementation and reproduction of mmWave radar sensing.
- We review the emerging applications of mmWave radar sensing and provide a taxonomy basis for a wide range of application scenarios in autonomous vehicles, smart homes, and industry. We conduct a comprehensive survey on related studies of the applications.
- We review current research efforts in solving practical challenges, and present our insights and solutions for future tendencies. Especially for the incoming LLM period, we give our insights into LLM-aided mmWave radar sensing.

The overall structure of the paper is shown in Fig. 1. In this paper, mmWave radar techniques are first presented in Section II. Section III introduces the widely exploited techniques of mmWave signal processing. Then, mainstream machine learning techniques especially the latest deep learning techniques in designing sensing applications are exhibited in Section IV. Section V introduces related hardware devices, public datasets and evaluation metrics. Then, this paper presents a taxonomy of mmWave radar sensing applications in Section VI, and gives broad visions of research works based on the taxonomy in Section VII. Finally, the current technical challenges and potential research directions are discussed in Section VIII, and the survey paper ends with a conclusion in Section IX.

II. MMWAVE RADAR TECHNIQUES

To realize sensing, a mmWave radar first transmits signals to sense environments and captures objective information. Signal modulation, transmission, reception and processing are the main contents of mmWave radar techniques. In this section, we first review frequency-modulated continuous-wave (FMCW) techniques [23], and introduce range estimation and velocity estimation enabled by FMCW techniques. We then present angle estimation and time-division multiplexing-multiple input multiple output (TDM-MIMO) techniques. Afterward, we review integrated sensing and communication (ISAC) signal design techniques.

A. Frequency-Modulated Continuous-Wave (FMCW)

FMCW techniques leverage modulated pulsed waves to sense environments and capture objective information. They are able to differentiate small distances due to the millimeter-level wavelengths, which provide high-resolution range and velocity estimation capability. The signal processing after mixing is performed at a low-frequency range, considerably simplifying the realization of the processing circuits. These properties have boomed FMCW techniques extensively exploited by the communities and occupy the current market.

FMCW techniques extend the capability of traditional continuous wave radars. Radars based on FMCW techniques can detect close objects with the minimum measurable distance equal to the wavelength while ensuring high measurement accuracy. With FMCW techniques, radars can estimate the distance and relative velocity of target objects. FMCW techniques modulate the transmitted mmWave signal into continuous waves with varying frequencies. The modulated wave signal operates in a frequency that changes linearly with time, which is also known as a linear frequency modulated pulse, i.e., a chirp. The frequency of a chirp can be defined as

$$f(t) = St + f_c, \quad (1)$$

where $f(t)$ is the frequency, S is the slope of the chirp, t is time, and f_c is the start frequency. The slope S of the chirp is determined by

$$S = \frac{B}{T_c}, \quad (2)$$

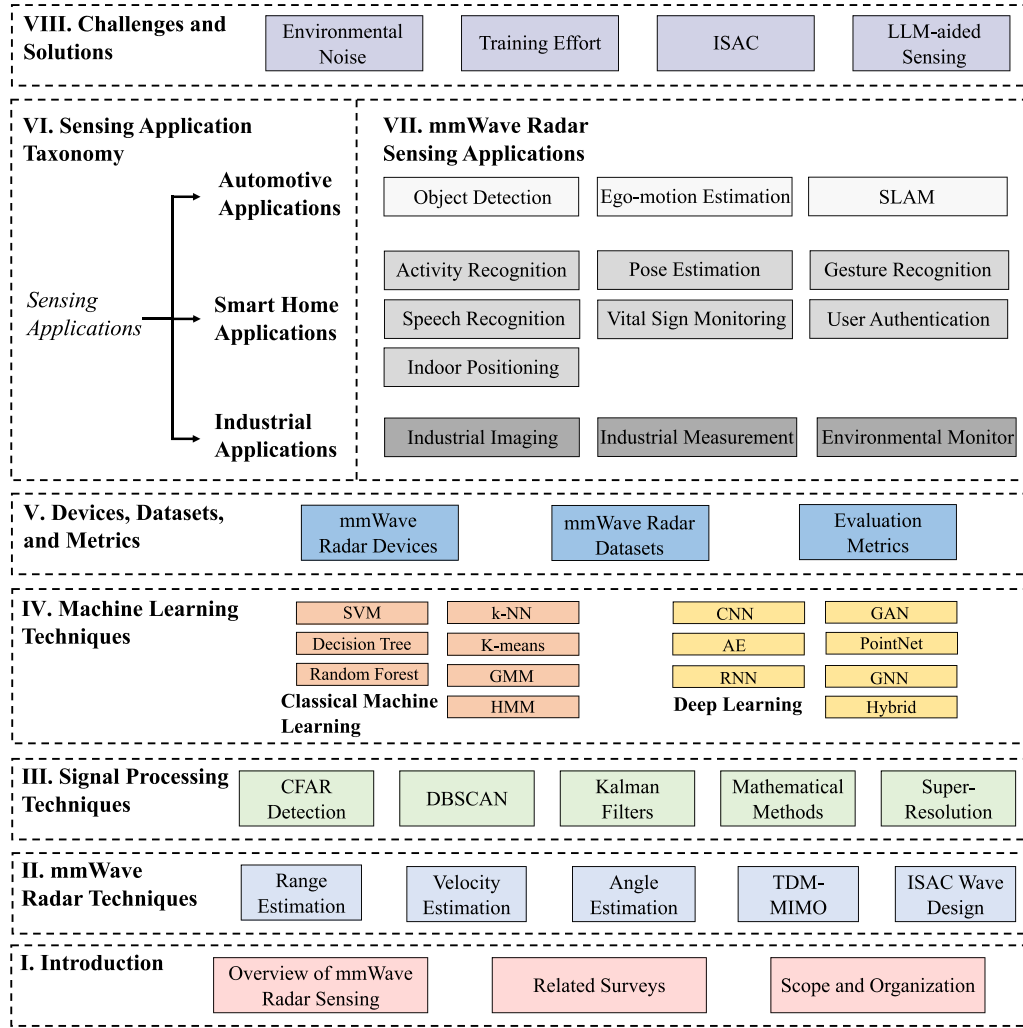


Fig. 1. An overall structure of the survey paper.

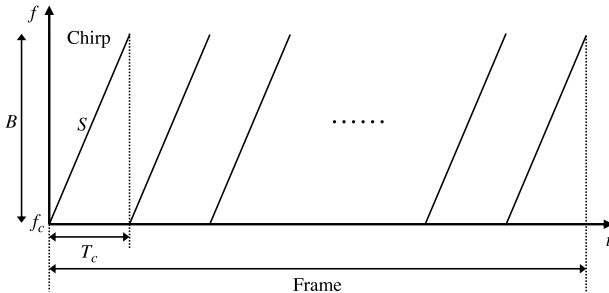


Fig. 2. An example of a chirp frame, where each chirp has a bandwidth B , duration T_c , slope S , and starting start frequency f_c .

where B is the bandwidth of the chirp and T_c is the duration of the chirp. mmWave radars usually transmit a number of equally-spaced chirp signals as a frame for sensing, as shown in Fig. 2.

A mixer is applied to combine transmitted signal and received signal to create a new signal. For the two sine signals denoted by x_1 and x_2 , we have

$$x_1 = \sin(\omega_1 t + \phi_1), \quad (3)$$

$$x_2 = \sin(\omega_2 t + \phi_2), \quad (4)$$

where ω_i and ϕ_i are the angular velocity and initial phase of the i -th signal respectively. The output signal of the mixer is

$$x_{out} = \sin((\omega_1 - \omega_2)t + (\phi_1 - \phi_2)), \quad (5)$$

which is also known as intermediate frequency (IF) signal [24].

Therefore, the generation process of FMCW radar signals can be summarized as follows. First, a mmWave radar generates a chirp frame, which is emitted by transmit antennas. Then, the chirp frame is received by the receive antennas after being reflected by environmental objects. Finally, a mixer mixes the transmitted signal and received signal, and outputs the IF signal. With the IF signal, mmWave radars can further process the data to estimate different physical quantities, such as the range and velocity of objects, which enables basic sensing functions.

B. Range Estimation

Range estimation is one of the basic functions of mmWave radars. Assume an object is located at a range d from a radar. As shown in Fig. 3, a transmitted chirp signal is reflected

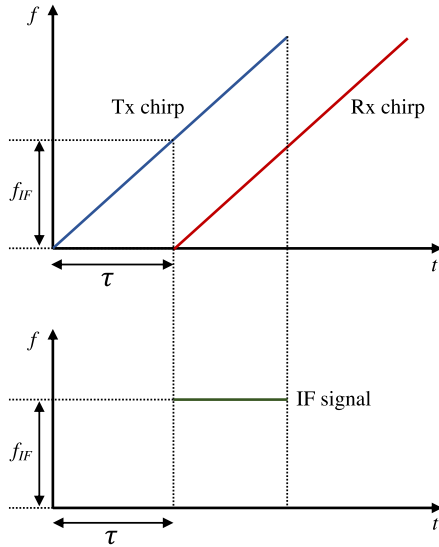


Fig. 3. The Tx signal and Rx signal are mixed to generate IF signal, which has a delay τ and constant frequency f_{IF} .

by the object and arrives at the receive antennas with a time delay. The frequency of IF signal is the difference between the transmitted signal and received signal. Hence, we have

$$\tau = \frac{2d}{c}, \quad (6)$$

$$S = \frac{f_{IF}}{\tau}, \quad (7)$$

where τ is the delay between the transmitted and received signals, d is the object's range, c is the light speed, S is the slope of the chirp, and f_{IF} is the frequency of IF signal. Based on the formulas, the range of the object can be estimated by

$$d = \frac{c T_c f_{IF}}{2B}, \quad (8)$$

where T_c is the chirp's duration and B is the chirp's bandwidth.

Moreover, if there are multiple objects in different ranges, each object reflects the transmitted chirp signal and produces a reflected chirp signal with a delay proportional to its range. Hence, the IF signal consists of multiple tones, each of which has a constant frequency and corresponds to a target. For the IF signal with multiple tones, a fast Fourier transform (FFT) [25] is employed to separate these tones in frequency spectrum, which is called Range-FFT. Each peak in the frequency spectrum denotes an object at a specific range. Therefore, the range of multiple objects can be estimated by FMCW techniques.

For mmWave radars, to conduct analog-to-digital converter (ADC) sampling, the sampling rate of radars should be greater than the frequency of IF signals. Hence, the IF frequency f_{IF} limited by the sampling rate leads to a maximal range that radars can estimate. According to the range estimation in eq. (8), the maximal range is given by

$$d_{max} = \frac{F_s c}{2S}, \quad (9)$$

where d_{max} is the maximal range, F_s is the sampling rate, c is the speed of light, and S is the chirp's slope.

Range resolution is the minimum distance at which two objects can be distinguished, reflecting the ability to distinguish multiple objects. The range resolution d_{res} is given by

$$d_{res} = \frac{c}{2B}. \quad (10)$$

where c is the speed of light and B is the bandwidth of the chirp signal [26].

As a basic function of mmWave radars, range estimation describes the relative distances between a radar and objects, which fundamentally facilitates distance-based applications and supports further processing of mmWave signals.

C. Velocity Estimation

Velocity is an important information that describes the instant motion state of the sensed objects. To estimate the velocity of a moving object, a radar transmits two chirp signals separated by T_c and receives the signals after being reflected by the object. Since T_c is usually measured in milliseconds, the movement of the object is less than the range resolution, which only results in a single peak in Range-FFT. However, the movement of the object leads to a phase difference between the reflected chirp signals. The phase of a chirp signal can be denoted as $\phi = (4\pi d)/\lambda$, where λ is the wavelength. The displacement of the object can be denoted as $\Delta d = vT_c$, so the velocity of the object can be derived by

$$v = \frac{\lambda \Delta \phi}{4\pi T_c}, \quad (11)$$

where v is the velocity, $\Delta\phi$ is the phase difference between the two reflected chirp signals.

If there are multiple objects moving simultaneously in the same range, the straightforward method could fail because the phase difference are a superposition of multiple objects. To estimate the velocity of multiple objects, a radar transmits a chirp frame with N_c equally-spaced chirps, and performs Range-FFT on the reflected chirp frame. These objects generate N_c peaks with the same range in frequency spectrum, but each has a different phase due to the movement of these objects. The movement of each object generates a phasor that contributes to the phase, as shown in Fig. 4. Then, another FFT operation, called Doppler-FFT, is performed to further resolve multiple objects and derive the phase difference of each object. Hence, the velocity of the i -th object can be calculated by

$$v_i = \frac{\lambda \omega_i}{4\pi T_c}, \quad (12)$$

where λ is the wavelength, ω_i denotes the phase difference between consecutive chirps of the i -th object, and T_c is the duration of the chirp.

Similar to range estimation, velocity estimation also has a maximal velocity that can be unambiguously differentiated by radars. Since the velocity is estimated by the phase difference as shown in eq. (12), it is unambiguous only when the phase difference is greater than π . Therefore, the maximal velocity can be denoted by

$$v_{max} = \frac{\lambda}{4(T_c + \tau_c)}, \quad (13)$$

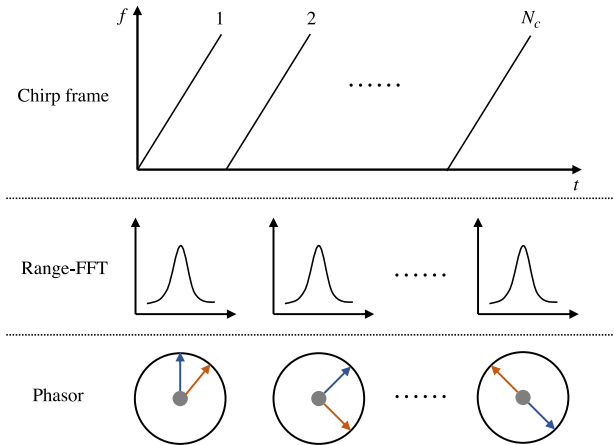


Fig. 4. A chirp frame generates multiple peaks in Range-FFT, each of which has a different phase and can be utilized to estimate velocity.

where \$\lambda\$ is the wavelength, \$T_c\$ is the duration of the chirp, \$\tau_c\$ is the interval of two adjacent chirps.

The resolution to estimate velocity can be derived based on how close two discrete frequencies can be resolved. According to the Fourier transform theory, two discrete frequencies can be resolved when their difference is larger than \$2\pi/N_c\$, where \$N_c\$ is the number of chirps. Hence, the velocity resolution can be given by

$$v_{res} = \frac{\lambda}{2T_f}, \quad (14)$$

where \$\lambda\$ is the wavelength, and \$T_f\$ is the time of the chirp frame (i.e., \$T_f = N_c T_c\$) [26]. The formula indicates that velocity resolution is inversely proportional to frame time.

Velocity estimation provides another key information related to the movement of targets. Based on velocity estimation, a radar can distinguish multiple objects of the same range according to their different radial velocity toward the radar, providing more precise sensing of multiple objects. Moreover, the estimated velocity describes how the objects move, which can support lots of motion-based applications.

D. Angle Estimation

The angle of signals arrived at a radar is also called angle-of-arrival (AoA). If the signals are reflected by an object, the angle of the object toward the radar can be estimated accordingly. Different from range and velocity estimation which is based on FMCW techniques, angle estimation exploits the information underlying multiple receive antennas. Consider a simple scenario where a mmWave radar is equipped with two receive antennas. The signals reflected by an object arrive at the two receive antennas and have different path lengths due to the relative angle of the object toward the radar, as shown in Fig. 5. The phase difference between the two paths can be denoted by

$$\Delta\phi = \frac{2\pi\Delta d}{\lambda}, \quad (15)$$

where \$\Delta\phi\$ is the phase difference, \$\Delta d\$ is the difference of the two paths, and \$\lambda\$ is the wavelength. Since the distance

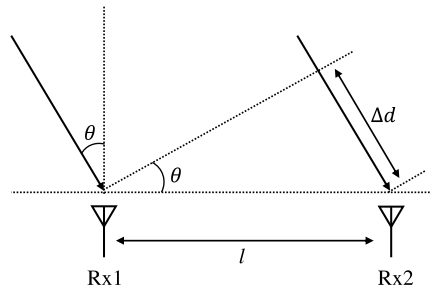


Fig. 5. The signals arrive at the two receive antennas with different path lengths.

of the two receive antennas is small and far less than paths' lengths, the two paths arrived at the antennas can be regarded as parallel lines. Hence, there is a geometrical relationship in paths' lengths and angle, i.e., \$\Delta d = l \sin(\theta)\$, where \$l\$ is the distance between the two receive antennas, and \$\theta\$ is the object's angle. Hence, the object's angle can be derived by

$$\theta = \sin^{-1}\left(\frac{\lambda\Delta\phi}{2\pi l}\right), \quad (16)$$

where \$\theta\$ is the angle. According to the property of trigonometric function, \$\sin\theta\$ and \$\theta\$ has a similar changing trend when \$\theta\$ is small. This indicates that the angle estimation has a more precise accuracy when the object is located with a small angle toward the radar [27].

To estimate the angle of multiple objects, radars require an antenna array consisting of multiple receive antennas and exploit the phase difference in each antenna. Assume there are two objects with different angles toward a radar equipped with \$N_{RX}\$ receive antennas. The signals reflected by the two objects are superposed at each antenna, which produces \$N_{RX}\$ phasors. The received signals of the \$N_{RX}\$ antennas can be considered as a discrete sequence, in which each antenna's signal contains two phasors of different angular frequencies. Then, a Fourier transform is performed on the sequence to calculate the angular frequency of the two phasors, so the angle of each object can be given by

$$\theta_i = \sin^{-1}\left(\frac{\lambda\omega_i}{2\pi l}\right), \quad (17)$$

where \$\theta_i\$ is the angle of the \$i\$-th object, \$\lambda\$ is the wavelength, \$\omega_i\$ is the angular frequency derived by FFT, and \$l\$ is the distance of two adjacent antennas. The Fourier transform that estimates the angle of objects is called an Angle-FFT.

The maximal angle that radars can estimate refers to the maximum angular field of view. According to eq. (16), the angle estimation stays unambiguous when the absolute value of phase difference is less than \$180^\circ\$. Hence, the maximal angular field of view can be given by

$$\theta_{max} = \sin^{-1}\left(\frac{\lambda}{2l}\right), \quad (18)$$

where \$\theta_{max}\$ is the maximal angular field of view for radars, \$\lambda\$ is the wavelength, and \$l\$ is the distance of adjacent antennas. When the distance \$l = \lambda/2\$, the radars achieve the maximal angular field of view, i.e., \$\pm 90^\circ\$.

The resolution of angle estimation refers to the minimum angular interval between two objects that can be distinguished by radars. The angle resolution can be deduced from Fourier transform theory, i.e.,

$$\theta_{res} = \frac{\lambda}{N_{RX} l \cos(\theta)}, \quad (19)$$

where λ is the wavelength, N_{RX} is the number of receive antennas, l is the distance of antennas, and θ is the angle [26]. The formula also indicates that the angle estimation is more precise with a small angle.

Angle estimation provides another view to spatially sense objects. Combining angle and range information, mmWave radars can localize objects and describe the shape of objects, enabling mmWave radar-based localization and objective detection applications.

E. Time Division Multiplexing Multiple-Input Multiple-Output (TDM-MIMO)

Due to the short wavelength of signals, multiple antennas can be integrated into a mmWave radar with a distance equal to half of the wavelength to estimate angles. According to the resolution of angle estimation in eq. (19), more receive antennas contribute to a more precise angle estimation. However, the physical space of mmWave radars limits the expansion of antennas. In order to leverage limited hardware resources for precise angle estimation, TDM-MIMO techniques are utilized in mmWave radars [28], which improves the resolution of angle estimation under limited antennas.

A mmWave radar with TDM-MIMO techniques is equipped with multiple transmit antennas and receive antennas. By generating a virtual antenna array based on TDM-MIMO techniques, the radar virtually expands the number of physical antennas. Using TDM-MIMO techniques, a radar with N_{TX} transmit antennas and N_{RX} receive antennas can perform as a radar with $N_{TX} \times N_{RX}$ receive antennas. Hence, even physically-small radars with fewer antennas can achieve precise angle estimation. Take a multiple-input multiple-output (MIMO) radar with 2 transmit antennas (Tx1 and Tx2) and 4 receive antennas (Rx1 to Rx4) as an illustration. The radar leverages TDM technique to transmit signals from different antennas in turn. Using TDM techniques, the radar can distinguish the signals transmitted by each transmit antenna according to different time slots. Assume that the distance between adjacent receive antennas is l and the distance between the transmit antennas is $4l$. The signals transmitted by Tx1 arrive at the 4 receive antennas with different phases, which are denoted as $\{0, \phi, 2\phi, 3\phi\}$. Since the distance between Tx1 and Tx2 is $4l$, the signals transmitted by Tx2 have an additional path length of $4l \sin(\theta)$ compared to that of Tx1. This results in additional 4ϕ phase of the signals transmitted by Tx2 for each Rx, which can be denoted as $\{4\phi, 5\phi, 6\phi, 7\phi\}$. It seems like another 4 receive antennas are added in the antenna array. Hence, although the radar has only 4 receive antennas, it generates a virtual antenna array of 8 receive antennas, which improves the resolution of angle estimation.

F. ISAC Signal Design

mmWave radar-based ISAC is also called joint radar communications (JRC), which jointly takes advantage of sensing and communication to provide ubiquitous sensing services while enabling more efficient communications. From the perspective of communication integration, signal design is a key step to enable both sensing and communication capabilities.

In designing mmWave ISAC signals, orthogonal frequency division multiplexing (OFDM) [29] is the fundamental. The basic principle of OFDM is to divide the available spectrum into multiple narrowband subcarriers, which are orthogonal to each other. The data are transmitted on the subcarriers' corresponding frequencies. OFDM adapts to severe channel conditions without complex time-domain equalization, and is robust against narrow-band co-channel interference. OFDM has been a basic technical component in realizing mmWave communication. Mathematically, the signal $x(t)$ can be expressed as the sum of modulated subcarriers: $x(t) = \sum_{n=0}^{N-1} X_n(t)$, where N is the number of subcarriers and $X_n(t)$ is the modulated signal for the n -th subcarrier. Each subcarrier is modulated using some form of digital modulation scheme, such as quadrature amplitude modulation (QAM) or phase shift keying (PSK). The modulated signal $X_n(t)$ for each subcarrier can be expressed as:

$$X_n(t) = A_n \cdot \text{mod}(f_n, t) \cdot e^{j2\pi f_n t}, \quad (20)$$

where A_n is the amplitude of the n -th subcarrier, $\text{mod}(f_n, t)$ is the modulated data signal (e.g., QAM or PSK) for the n -th subcarrier, f_n is the frequency of the n -th subcarrier, and $e^{j2\pi f_n t}$ is the carrier frequency at f_n .

To enable ISAC of mmWave using OFDM, several techniques are applied to aid the combination of communication and sensing. Different linear frequency modulation (LFM) methods are designed for high-accurate mmWave radar sensing and FMCW is one of them. For highly efficient communications and radar resolution, [30] designs IF signal through the angle modulation of LFM radar carrier by OFDM communication signal. It aims to generate mmWave ISAC signal with multiplied instantaneous bandwidth and phase modulation index for high-resolution radar function and noise-robust OFDM communication. Reference [31] designs a photonics mmWave ISAC system that acquires FDM schemes while improving spectral efficiency using super-resolution techniques. The key idea is to utilize coherent fusion processing of sparse sub-band LFM radar signals, and enable a full-band-equivalent range resolution and more spectrum resources with a small fraction of the total bandwidth. Reference [32] integrates waveform generation using OFDM-based non-orthogonal multiple access (NOMA) communication signal and LFM radar signal. They try to keep the optimal power ratio consistent on different subcarriers and therefore improve the communication performance.

Phase coding is another technique utilized with OFDM, which optimizes the peak sidelobe ratio and modulates specific phase sequences into the subcarrier of OFDM. Phase coding and LFM are combined to achieve a high time-bandwidth product and reduce peak to average power ratio. Reference

[33] designs phase-coded orthogonal frequency division multiplex waveform and the phase sequence is controlled by transmitted messages. For sensing, it also builds radar data processing for joint estimation of the range and velocity of the single-scatter-point target within one single transmitted pulse. Reference [34] combines communication and radar sensing in OFDM signal by analyzing the ambiguity function of OFDM signal with each pulse composed of one or more continuous symbols. Besides the above direct phase coding sequence modulation, phase modulated continuous waveform (PMCW) is another modulation method for sensing [35]. Reference [36] utilizes PMCW to retain reduced range-Doppler ambiguity property in ISAC. Reference [37] studies multicarrier PMCW to provide degrees of freedom (DoF) to confine AoA, Doppler shifts, ranges, and communication symbols in different dimensions. By leveraging multicarrier feature of OFDM and the code sequence of PMCW, it promotes conventional PMCW and OFDM waveforms.

In ISAC systems, beamforming is utilized to dynamically steer antenna beams towards specific directions. Thus, it allows for spatial separation of sensing and communication by steering the radar beam towards the desired direction, facilitating targeted transmission of signals and sensing of objects. Also, it enables ISAC systems to dynamically adapt their beam patterns in response to changing environmental conditions. Researchers usually consider combining beamforming techniques in implementing mmWave radar-related ISAC [38], [39], [40].

G. Summary and Insights

This section reviews mmWave radar techniques that underpin fundamental sensing functions. Among these techniques, FMCW methods serve as the cornerstone, providing essential sensing capabilities by modulating signals into continuous waves. Range, velocity and angle estimation are fundamental functions crucial for mmWave radars. Range and velocity estimation is driven by FFT operation on FMCW IF signals, which enables detecting and ranging the targets. Angle estimation is supported by employing multiple antennas and TDM-MIMO techniques. It enables the radar system to determine the angles of arrival for incoming signals, thereby spatially characterizing targets within the plane of the radar. For FMCW-based mmWave radars, these techniques are integrated into the basic processing flow. Hence, sensing applications leveraging FMCW radars typically incorporate these methods collectively to extract essential sensing information.

To integrate sensing and communication, wave signals are designed based on OFDM techniques to ensure highly efficient transmission. OFDM divides the available spectrum into orthogonal subcarriers, facilitating parallel data transmission and robust communication in wireless systems. With OFDM, various LFM techniques are integrated for joint radar and communication. They provide high resolution in range and robustness to Doppler effects, making them invaluable for radar sensing applications. Moreover, phase-coded signals modulate the phase of subcarriers to encode information. This

ensures reliable communication while simultaneously supporting radar sensing functionalities within the same waveform. PMCW techniques contribute significantly to the sensing capabilities of ISAC systems. PMCW radar operates by modulating the phase of continuous wave signals, allowing for precise range measurements and target detection without relying on traditional FMCW methods. Beamforming is instrumental in enabling the integration of radar sensing and wireless communication by efficiently utilizing signal resources. These ISAC signal design techniques empower mmWave radars with the capability to perform sensing tasks independently of only FMCW-related techniques. By leveraging the unique advantages of each technique, mmWave radars are endowed with integrated capability of radar sensing and communication.

With radar techniques, mmWave obtains essential spatial information to describe objects. Based on the spatial information, further processing of signals will be conducted for building various sensing systems.

III. SIGNAL PROCESSING TECHNIQUES

After the signals are initially acquired with spatial information by mmWave radar techniques, the intermediate sensing data need to be further processed to extract denoised and compressed representations to realize sensing. In this section, we present key techniques in mmWave signal processing, including constant false alarm rate (CFAR), density-based spatial clustering of applications with noise (DBSCAN), Kalman filter (KF), mathematical methods, and super-resolution methods.

A. Constant False Alarm Rate (CFAR)

CFAR detection [41] is a typical algorithm in radar signal processing, which aims to detect target reflections and filter out background noises. A threshold is determined in CFAR to judge if the reflections come from a target or a false source. The reflections exceeding the threshold will be judged as real targets while those lower than the threshold will be considered as false sources. Therefore, determining the threshold is critical in CFAR to accurately detect target reflections and filter out background noises. A low threshold could detect more real targets but at the cost of an increase in false alarms, while a high threshold may lead to fewer real targets being detected.

A number of CFAR techniques have been studied in radar systems, such as cell averaging (CA)-CFAR, clutter map CFAR and two-dimensional CFAR [42]. CA-CFAR is widely applied in mmWave radars for target detection. In CA-CFAR, the estimate of noise level E is calculated by using samples from the reference window x_{iN} around the test cell, where N is the number of units in the reference window and x_i is the number of units in the window. The threshold T is the product of estimated noise level E and predetermined detection scale factor B , i.e., $T = EB$. If the value of the cell under x_0 exceeds the threshold T , i.e., $x_0 > T$, the target is detected. The noise level is estimated by averaging the output of the reference unit

around the unit, i.e.,

$$E = \frac{1}{N} \sum_{i=1}^N x_i. \quad (21)$$

And the scaling factor B is calculated by

$$B = N(P_{FA}^{-1/N} - 1), \quad (22)$$

where P_{FA} is a desired probability of false alarm [41]. CA-CFAR detection is effective in the presence of background noises and interference to detect target reflections, which is a basic signal processing operation in mmWave radar sensing.

B. Density-Based Spatial Clustering of Applications With Noise (DBSCAN)

The target reflections detected by radars can be presented by points in the dimensions of range, angle, and velocity. These reflection points are usually numerous and dense, along with noise reflections and outliers being detected as well. Hence, a clustering method is expected to cluster target points and remove isolated points to describe a target. DBSCAN [43] is a classical density-based clustering method for radar systems, which can discover clusters of arbitrary shape and size containing even noise and outliers.

The basic idea of DBSCAN is that the high-density points are grouped as clusters while these isolated points are discarded according to the spatial distribution and local density. For each point in the cluster, the neighborhood of a radius contains a minimum number of points, which means that the cardinality of the neighborhood has to exceed a threshold. The ε -neighborhood of an arbitrary point p is defined as

$$N_r = \{q \in S | d(q, p) < r\}, \quad (23)$$

where q is a neighborhood point, S is the set of points, $d(q, p)$ represents the distance between q and p , and r is the radius [44]. The points whose ε -neighborhoods contain at least a minimal number of points is called the core point. The clusters are discovered by checking the ε -neighborhood of each point in the set. If the ε -neighborhood of a point p contains points more than the minimum number, a new cluster with p as the core point is created. Then, density-reachable points of these core points are further collected iteratively, which can be utilized to merge a new density-reachable cluster. The iterative process ends when no new points are added to any cluster. Finally, one or more clusters are discovered that represent high-density regions while the isolated points are referred as outliers.

As an unsupervised method, DBSCAN does not need to know the number of clusters in advance while only needing to set a few parameters during the training process, e.g., the threshold and the radius. The parameters usually remain valid for different cluster numbers, scenarios, and hardware settings. Moreover, DBSCAN releases the requirement of the spherical shape of clusters, which works in different shapes of clusters under random noises. The strengths have facilitated DBSCAN to be extensively applied in mmWave radar sensing.

C. Kalman Filters (KFs)

Kalman filters [45] are a kind of filter that works in dynamic systems with noise and inaccuracy. They can estimate accurate state of dynamic systems by using a series of observations that change over time, which filters unexpected noises and interferences. KFs are extensively used in a variety of fields including navigation, localization, autopilot, digital image processing, etc. Besides traditional KFs, extended Kalman filters (EKFs) and unscented Kalman filters (UKFs) have been developed for more complex scenarios such as non-linear systems. For mmWave radar sensing, applying KFs provides an accurate estimation of targets' trajectories.

A typical workflow of KFs can be divided into two major steps, i.e., estimate and update. KFs first define a state function that describes the current state of a target. In the estimate step, KFs estimate the state of the target at the current timestep and also calculate the variance of the estimated state. In the update step, KFs obtain the measurement of the state at the current timestep and also calculate the variance correspondingly. KFs update the estimated state using a state transition model and the measurement. The update process can be expressed by

$$\hat{s}_{t+\Delta t} = K_{t+\Delta t} \cdot z_{t+\Delta t} + (I - K_{t+\Delta t} H) s_{t+\Delta t}, \quad (24)$$

where $\hat{s}_{t+\Delta t}$ is the updated state of the target, $K_{t+\Delta t}$ is the Kalman Gain calculated by the two variances, $z_{t+\Delta t}$ is the measurement, I is a unit matrix, H is a transformation matrix, and $s_{t+\Delta t}$ is the estimate [46]. With the update process combining the estimate and measurement, KFs obtain an updated and more accurate state of the target. The two steps are in a recursive process, continuously estimating the state and then updating the state with real measurement.

The combination of estimate and measurement in KFs addresses random noise and frame loss in mmWave radars, which can accurately identify the center of targets and continuously track their trajectories. Many applications based on mmWave radar sensing employ extended KFs for indoor localization and tracking, which develops various types including linear regression correction-based extended Kalman filter [47], non-linear extended Kalman filter [48], recursive Kalman filter tracking with data association [49], coordinate-corrected extended Kalman filter [50], etc.

D. Mathematical Methods

There are some mathematical methods utilized in mmWave radar sensing applications for noise removal and dimension reduction. For example, to remove signal interferences and retain accurate sensing data, some studies exploit simple but effective mathematical operations. Geometric mean subtraction [51] can be performed for mean clustering, which eliminates random noises and retains regular signal components like faint physiological signals. Dual-differential background removal [52] leverages two differentials computed at different time points and adds them together to get background canceled points for filtering signals and removing noises. Line fitting [53] fits a line to IF signal phase with a low-pass filter to obtain accurate y-intercept of the demodulated IF signals, which can accurately estimate the phase of IF

signals. Different cosine-sum and adjustable windows can also be employed to reduce spectral leakage in signal transformation, such as Hann windows [54], Hamming and Kaiser windows [55], Chebyschev windows [56], etc. The effect of background reflections can also be manually subtracted by removing point clouds with zero Doppler velocity [57] or removing averages in spectrograms [58]. Other than noise removal, data dimension reduction is also an important operation for mmWave radar sensing works to obtain compressed and high-level data representations. As a statistical technique, principal component analysis (PCA) [59] has been successfully employed in mmWave radar sensing. PCA can linearly transform the data into a new coordinate system of small variations, which is an effective and lightweight dimension reduction and feature extraction method.

E. Super-Resolution Method

FMCW-based mmWave radars obtain data representation by the above signal processing techniques. Furthermore, super-resolution methods can be utilized in mmWave signal processing, including MUSIC, ESPRIT, and MVDR. In this section, we review these super-resolution methods utilized to process mmWave signals.

Multiple signal classification (MUSIC) [60] is a well-known algorithm that utilizes matrix eigenspace decomposition to classify signals. MUSIC is widely used in array signal processing for estimating AoA of the signals. In mmWave communication, MUSIC can be applied to enable signals with radar capability of estimating angles. The basic idea of MUSIC is to decompose the spatial covariance matrix of received signals into its eigenvalues and eigenvectors. With the eigenvalues and eigenvectors, MUSIC uses the fact that eigenvectors corresponding to the noise subspace span the nonsignal space, while the eigenvectors corresponding to the signal subspace span the signal space. Through spectral analysis of the eigenvalues, MUSIC detects the peaks corresponding to the potential AoA. The AoA estimation is based on the difference between antennas. In a similar way, the phase difference in OFDM subcarriers can be used to estimate distance of arrival. The phase difference in OFDM symbols can be used to estimate the velocity of target. Hence, the mmWave communication systems that do not rely on FMCW radar techniques can also be enabled with sensing capability. Some works modify MUSIC algorithms for mmWave radar sensing. Reference [61] uses random matrix sketching to estimate the signal subspace via approximated computation, developing a fast randomized-MUSIC algorithm. Reference [62] designs a low complexity MUSIC-based angle of arrival detection algorithm. It employs the characteristics of distance between adjacent arrays to balance the trade-off between field of view and resolution. Reference [63] focuses on step-scanned radar antennas and extends the application of MUSIC to improve the cross-range resolution of closely spaced point targets with a step-scanned mmWave radar.

Estimation of signal parameters via rotational invariance technique (ESPRIT) [64] is another technique used to estimate AoA. The basic idea of ESPRIT is to exploit the rotational

invariance property of uniform linear arrays to directly estimate AoA of signals without covariance matrix computation. Using the rotational invariance property of uniform linear arrays, ESPRIT estimates the signal subspace of the received signals. With the estimated signal subspace, ESPRIT directly estimates the AoA of the sources using pairs of antenna elements and the phase differences between them. This avoids the need to calculate the covariance matrix, thus reducing the computational complexity compared to MUSIC and achieving accurate AoA estimation. Reference [65] exploits ESPRIT for joint angle of arrival and range estimation in a monostatic MIMO radar with a frequency diverse array. A phase ambiguity removal method is proposed based on phase periodicity of the transmitting array steering vector. Reference [66] designs a 2D-unitary ESPRIT-based joint range and velocity estimation algorithm of multiple targets for radars. It aims to solve the problem of estimating the range-velocity information with high accuracy simultaneously and discriminating the targets with either closely spaced ranges or closely spaced velocities in the 2D range-Doppler spectrum.

Minimum variance distortionless response (MVDR) method is a popular adaptive super-resolution technique. It aims to estimate the weight of an antenna array and optimally suppress interference. MVDR method operates by applying spatial filtering to the received signals at an array of sensors. It forms a beam pattern that maximizes the output signal-to-interference-plus-noise ratio (SINR) in the direction of the desired signal while minimizing the power from interference and noise. MVDR first estimates the covariance matrix of the received signals to capture statistical properties of the signals and noise observed by the array. With the estimated covariance matrix, MVDR calculates the optimal beamforming weights by minimizing the output power subject to a constraint on the desired response in the desired direction. This optimization problem is typically solved by using inverse of the covariance matrix. Hence, MVDR provides another solution of enhancing the sensing of desired signals in the presence of interference. Some works directly exploit MVDR method and combine it with radar techniques to enhance sensing resolution. Reference [67] combines MVDR and MUSIC to gain the angle of arrival. Reference [68] leverages MVDR to promote spatial resolution by digital beamforming, thus helping to passively localize multi-person using mmWave radars. Some works exploit MVDR to obtain highly accurate range-angle images from mmWave signals [50], [69].

F. Summary and Insights

This section reviews techniques utilized to process mmWave signals. These signal processing techniques are basic processing flows for sensing systems because of the demand for handling mmWave signals. A comprehensive workflow of FMCW mmWave radar signal processing is depicted in Fig. 6.

With ADC sampling of mmWave radar signals, signal processing contains several stages to extract sensing information of the targets. Range-FFT is first employed to estimate the distance of objects from the radar, providing spatial distribution of detected targets within the radar's field of view. Following

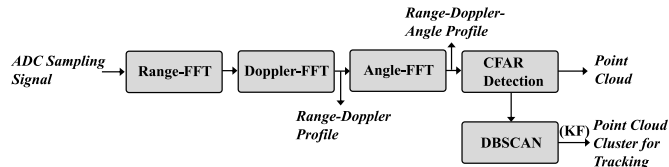


Fig. 6. A typical signal processing workflow of FMCW-based mmWave radars.

Range-FFT, a Doppler-FFT is applied across multiple chirps to analyze the frequency shifts induced by the motion of objects relative to the radar. With Doppler shifts, the velocity of the targets can be estimated. Combining the results from the Range-FFT and Doppler-FFT, Range-Doppler profiles are constructed. These profiles represent the spatial distribution and velocity information of detected targets, with higher intensity indicating the presence of significant objects. To provide more spatial information of the detected targets, an Angle-FFT is employed to extract angular information, which creates Range-Doppler-Angle profiles. The profiles provide a more comprehensive characterization of target locations and motions in three-dimensional space. Subsequently, CFAR detection algorithm is utilized to distinguish real targets from background noise, thereby improving the accuracy of target detection. Moreover, to facilitate the tracking and differentiation of multiple objects, point clouds can be further processed through techniques such as DBSCAN. This clustering approach groups point clouds corresponding to individual objects, enabling their distinct identification and tracking. To enhance target trajectory estimation and smoother tracking, techniques like Kalman filters can be applied. These filters utilize probabilistic models to estimate the state of tracked targets, providing more accurate predictions of their future positions and velocities.

In addition to the FMCW techniques described earlier, mmWave radars that do not utilize FMCW can leverage alternative methods, such as super-resolution techniques, to enhance their sensing capabilities. These methods, including MUSIC, ESPRIT, and MVDR, offer high-resolution sensing capabilities, particularly in the angular domain. These techniques are pivotal in overcoming limitations related to spatial resolution and signal ambiguity inherent in conventional radar systems. MUSIC, ESPRIT, and MVDR can extract detailed spatial information from received radar signals, which enables precise localization and characterization of targets. By integrating super-resolution algorithms into ISAC mmWave radars, researchers and engineers can achieve superior performance in target detection, tracking, and localization tasks.

With the processed mmWave signals that comprise physical meanings, various sensing systems can be built by further utilizing machine learning techniques.

IV. MACHINE LEARNING TECHNIQUES

The processed mmWave signals contain basic sensing information. To realize mmWave radar sensing applications, machine learning techniques, especially deep learning, are

broadly adopted and elaborately designed for sensing tasks. With machine learning and deep learning techniques, we can build the ultimate bridge between sensing tasks and signals to enable various novel sensing applications. In this section, we review mainstream and latest machine learning techniques, including classical machine learning algorithms and the latest deep learning models.

A. Overview of Machine Learning in mmWave Radars

Machine learning is a type of artificial intelligence technology that enables machines to think and learn how to process data efficiently and make predictions and decisions. Given the input data, machine learning techniques learn high-dimensional structures and relations behind the data. Based on the learned structures and relations, they can give predictions or decisions for newly arrived data. Machine learning techniques are used in a wide variety of applications, such as data mining, computer vision, speech recognition, medical diagnosis, financial forecasting, etc.

The task of sensing applications based on mmWave radars usually involves classification and regression. The ultimate goal requires techniques to output inferential results for the newly arrived radar data. Therefore, machine learning techniques can be naturally applied in mmWave radar sensing applications. Some unsupervised machine learning methods (e.g., DBSCAN and PCA) are included in signal processing techniques and those presented in this section focus on solving specific tasks.

B. Classical Machine Learning Algorithms

In sensing applications, classification and regression are the most common tasks that intuitively reveal the interrelationships of the data and give inferential results for the newly arrived radar data. Typically, feature extraction of the data is required to reduce data dimensions and extract compressed information. The feature extraction methods could be either signal processing techniques or machine learning techniques. A surge of classical machine learning algorithms has arisen in designing mmWave radar sensing systems.

Support vector machines (SVMs) [70] are a classical supervised learning model whose purpose is to determine the class a new data point belongs to for classification. For given data points, SVMs aim to decide a hyperplane of lower dimension that best separates the data points. Among many hyperplanes that could classify data points, SVMs find the one with the largest margin between classes as a target hyperplane. The largest margin can be determined by maximizing its distance from a data point on each side, which is called a maximum-margin hyperplane or maximum-margin classifier. For different datasets and classification tasks, hyperplanes could be non-linearly separable in the dimensional space. In that case, the dimensional space is mapped into a higher-dimensional space where the separation of data points becomes easier. Kernel functions are defined in the mapping to ensure that the dot product of data vectors can be calculated. In mmWave radar sensing tasks, SVMs are usually used to classify data representations constructed by processed mmWave

signals, leveraging the constructed hyperplanes. Hence, using SVMs to solve classification problems, SVMs are first trained and then classify data representations of the signals by the constructed hyperplanes. Through giving inferential classification results, SVMs enable various recognition-based applications. For example, we can exploit one-versus-one SVMs [71] or support vector domain descriptions (SVDDs) [72] to classify different samples and therefore output recognition results, enabling recognition-based mmWave radar sensing applications, such as activity recognition, gesture recognition, object recognition, etc.

Decision trees [73] are a common and popular machine learning algorithm that uses flowchart-like structures for classification. In decision trees, internal nodes represent binary attribute tests, branches represent the outcomes of node tests, and leaf nodes represent class labels. The paths from a root to leaves represent classification rules. Given a constructed decision tree, the data that needs to be classified will travel through the entire tree and finally be decided into a leaf node as the classification result. Random forests [74] that are composed of a multitude of decision trees are more popular and achieve more accurate classification performance for complex tasks. The output of random forests is the class that most trees decide. Utilizing random forests can run efficiently on large data sets and correct the defect of decision trees on overfitting training sets. Similar to SVMs, decision trees and random forests are specialized in giving inferential classification results to solve classification problems. With the feature representations of mmWave signals, we can use decision trees and random forests to construct small training costs and effective machine learning models, which can be utilized in various recognition applications.

Besides, there are other lightweight yet effective machine learning algorithms utilized in mmWave radar-based smart home applications. For example, k-nearest neighbors (k-NN) [75], a non-parametric supervised learning method, uses proximity to classify targets by grouping them based on similarity. It has been exploited in mmWave radar sensing applications [55], [76], [77]. for classification due to its lightweight complexity and high accuracy. Besides, a simple and popular unsupervised clustering algorithm, K-means clustering [78], also appears in mmWave radar sensing applications [79], [80], [81]. It groups unlabeled data into different clusters by referring to their distances, which gives self-adapting classification results without known classes. Gaussian mixture models (GMMs) [82] are a probabilistic algorithm used for classifying targets into different categories based on probability distribution. Since a GMM applies multiple Gaussian distributions, it can fit arbitrary types of distribution to deal with the data that are generated from different distributions. Hence, mmWave radar sensing systems [80], [83], [84] could take advantage of GMMs for clustering. Hidden Markov models (HMMs) are a commonly used statistical method for sequence modeling. Based on observed sequences, HMMs calculate the probability of hidden states underlying the events, which can give predictions for the current and future. This characteristic has made HMMs specialized in sequential problems. In mmWave radar sensing, some problems, such

as activity/gesture recognition, and object detection, also have strong relations in time. Therefore, it is suitable to use HMMs to build applications involving temporal change, such as mmWave radar-based gesture recognition [85], [86], [87], accidents detection [88], etc.

C. Deep Learning

Over the last decade, neural networks, especially deep learning technologies, have made tremendous progress and been extensively employed in a number of applications including pattern recognition, natural language processing, financial prediction, adaptive controlling, etc. A neural network model is usually structured by multiple layers of neurons to extract high-level feature representations from input data. By training a neural network model with sufficient data, it learns the knowledge underlying the data and can make intelligent predictions and decisions. Similar to other fields, the applications based on mmWave radar sensing also integrate different types of neural networks to extract features and give predictions to realize different sensing tasks.

Convolutional neural networks (CNNs) [89] are a very popular type of neural network for visual imagery analysis problems and have been broadly applied in mmWave radar sensing applications. The prominent characteristic of CNNs is a special operation called convolution, which performs matrix multiplication on small regions sliding along the whole input for extracting convolved features. A typical CNN consists of an input layer, hidden layers, and an output layer. Each hidden layer performs convolutional operations by the dot product of convolution kernels with input matrix of the layer. As convolution kernels slide along the input matrix of the layer, the convolution operation generates a feature map that acts as the input of the next layer. A convolutional layer is usually accompanied by a pooling layer to reduce the dimensions of the feature map, and a normalized layer to prevent gradient explosion or dispersion. Fully-connected layers are also important components in CNNs to integrate the extracted features and map the feature representations to the sample space for final predictions. CNNs are specialized in feature extraction among a variety of problems, and mmWave radar sensing is one of them. CNNs are widely applied in mmWave radar sensing to process the data representations composed by range, angle, and Doppler measurements. The feature representations extracted by CNNs abstract imagery embeddings under radar spectrums, which can be further utilized to facilitate various sensing applications. Together with deep learning techniques, many applications based on mmWave radar sensing have exploited CNNs with deep layers or modified components, such as deep convolutional neural network (DCNN) [90], [91], [92], residual neural network (ResNet) [93], [94], [95], [96], [97], [98], dual-view CNN [99], etc., to extract imagery features for realizing various applications.

Autoencoders (AEs) act as a common feature extractor in mmWave radar sensing applications. As unsupervised learning techniques, autoencoders learn compressed feature representations by reducing feature dimensions and ignoring insignificant

information underlying the data. An autoencoder consists of two main components, i.e., an encoder and a decoder. The encoder compresses the input into an intermediate feature representation of low dimensions called code, and the decoder then reconstructs the input using the code. Through outputting the reconstructed input that approaches the real input, autoencoders learn compressed feature representations in the intermediate process. This characteristic of autoencoders makes them popular and effective in dealing with various kinds of data representations to extract compressed features. For many mmWave radar sensing applications, the signal representations are usually complex and the features are hidden in the representations. Hence, autoencoders are widely exploited by researchers as a basis for constructing deep learning models, [96], [98], [100], [101], [102] to extract features from mmWave radar signals. Autoencoders have been utilized to extract features from mmWave radar signals for fall detection [103], face verification [104], human tracking [105], finger tracking [96], target detection [106], etc.

Recurrent neural networks (RNNs) [107] are another classical neural network model that exploits sequential relationships in the data to solve temporal problems, such as speech recognition, natural language processing, language translation, and radar sensing applications. RNNs can memorize historical information of prior inputs to deal with sequential data. They have a feedback process in which the output of hidden units at time step $t - 1$ is further fed to hidden units along with the current input of time step t . Among RNNs, long short-term memory (LSTM)-based RNNs [108], gated recurrent unit (GRU)-based RNNs [109], and bi-directional RNNs [110] have become the focus of solving temporal tasks. For mmWave radar data, the sequential relationships underlying serial inputs describe how a target moves over time, which supports temporal-related sensing applications like activity recognition and object tracking. Hence, researchers in mmWave radar sensing field have exploited different RNN-based models, e.g., deep RNN (DRNN) [111], LSTM-based RNN [112], convolutional-RNN [50], [58], spiking recurrent neural network (SRNN) [113], etc., to facilitate mmWave radar sensing applications.

As generative modeling methods, generative adversarial networks (GANs) have been successfully applied in various generative applications and have drawn considerable attention in mmWave radar sensing. GANs learn knowledge from the patterns of input data and utilize the learned knowledge to generate realistic new samples that resemble the original data. By generating realistic and synthetic samples, GANs enable the crossing in a range of problem domains, such as image-to-image translation across domains. Two sub-models called generator and discriminator are integrated into a GAN, where the generator aims to generate new samples and the discriminator tries to discriminate the samples as real or generated samples. The two sub-models are trained in a zero-sum game to discriminate the two types of samples fail, so that GANs can output the samples that are realistic and synthetic enough as real samples but in different domains. Some mmWave radar sensing applications are generative problems that either require to output new synthetic samples, or generating usable samples

from other domains. The prominent capability makes GANs promising in mmWave radar sensing applications. For example, researchers utilize conditional GAN [114], [115], [116], GAN denoising model [117], etc., to reconstruct the map of environments [116], recover user audios for eavesdropping [114], [115], generate training samples of micro-Doppler signatures [118], 3D shape reconstruction [119], [120], high-resolution imaging [121], etc.

In addition to the above dominant neural network types, some dedicated neural networks have also achieved promising performance in mmWave radar sensing applications. For example, PointNet [122] and its modification PointNet++ [122], novel types of neural networks that directly consume point clouds, have been exploited to process point clouds of mmWave signals for objective detection [123], [124], objective classification [125], semantic segmentation [126], etc. Other studies treat data representations of mmWave signals as graphs and utilize graph neural networks (GNNs) [127] to further process data and extract features, yielding mmpoint-GNN [128], spatial temporal-GNN [129], etc., for human activity recognition or gait recognition. Spiking neural network (SNN) [130] is also studied to take advantage of the intrinsic characteristics of SNNs in processing noisy and sparse data. SNN could better address noise and sparsity issues in mmWave radar sensing. Besides, hybrid deep models that integrate different neural networks also attract a lot of attention. Each component in a hybrid deep model is a type of neural network specially designed for a relatively individual task. By combining these components, hybrid deep models achieve a better performance by jointly taking advantage of each neural network. For example, some works design hybrid deep models using CNNs and RNNs [131], [132], CNNs and GRUs [133], autoencoders and RNNs [134], etc., to extract features from different perspectives and jointly fuse these features.

D. Summary and Insights

The comparison of these machine learning techniques is listed in Table II. The training type shows how the machine learning method is trained in a supervised or unsupervised manner. The objective indicates the ultimate goal of learning, such as classification, feature extraction, time series prediction, etc. The characteristic demonstrates the main features or technical means that make this method different from other methods. The applicable task shows the application fields the technique is suitable.

Machine learning techniques, particularly deep learning methods, have revolutionized the field of sensing and enabled significant advancements in various sensing tasks. The selection and design of these techniques are crucial in mmWave radar sensing design. Classical machine learning algorithms are usually utilized for processing low-complexity feature representations extracted from mmWave signals. These algorithms are suitable for tasks such as sample classification. For instance, SVMs, SVDD, decision trees, k-NN, and GMM are commonly employed for tasks like target recognition and activity recognition. HMMs are particularly skilled in sequential modeling, making them suitable for problems

TABLE II
COMPARISON OF MACHINE LEARNING TECHNIQUES

Techniques	Type	Objective	Characteristic	Applicable task
Support vector machine	Supervised	Classification	Determine the class a sample belongs to	Recognition, classification, detection
Support vector domain description	Supervised	Classification	Determine whether a sample belongs to a specific class	Recognition, classification, detection
Decision tree	Supervised	Classification	Determine the class a sample belongs to	Recognition, classification, detection
Random forest	Supervised	Classification	Determine the class the sample belongs to with multiple decision trees	Recognition, classification, detection
K-nearest neighbors	Supervised	Classification	Determine the class a sample belongs to using proximity	Recognition, classification, detection
K-means	Unsupervised	Classification	Groups unlabeled data to different classes	Recognition, classification, detection
Gaussian mixture model	Unsupervised/Semi-supervised	Classification	Determine the classes using probability distribution	Recognition, classification, detection, identification
Hidden Markov model	Supervised & unsupervised	Sequence labeling	Predict the hidden states of an event	Recognition, detection
Convolutional neural network	Supervised	Feature extraction	Extracting regional features using convolutional operation	Recognition, classification, detection, identification
Residual neural network	Supervised	Feature extraction	Extracting regional features with deeper convolutional layers	Recognition, classification, detection, identification
Autoencoder	Unsupervised	Feature extraction	Extracting compressed feature representation	Recognition, classification, detection, identification, tracking
Recurrent neural network	Supervised	Time series prediction	Extracting sequential features with recurrent process	Recognition, detection, tracking
Convolutional recurrent neural network	Supervised	Time series prediction	Extracting sequential features	Recognition, detection, tracking
Generative adversarial network	Unsupervised	Sample generation	Generating samples that resemble original data	Recognition, detection, monitoring, imaging
PointNet/PointNet++	Supervised	Feature extraction	Extracting features from point cloud data	Recognition, classification, detection

involving temporal changes in mmWave radar sensing. They are often utilized in recognition tasks involving temporal dynamics.

Other deep learning technologies leverage deep neural networks to automatically learn complex feature representations from mmWave signals. CNNs and their variants are popular choices for extracting features from range-angle spectrums constructed from mmWave signals, based on the ability to perform convolutional operations on image-like features. AEs are specialized in encoding various representations of mmWave signals into compressed features, which can be utilized in a wide range of mmWave sensing tasks. RNNs are suitable for handling temporal-related sensing applications, including gesture recognition and object tracking. GANs are suited for generative tasks and are increasingly used in mmWave-based applications such as map reconstruction, sample generation, and imaging. Therefore, researchers must carefully consider the nature of the sensing task and select appropriate methods for each phase of the process.

Machine learning techniques, especially deep neural networks, serve as the ultimate bridge between mmWave signals and practical applications. Through thoughtful selection and design, these techniques enable the development of sensing systems capable of addressing a wide range of real-world challenges.

V. DEVICES, DATASETS AND METRICS

Millimeter wave radar devices, public radar datasets, and evaluation metrics are important implementation tools of mmWave radar sensing applications. With the rapid development of mmWave radar sensing research and products in recent years, researchers in academia and industry have introduced numerous radar devices, public datasets, and evaluation metrics related to mmWave radars, which have been widely recognized by the public. In this section, we first review the radar devices that are designed for sensing. Then, we present available public datasets and introduce the key evaluation metrics for evaluating mmWave sensing systems.

A. mmWave Radar Devices

Devices are the fundamental that supports sensing techniques and applications. There are many mmWave radar devices manufactured by commercial corporations or academic researchers. Although they have different hardware components and properties, most of them share a typical hardware processing flow. Fig. 7 shows a typical block diagram of hardware processing for a commercial mmWave radar.

As shown in Fig. 7, there are multiple transmit antennas and receive antennas in a radar. For transmission, the radar uses a voltage-controlled oscillator, in which the frequency is controlled by a voltage input and allows for the frequency to

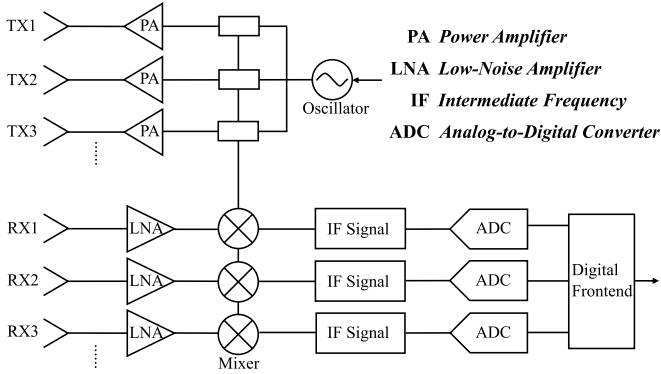


Fig. 7. A typical block diagram of hardware processing for a commercial mmWave radar.

be adjusted as needed. Therefore, the oscillator can generate mmWave signals with linearly increased frequency, i.e., the chirp signals. With power amplifiers (PAs) at each transmit antenna, the amplified chirp signals are transmitted from the TX to the space. The receive antennas capture the chirp signals reflected by the space. Since the received signals from the target could be very weak, the low-noise amplifiers (LNAs) are used immediately after the antennas to amplify the received signal from the antennas, which aims to increase the signal strength while introducing as little noise as possible. The received signals are then mixed with a portion of the transmitted signals using a mixer, which performs frequency mixing to produce IF signals that are proportional to the difference between the transmitted and received frequencies. The analog IF signals are converted to digital signals through analog-to-digital converters (ADCs). The ADC samples the analog signals at a high rate to produce digital signals that represent the amplitude and phase of the analog signals at each sample point. Therefore, the digital signals can be processed by digital signal processors (DSPs) in the digital frontend to obtain sensing information.

Based on the typical hardware processing flow, many mmWave radar devices have been manufactured in recent years. Texas Instrument (TI) mmWave radar sensors [4] are very popular commercial products, which are widely applied owing to their high integration, mature industrial supporting equipment and flexible designing capability. The radar sensors operate in the 60GHz/77GHz band and are integrated with FMCW techniques to enable high-accuracy sensing in automotive and industrial applications. TI mmWave radar sensors are typically integrated with DSP for data analysis, configurable RF frontends for more flexible system design, antenna-on-package (AOP) technology for compact form factors, and MIMO interfaces for easy integration into systems. As their high integration and flexible design, the researchers have paid a great deal of attention to utilizing TI mmWave radar sensors to realize various sensing applications.

There are many types of TI mmWave radar sensors, such as IWR/AWR1443 [135], IWR/AWR1642 [136], IWR/AWR1843 [137], IWR/AWR6843/6843AOP [138], etc., which have been extensively exploited in a number of system designs. The 1642 series has 2 on-board transmit antennas

and 4 on-board receive antennas, while the others have 3 on-board transmit antennas and 4 on-board receive antennas. The 1443,1642 and 1843 series are single-chip solutions that operate in the frequency range of 76GHz to 81GHz, while the 6843 series operates in the frequency of 60GHz to 64GHz. Among them, AWR and IWR are two different sensor families that operate in the same frequency range and use similar technology but apply to different sensing ranges. The AWR sensors usually have a maximum range of up to 300 meters, which is designed for long-range radar applications, such as automotive radar and radar for drones and autonomous vehicles. They are typically used as a complete system solution with evaluation boards and software. The IWR sensors are designed for short-range radar applications, such as industrial applications usually with a maximum range of up to 70 meters. They are used as discrete components that can be integrated into customer systems.

Besides TI mmWave radar sensors, there are many other mmWave radar types developed by commercial corporations, which are also utilized by researchers to implement mmWave radar sensing applications. For example, some studies [139] utilize ARS 408-21 radars that are manufactured by German Continental [140] to realize automotive-related sensing. The ARS 408-21 radar operates in 77GHz mmWave radar based on FMCW techniques. It has two modes of short range (SR) and far range (FR), which can effectively detect targets with a radius of up to 70 meters or up to 250 meters respectively. Navtech CTS350-X is another type of mmWave radar manufactured by Navtech Radar [141]. It is designed based on FMCW techniques and has compact designs that allow easy handling and installation. The researchers in [142], [143] exploit the radar to realize automobile-related applications. Soli [144] is a kind of mmWave radar developed by Google and Infineon. The radar operates in 24GHz/60 GHz with a short-range sensing capability driven by FMCW techniques. The radar is well known as a commercial gesture recognition product in smartphones. INRAS RadarLog [145] is a FMCW radar operating between 77GHz and 81GHz, which is equipped with one transmit antenna and 16 receive antennas. Some studies [105] utilize the radar to implement gait recognition based on mmWave signal sensing. Ahmad et al. [146] design a 60GHz mmWave radar sensor chip set with FMCW techniques. The radar sensor is equipped with a maximum of 4×4 transmission pairs. Pohl et al. [147] propose a compact ultra-wideband mmWave radar, which is designed with a wide bandwidth of 25 GHz around a center frequency of 80 GHz. Hansen et al. [148] present a D-band FMCW radar based on a fully integrated monostatic single-channel silicon-germanium (SiGe) transceiver (TRX) chip. It enables sweep within a single-loop phase-locked loop circuit from 174.5 to 121.5GHz, which achieves a spatial resolution of 3mm. The radar is proven with high capability in various industrial applications. Kueppers et al. [149] design a D-band FMCW radar working in 126–182 GHz with 1TX and 2RX. It is manufactured in Infineon's B11HFC 130 nm BiCMOS process, with a multichannel edge-launch waveguide frontend-module architecture. The designed radar is suitable for industrial and scientific applications. In addition, many

research works do not specify the details of their radars. These radars could typically work under 24GHz, 60 GHz, 76GHz, 77GHz, 79GHz, etc., with a typical 2GHz or 4GHz band. Usually, multiple transmit and receive antennas are applied to enable high angular estimation, such as 2TX with 4RX, 3TX with 4RX, etc. Combining FMCW techniques, these radars bring about similar capabilities to support different mmWave radar sensing applications.

B. mmWave Radar Datasets

The recent emergence of mmWave radar sensing works has promoted the growth and enrichment of public datasets. These public datasets release the heavy data collection process, which provides researchers with easily acquired radar data to design and implement new applications. Also, they offer the possibility to fairly evaluate different methods for comparison, inspiring more participants to step into the field.

nuScenes [150] is a well-known public dataset related to mmWave radars. It is a multimodal dataset that combines several autonomous vehicle sensors including 6 cameras, 5 mmWave radars and 1 lidar. The radars operate in 77GHz to 81GHz with FMCW techniques. The dataset comprises 1000 scenes, each 20s long and fully annotated with 3D bounding boxes for 23 classes and 8 attributes. nuScenes has contributed to some works in automobile applications especially multi-sensor fusion works [164], [165].

ColorRadar [151] is a multimodal dataset involving mmWave radar data. ColoRadar includes 3 different forms of dense, high-resolution radar data from 2 mmWave radar sensors and also the data from 3D lidar and (Inertial measurement unit) IMU sensors, where the mmWave radar data is collected by TI AWR1843. It also includes highly accurate groundtruth for the sensor rig's pose over approximately 2 hours of data collection in highly diverse 3D environments, including labs, hallways, creek paths, mine, etc. The dataset aims to provide radar sensor data for robotics perception works.

Wang et al. [152] share a dataset of mmWave radars in vehicle trajectory tracking. The dataset is collected in real-world road environments, including two freeways, a bridge, and an expressway. mmWave radars are installed on one side or both sides of road sections to cover the traffic.

3DRIED [153] is a 3D mmWave radar dataset for imaging. The dataset contains the raw echo data and the imaging results, in which 81 high-quality raw echo data are presented mainly for near-field safety inspection. The dataset is constructed by TI IWR1443 radar sensors operating in 77GHz to 81GHz.

Gambi et al. [154] propose a mmWave radar dataset of people walking. The dataset consists of 29 users' data under 6 different walking types, including fast walking, slow walking, slow walking with pocket, walking hiding bottle, walking with a limp, and slow walking with swinging hands, with a total of 231 acquisitions. The data is collected by TI AWR1642.

RadHAR [71] presents a point cloud dataset named MMActivity collected using TI IWR1443 mmWave radar. The dataset contains two users' data on 5 activities, including walking, jumping, jumping jacks, squats and boxing. Overall 93 minutes of data are collected.

HuPR [155] is a dataset of human pose estimation based on mmWave radars. The dataset contains 6 users' data under 3 different activities, including static actions, standing and waving hands, and walking with waving hands. Two TI IWR1843 and one camera are used for data collection, where the two radars are placed vertically for capturing high angular resolution mmWave signals. The two radars and the camera are synchronously configured to capture data with a total of 235 sequences and 141,000 triplets.

MARS [156] is a human pose activity dataset based mmWave point cloud. The data is collected by a TI IWR1443 and a Microsoft Kinect. The dataset involves 4 users with 10 activities, which can be utilized in pose estimation and rehabilitation assistance.

A similar dataset mri [157] also focuses on human pose estimation. The dataset is constructed by mmWave (TI IWR1443), RGB-D, and inertial sensors. It consists of over 160k synchronized frames from 20 users with various rehabilitation exercises.

mmBody [158] is another mmWave signal-based dataset for human pose estimation. They employ a Phoenix type mmWave radar from Arbe Robotics due to its high resolution. The dataset is built with mmWave radar point clouds and RGB(D) images in different scenes and skeleton/mesh annotations for humans.

mmMesh [159] collects mmWave point clouds of human body activities and constructs a human mesh dataset. The dataset is collected by TI AWR1843 and VICON system, which is a professional motion capture system for obtaining human meshes' ground truth.

M-Gesture [160] is a mmWave signal dataset of hand gestures. It consists of 144 users' data with 54,620 instances. The data is collected under not only direct sensing, but sensing under paper, corrugated paper, metal board, etc.

Mimogr [161] is a mmWave radar dataset that contains 7 types of gestures, including waving up, waving down, waving left, waving right, waving forward, waving backward, and double-tapping. The dataset consists of dataV, seven sets of gestures performed by 10 volunteers in an ideal indoor setting with a total of 6847 samples, and dataS, 2800 samples from a variety of complex environments and random users.

mHomeGes [86] is a arm gesture dataset based on mmWave radar sensing. The dataset focuses on arm movement of human, which are collected by TI IWR1443. It consists of 22,000 samples from 25 persons under 10 arm gestures.

Pantomime [162] is another gesture dataset of mmWave signals. The mmWave signals are collected with IWR1443. The dataset contains 21 gesture types performed by 41 users in two indoor environments.

mmGait [97] presents a human gait dataset collected by mmWave signals. The collection process involves 95 participants. In multi-user scenarios, up to 5 users walk simultaneously. The users can walk in fixed roads and freely.

MiliPoint [163] provides a large-scale mmWave radar-based human activity dataset. It consists of 11 users' data in identification, keypoint estimation, and action classification.

We summarize the reviewed mmWave radar datasets in Table III. The hardware devices that each dataset is collected

TABLE III
COMPARISON OF MMWAVE RADAR DATASETS

Dataset	Device	Data representation	Objective	Setting	Data composition
nuScenes [150]	TI AWR1443 & cameras & lidar	Multimodal	Autonomous driving	Road	1000 scenes, 3D bounding boxes for 23 classes and 8 attributes
ColorRadar [151]	TI AWR1843 & lidar & IMU	Multimodal	Autonomous robots	Lab, large buildings, urban walkways, mine	2 of 6D pose data across 52 datasets
Wang et al. [152]	Unspecified	Vehicle trajectory data	Autonomous driving	Freeways	4 freeways' trajectory data
3DRIED [153]	TI IWR1443 & camera	Echo data & imaging results	Near-field safety inspection	Unspecified	81 raw echo data and 2.8mm × 2.8mm × 3.75cm resolution
Gambi et al. [154]	TI AWR1642	Raw data	Walking activity monitoring	Hallway in university	6 activities, 29 subjects, 231 acquisitions
RadHAR [71]	TI IWR1443	Point cloud	Activity recognition	Indoor environment	5 activities of 2 users
HuPR [155]	TI IWR1843	Raw data	Pose estimation	Indoor environment	Horizontal and vertical frames, 141,000 triplets in 235 sequences
MARS [156]	TI IWR1443 & Kinect	Point cloud	Human pose estimation	Indoor environment	4 users, 10 activities
mri [157]	TI IWR1443 & RGB-D & Inertial sensors	Point cloud	Human pose estimation	Indoor environment	20 users, 160k frames
mmBody [158]	Phoenix radar of Arbe Robotics & Kinect	Point cloud	Human pose estimation	Indoor environment	100 motions, 20 volunteers, 6 environments
mmMesh [159]	TI AWR1843 & VICON	Point cloud	Human mesh construction	Indoor environment	20 users, 8 activities
M-Gesture [160]	TI IWR1443	Point cloud	Gesture recognition	Indoor environment	144 users, 54,620 instances, different blockage
Mimogr [161]	Unspecified	Raw data	Gesture recognition	Indoor environment	7 gestures of 10 users (dataV), 2 from different environments and random users(dataS)
mHomeGes [86]	TI IWR1443	Point cloud	Gesture recognition	Indoor environment	25 users, 10 arm gestures
Pantomime [162]	TI IWR1443	Point cloud	Gesture recognition	Indoor environment	41 users, 21 gestures
mmGait [97]	TI IWR1443 & TI IWR1843	Point cloud	Gait recognition	Indoor environment	95 users, 5 simultaneous users
MiliPoint [163]	TI IWR1843	Point cloud	Activity recognition	Indoor environment	11 users for identification, key-point estimation, and action classification

based on are given. We present data representation of each dataset, such as multimodal data, point cloud, raw data, etc. We summarize the objective of constructing each dataset to directly indicate which field this dataset can be used. The environmental settings when collecting data are given. Finally, the data composition of each dataset, i.e., the number of participants, number of types, etc., are summarized. The table of mmWave datasets gives a direct and comprehensive understanding of the currently available dataset, which can help researchers acquire resources quickly.

C. Evaluation Metrics

To effectively evaluate mmWave radar sensing works, various evaluation metrics have been proposed for different sensing applications. These evaluation metrics provide researchers with a critical criterion to judge the quality of each work, which is an important element in sensing applications.

Accuracy is one of the bases to evaluate the capability of recognition-related works. It is usually calculated by the

probability that a target is correctly recognized as the target itself rather than other types of targets. As a simple but intuitive evaluation metric, accuracy has been widely utilized in object detection accuracy [166], human activity recognition [167], gesture recognition [168], speech recognition [98], user authentication [169], etc. By obtaining the mean/average accuracy expressed by percentage, the performance of the designed application systems in recognizing specific targets can be directly inferred.

Precision and recall are two evaluation metrics that usually appear in evaluating classification models. Precision measures the proportion of true positives (TP) among all the instances that the model classified as positive (TP+FP). Precision measures how many of the positive predictions made by the model are actually correct. Recall, on the other hand, measures the proportion of true positives among all the instances that are actually positive (TP+FN). It measures how many of the positive instances in the dataset are correctly identified by the model. Therefore, precision and recall are widely used in object detection works to judge the probability

that the object is accurately detected [164], [165], [170]. Besides, mean average precision (mAP) is commonly used with Intersection over Union (IoU) to evaluate object detection capability. IoU is the ratio of the area of overlap and area of the union between the predicted box and ground-truth box, which is used to judge true positive or false positive [171], [172].

In motion estimation tasks, errors are an important evaluation metric. Errors are typically defined as the difference between the estimated values and the ground truth values. Hence, they are naturally suitable to reveal the capability to accurately estimate different motion parameters. For example, in radar-based motion estimation works [142], [173], rotation errors, translation errors, velocity errors, drift errors, etc., have been widely applied to evaluate the motion estimation in different aspects compared to ground truth. In human pose estimation, errors are also important metrics to evaluate the performance in estimating the coordinates of human skeleton joints [50]. The errors in human pose estimation are usually presented in azimuth (X), elevation (Y), and depth (Z) to show the 3D pose estimation results. In addition, estimation errors can also be utilized in vital sign monitoring, such as heartbeat and respiration monitoring. The errors of estimating heartbeat rate per minute (bpm) and respiration rate per minute (rbm) describe the accuracy in monitoring the two types of vital sign with mmWave radars, which have been widely exploited in evaluating such work [174]. Moreover, in mmWave radar-based positioning, the positioning errors or tracking errors show the difference in coordinate between the estimated position and the real position, which are basic metrics for indoor positioning and tracking works [47].

False accept rate (FAR) and false reject rate (FRR) are commonly used for evaluating biometric systems, such as fingerprint recognition, face recognition, and voice recognition. The FAR represents the probability that the system incorrectly accepts an unauthorized person, and the FRR represents the probability that the system incorrectly rejects an authorized person. Therefore, the researchers in mmWave radar sensing also exploit the two evaluation metrics to evaluate the performance of user authentication [104], [175].

The signal-to-noise ratio (SNR) is an important metric to evaluate the quality of synthetic speech. It is defined as the ratio of signal power to noise power and is usually expressed in decibels (dB). SNR has been widely employed in mmWave radar-based speech synthesis works [101], [117]. Besides SNR, Mel-Cepstral distortion (MCD) is another metric of speech synthesis quality. Researchers in mmWave radar sensing employ MCD to measure the spectral difference between synthetic speech signals and real speech signals for evaluating speech synthesis capability [114], [115], [176].

D. Summary and Insights

In this section, we review three crucial components in implementing mmWave radar sensing, i.e., radar devices, public datasets, and evaluation metrics. These components play vital roles in advancing future research design and evaluation.

Radar devices serve as the hardware foundation for transmitting and receiving signals with mmWave radars. The design

of radar devices significantly influences sensing capabilities. For instance, the number and configuration of antennas directly impact the resolution of angle estimation. Both commercial corporations and academic researchers meticulously design radar devices to meet the requirements of specialized sensing applications. The devices have been manufactured with the characteristics of specialization and complication, which has become a popular tendency for mmWave radars.

mmWave radar datasets play a crucial role in the development and evaluation of mmWave radar sensing applications. These datasets provide researchers with real-world data to implement systems and evaluate algorithms more effectively. Recent efforts in mmWave sensing have led to the release of numerous public datasets tailored for different sensing tasks. This availability alleviates the burden of data collection and facilitates fair evaluation of sensing applications. New researchers are encouraged to leverage public datasets to validate their work, and the community welcomes the creation of more datasets for a wider range of sensing tasks.

Evaluation metrics are indispensable for assessing the performance of designed sensing applications. Researchers carefully select appropriate metrics tailored to specific sensing tasks to ensure fair and comparable evaluation results. These metrics enable researchers to quantitatively evaluate the accuracy and robustness of sensing systems, which facilitates advancements in mmWave radar sensing technology.

Radar devices, datasets, and evaluation metrics are essential tools that support the deployment and development of mmWave radar sensing applications. As new application scenarios emerge, we expect to witness advancements in hardware designs with enhanced sensing capabilities and the continued expansion of public datasets.

VI. SENSING APPLICATION TAXONOMY

A great diversity of mmWave radar sensing applications are designed for different scenarios. As a result, a taxonomy for the sensing applications is highly desired. The taxonomy can not only enhance the understanding of sensing applications but also reveal the commonalities and connections between different applications. From the perspective of application scenarios, this survey categorizes mmWave radar sensing applications into three major categories, i.e., **Automotive Applications**, **Smart Home Applications**, and **Industrial Applications**. The three major categories represent three typical scenarios of autonomous driving, human daily life, and industrial manufacture respectively, which cover most sensing-driven scenes. The property of different mmWave radar-based sensing applications is shown in Fig. 8.

A. Automotive Applications

Utilizing radars to sense the environment for automotive driving is an original task in mmWave radars. Hence, automotive applications have been widely studied by academic researchers and industrial practitioners, and lots of

Application	Object	Basic Approach	Evaluation Metric
Automotive Applications	Object Detection Obstacle/Automobile	Localizing bounding box	Detection Precision
	Ego-motion Estimation Automobile/Robot	Estimating motion parameter	Estimation Error
	SLAM Robot/Environment	Estimating the map	Estimation Error Reconstruction Error
	Activity Recognition Human Activity	Classifying human activity	Recognition Accuracy
	Pose Estimation Human Body Pose	Estimating position of skeleton joint	Estimation Error
	Gesture Recognition Human Hand Gesture	Classifying & estimating gesture	Recognition Accuracy Estimation Error
Smart Home Applications	Speech Recognition Human Voice/Audio	Classifying & generating voice content	Recognition Accuracy Speech Quality
	Vital Sign Monitoring Breathing/Heartbeat	Estimating chest or skin's movement	Breathing/Heartbeat Rate Estimation Error
	User Authentication Behaviors/Biometrics	Classifying human identity	Authentication Accuracy FAR&FRR
Industrial Applications	Indoor Positioning Human Location	Estimating location of target	Positioning Error Tracking Error
	Industrial Imaging Machine/Object	Generating heatmap of target	Estimation Error Accuracy
	Industrial Measurement Equipment/Phenomenon	Measuring physical parameters	Measurement Error Accuracy
	Environmental Monitoring Weather/Living matter	Measuring physical parameters/imaging	Prediction accuracy Detection accuracy

Fig. 8. The property of different mmWave radar-based sensing applications. These applications are categorized in terms of object, basic approach, and evaluation metrics.

commercial products are already available. In automotive-related scenarios, 1) *Object Detection* that utilizes mmWave radars to sense and detect various vehicles, pedestrians, and roadblocks is an important task. A typical workflow of object detection is to first derive point clouds or heatmaps based on mmWave signals, and then localize the bounding box of target objects. Accuracy or precision are the main criteria that value the applications' performance. Besides, the respective strength of mmWave radars and cameras also inspires many works fusing mmWave radars and cameras in object detection. 2) *Ego-motion Estimation* aims to estimate the motion parameters of vehicles or robots by the built-in mmWave radars. Localization, translational, and rotational errors are common evaluation metrics for mmWave radar-based ego-motion estimation systems. Besides, another application named 3) *Simultaneous Localization and Mapping (SLAM)* is also an important component in automotive applications. SLAM lays more emphasis on building a map

of the target and environment compared to only localization. The criteria to judge SMAM works mainly include estimation errors, reconstruction errors, etc.

B. Smart Home Applications

The integration of RF modules of mmWave and IoT devices in indoor environments has facilitated many smart home applications. These applications mainly provide human-centric services ranging from user monitoring to security surveillance in indoor environments. 1) *Activity Recognition* refers to using mmWave signals to sense various human daily activities (e.g., walking, eating, and typing) and classifying the type of activity, which plays a key role in smart homes. Recognition accuracy is a major evaluation metric for human activity recognition. Similar to activity recognition, 2) *Pose Estimation* also focuses on human activities and can reconstruct the pose of a person. This is realized by estimating the coordinates

of a person's skeleton joints (typically 17, 19, and 25 joints) through the mmWave signals that sense the person's pose. Its evaluation metrics are usually estimation errors of each joint's coordinate in different axes. 3) *Gesture Recognition* is another important human-centric application, which can be realized by mmWave radar sensing technologies. The mmWave signals reflected by the hand can be processed to classify the type of gestures or estimate the location of the hand. Hence, recognition accuracy and estimation error are two main evaluation metrics. 4) *Speech Recognition* can also be realized by mmWave radar sensing. The mmWave signals reflected by the human mouth, throat, or a device's speakers capture specific vibration information, which can be utilized to recognize and recover the content of speeches. The evaluation metrics for speech recognition are mainly recognition accuracy and speech quality, such as the SNR and Mel-Cepstral distortion. 5) *Vital Sign Monitoring* is a healthcare-related application that can estimate respiration and heartbeat activities. Using mmWave radars is able to sense the movement of human chest or skin, therefore providing the foundation to estimate the circle rate of vital sign activities. The breathing rate and heartbeat rate are two typical evaluation metrics in mmWave radar-based vital sign monitoring. 6) *User Authentication* based on mmWave radars can provide a ubiquitous and contactless security protection manner by wireless sensing. This is realized by extracting behavioral or biometric features of the user and classifying identity labels using machine learning techniques. The evaluation metrics mainly include authentication accuracy, FAR, and FRR. 7) *Indoor Positioning* is a fundamental function in smart homes, which can be carried out by mmWave radar sensing due to the range and angle information estimated by FMCW techniques. Positioning errors or tracking errors are common evaluation metrics for mmWave radar-based indoor positioning.

C. Industrial Applications

mmWave radars also act as sensors to assist in building industrial applications or acquiring sensing information for industrial systems. The radars have the strength of high sensing capability, privacy-preserving and low cost. Hence, mmWave radars are suitable to replace some traditional sensors in some scenarios, such as imaging in privacy-sensitive scenes. Also, the characteristic of low cost makes them widely equipped in factories to enable manufacture-assist applications. Many industrial applications have emerged in recent years, which can be classified by 1) *Industrial Imaging*, 2) *Industrial Measurement* and 3) *Environmental Monitoring*. *Industrial Imaging* refers to utilizing mmWave radars to derive spatial information (such as azimuth and elevation angles) and generating images that describe the target. The imaging based on mmWave radars is an alternative to other sensors. It expands the usage scenarios under barriers and poor weather compared to cameras, and achieves high sensing capability with capable sensing ranges. Hence, the imaging applications are designed in various industrial scenarios such as parking lots, mine environments, etc. Estimation error and accuracy are two typical evaluation metrics in industrial imaging.

Industrial Measurement is another important application scenario in the industry. Since the signals are with millimeter-level wavelength and centimeter-level range estimation capability, mmWave radars are naturally utilized to measure physical parameters with high accuracy in industrial systems. The measurement of various physical parameters has led to many novel industrial applications. The metrics to evaluate these industrial measurement applications mainly include measurement errors and measurement accuracy. *Environmental Monitoring* refers to utilizing mmWave radars as environmental sensors to monitor weather, soil, liquid, or detect insects. The monitoring of weather conditions is particularly realized by joint radar and communication, which helps climate prediction and agricultural production. It typically involves exploiting the effect of environmental changes such as rain and clouds on mmWave communication links. Prediction accuracy or detection accuracy are common evaluation metrics.

VII. MMWAVE RADAR SENSING APPLICATIONS

Nowadays have witnessed the emergence of mmWave radar sensing applications deploying in different scenarios. The applications mainly involve the use of mmWave signals to detect, identify and monitor targets in the environment to achieve the perception of the physical world. Based on the perception of the physical world, mobile devices and smart facilities can be given more intelligent capabilities to serve humans. Together with more mmWave radars appearing in different scenarios including autonomous vehicles, smart homes and industry, the applications and related studies also increase rapidly. In this section, we give a comprehensive review of the emerging mmWave radar sensing applications.

A. Automotive Applications

As common sensors deployed in various vehicles, mmWave radars have been extensively utilized to realize detection, ranging, and localization for vehicles. The combination of mmWave radars, lidars and cameras now is boosting the realization of automatic driving. The automotive applications can be further divided into *object detection*, *ego-motion estimation*, and *SLAM*.

1) *Object Detection*: The purpose of object detection is to detect the existence of targets in the sensing region, which is also called semantic segmentation in much literature. Utilizing the range estimation capability enabled by the FMCW technique, mmWave radars can provide a weather-robust detection of objects, which plays an important role in automatic obstacle avoidance. Therefore, many works employ mmWave radars for object detection in many application scenarios, such as automatic driving and unmanned aerial vehicles (UAVs). Fig. 9 shows the basic idea of object detection with mmWave radars for automobiles. Object detection can be realized by using only mmWave radars or fusing mmWave radars with other sensors such as cameras.

The radar-only works develop different methods including grid mapping and deep neural networks to detect objects using only mmWave radars. The grid maps are accumulated by multiple frames of data, and the segmentation for grid maps

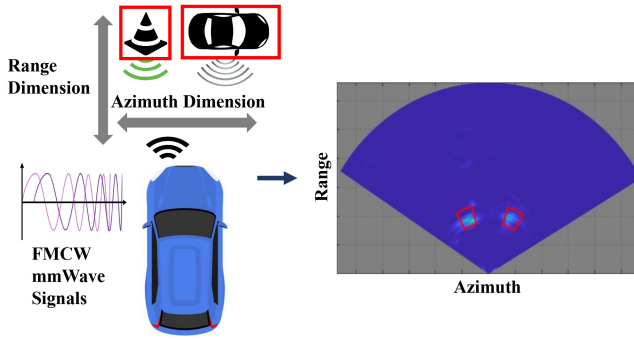


Fig. 9. Detecting objects based on mmWave radars in automobiles with FMCW techniques.

can detect different objects. For example, the point clouds of mmWave radar that capture environmental information can generate grid maps [166], [177]. Applying image-processing methods on these grid maps can detect different objects, realizing mmWave radar data-based object detection. Other works rely on deep neural networks for object detection with radar point clouds. For instance, a deep neural network incorporating multi-scale grouping module (MSG) and feature propagation module (FP) are proposed in [126]. With the whole radar point cloud as input, it releases the requirement of clustering algorithms and manually selected features in object detection. Scheiner et al. [178] propose recurrent neural network ensembles based on one-vs-all correction classifiers, which achieves more accurate performance in identifying novel classes. Huang et al. [179] use two mmWave radar sensors for accurate object detection and tracking. They particularly focus on two noise reduction stages to reduce noise and distinguish cluster groups. The system is able to visualize the objects' information acquired by one radar on another radar. Tan et al. [180] focus on 4D mmWave radars, in which the elevation can be used to provide valuable sensing information. They propose a 3D object-detection framework based on multi-frame 4D mmWave radar point clouds. The relative velocity is utilized as compensation to construct multi-frame mmWave point clouds for object detection.

A number of works fuse mmWave radars and cameras together to enable object detection in automotive driving. The fusion of mmWave radars and cameras provides sight for objects in poor visibility and illumination where cameras could fail. A pioneer work [150] presents a dataset named nuScenes constructed by mmWave radars, cameras and lidar. Based on the dataset, the following works develop different methods to achieve precise object detection. For example, Nobis et al. [164] propose a CameraRadarFusionNet (CRF-Net) to automatically learn the most beneficial level of fusion. They leverage a Dropout-based learning strategy for learning on a specific sensor type, which enables better performance than the image-only method. Another work [165] proposes a spatial attention fusion (SAF) method to detect objects. The method embeds the features of mmWave radar and vision in the feature-extraction stage, and a deep learning framework is finally used for objective detection. Besides, Dong et al. [181] explore feature-level interaction and global

reasoning by deep representation learning. With a loss sampling mechanism and an innovative ordinal loss, this work addresses imperfect labeling and enables critical human-like reasoning. RODNet [182] designs a deep radar object detection network, which is cross-supervised by fusing camera and radar without laborious annotation, to detect objects from the radar spectrums. A deep learning object detection network MS-YOLO [139] is proposed to make radar information and visual information at the same scale. milliEye [172] aims to adapt to new scenes with only small labeled images or radar data. It designs a learning-based fusion and a novel decoupling architecture to robustly detect objects on edge platforms, enabling performance gains over only image-based object detectors while generating lower computing overhead on edge platforms. Sengupta et al. [183] focus on a decision-level fusion of mmWave radars and cameras for robust multiobject classification and tracking. Some works focus on object detection in UAV scenarios. For example, mmWave radars and cameras can be fused in unmanned surface vehicles (USVs) [170] for detecting objects on the water surface. This work designs a novel representation format of mmWave point clouds, and leverages a deep-level multi-scale fusion of images and radar data to improve the accuracy and robustness of small object detection on water surfaces. mmWave radars and cameras can also be integrated into drones [171]. A drone fusing the two sensors can address the aggravated sparsity and noise of radar point clouds, which enables object detection in poor weather and illumination conditions. A summary of mmWave radar-based object detection works is given in Table IV.

2) *Ego-Motion Estimation*: Ego-motion estimation is a technology that estimates a device's motion using the information captured by the device itself. The technology originates from computer vision, which is developed to estimate the motion of a camera itself by the captured visual information. It is essential for navigation and interaction with the environment. Since the signals can capture environmental information, ego-motion estimation using mmWave radars has become an attractive topic and plays an important role in autonomous vehicles, robotics, etc. Fig. 10 shows the illustration of estimating a vehicle's ego motions by radars.

mmWave radars work under variable illumination and atmospheric conditions and can detect long-range surroundings, which is a promising solution for automobiles' ego-motion estimation. Ghost objects are a common issue in radar-based ego-motion estimation. To address the reflection of ghost objects, Cen and Newman [142] utilize a landmark extraction method and design a radar-only scan matching algorithm to robustly estimate ego-motions under different rotations and large translations. It achieves robust ego-motion estimation under various conditions that visual odometry and GPS/INS could fail. A following work [143] further designs a gradient-based, one-parameter keypoint extraction algorithm. The algorithm makes ego-motion estimation highly robust to radar artifacts (e.g., speckle noise and false positives) with only one input parameter. Manzoni et al. [185] analyze the effects of trajectory estimation errors induced by navigation in terms of defocusing and wrong targets' localization. The

TABLE IV
COMPARISON OF MMWAVE RADAR-BASED OBJECT DETECTION WORKS

Work	Type	Device	Key method	Performance
Prophet et al. [166]	Radar-only	79GHz radar	Semantic segmentation networks SegNet and U-Net	Overall accuracy of 95 and 90%
Lombacher et al. [177]	Radar-only	76GHz radar	Cell level classification & CNN	True positive rates of 80% with limited training data
Schumann et al. [126]	Radar-only	77GHz radar	Multi-scale grouping module & feature propagation module	Accuracy of 88.1% for cars
Scheiner et al. [178]	Radar-only	77GHz radar	RNN ensembles & one-vs-all correction	Final score of 91.46% for 6 class
Huang et al. [179]	Radar-only	TI IWR1642	Density-based clustering & Unscented Kalman Filter	Clustering accuracy of 84% to 99%
Tan et al. [180]	Radar-only	4D radar	Velocity compensation & point-cloud-detection network	3D average precision of 29.36 for cars
Nobis et al. [164]	Sensor fusion	77GHz radar & camera & lidar	CRF-Net & Dropout-based learning strategy	Mean average precision of 55.99%
Chang et al. [165]	Sensor fusion	77GHz radar & camera & lidar	Spatial attention fusion & generation model	Average precision(100) of 72.4
Dong et al. [181]	Sensor fusion	mmWave radar & camera	Deep representation learning & loss sampling mechanism	F1 score of 92.2%
RODNet [182]	Sensor fusion	77GHz radar & camera	M-Net & temporal deformable convolution & CRF supervision framework	Average precision of 86% and average recall of 88%
MS-YOLO [139]	Sensor fusion	ARS 408-21 & camera	Double backbone network	Mean average precision of 0.888 for large model and 0.841 for small model
milliEye [172]	Sensor fusion	TI IWR6843 & camera	Box proposal aggregation and box refinement	Improvement of 5.5 mean average precision with IoU of 0.5
Cheng et al. [170]	Sensor fusion	TI AWR1843 & camera	Encoding & attention-based deep learning	Average precision 90.05% with IoU of 35%
Sengupta et al. [183]	Sensor fusion	TI AWR1843 & camera	Decision-level fusion & tri-Kalman filter	Accuracy of 75.83% and precision of 0.26m
Deng et al. [171]	Sensor fusion	TI IWR6843 & camera	Saliency area extraction & parallel transmission and inference	Mean average precision of 96.51% with IoU of 0.5
Zhang et al. [184]	Sensor fusion	TI AWR1642 & camera	Fusion-extended Kalman filter	Range accuracy of 0.29m and angular accuracy of 0.013rad

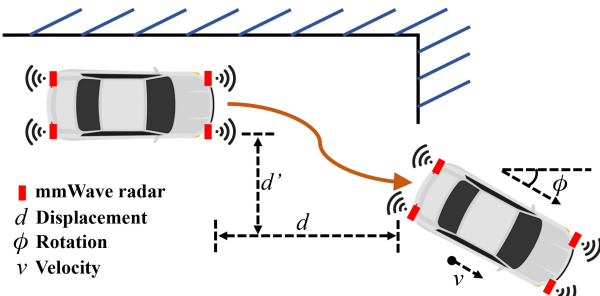


Fig. 10. Ego-motion estimation based on mmWave radars for automobiles.

work designs a motion estimation and compensation system leveraging stationary ground control points (GCPs) in low-resolution radar images, which allows obtaining cm-accurate images of urban environments for ego-motion estimation of vehicles. A probabilistic approach [186] can also be employed to address unstable and phantom measurements and a high rate of outliers in ego-motion estimation. Zeng et al. [187] try to solve radar odometry algorithm invalidation caused by radar velocity ambiguity. They study a joint velocity ambiguity resolution and ego-motion estimation radar odometry method. A signal model for the radar odometry is first built and then

an angle-velocity point cloud clustering algorithm is designed. With the proposed method, they can estimate vehicle poses in the presence of velocity ambiguity. The coherent synthetic aperture radar (SAR) imaging problem is closely related to ego-motion estimation. Therefore, researchers also study improving the resolution of mmWave radar-based imaging in automotive applications [188], [189].

Despite the success in automotive scenarios, indoor ego-motion estimation is also developed to enable location-based services of robots. For example, a mmWave radar can work with an Inertial measurement unit (IMU) together in a system Milli-RIO [190] to estimate six-degrees-of-freedom ego-motion. The system designs a point association technique to match the sparse measurements of mmWave radars, and realizes model-free motion dynamics estimation for indoor environments. Others mainly rely on the power of deep learning to realize indoor ego-motion estimation for mobile agents. For example, a deep learning method milliEgo [173] is proposed to perform robust ego-motion estimation. This work is distinguished by a DNN-based odometry approach to reliably estimate ego-motion from the sparse and noisy data, and a two-stage cross-modal attention layer to promote complementary sensor behaviors in the wild. The comparison of these works is given in Table V.

TABLE V
COMPARISON OF MMWAVE RADAR-BASED EGO-MOTION ESTIMATION WORKS

Work	Device	Key method	Target	Performance
Cen et al. [142]	Navtech CTS350-X	Scan matching & landmark extraction	Automobile	Median error of 0.106 m/s in translation and 0.321 deg/s in rotation
Cen et al. [143]	Navtech CTS350-X	Gradient-based one-parameter keypoint extraction	Automobile	Scan matching accuracy of approximately 5.20 cm and 0.0929 deg
Manzoni et al. [185]	TI AWR1243	Motion estimation and compensation based on stationary GCPs	Automobile	Velocity estimation accuracy of 1.08m/s and 3.06m/s for X and Y
Haggag et al. [186]	TI AWR1843	Probabilistic approach	Automobile	N/A
Zeng et al. [187]	TIMMWCAS radar	Radar odometry signal model & point cloud clustering	Automobile	Average translation error of less than 0.28 m
MIMO-SAR [188]	TI AWR1843	Time-domain backprojection SAR	Automobile	Average run time of 1.17s per frame
Steiner et al. [189]	77GHz FMCW radar	Multi-sequence SAR	Automobile	Subapertures of up to 64λ
Milli-RIO [190]	TI AWR1843 & IMU	Unscented KF & RNN	Moving radar	Translational error of 2.57cm and rotational error of 1.38°
milliEgo [173]	TI IWR6843	DNN-based odometry	Robot	3D absolute trajectory error of 0.814m and drift error of 1.3%
Meiresone et al. [191]	TI IWR1443	Key point matching & extracting loop closures	UAV	Relative trajectory yaw error between 2° and 5°
Cho et al. [192]	79GHz radar	Deep Complex-Valued Network	Automobile	N/A

3) *SLAM*: Some works pay more attention to simultaneous localization and mapping (SLAM) using mmWave radars, which can reconstruct an environment and localize target objects. SLAM refers to the process of building a map of the surrounding environment while simultaneously localizing the sensor. SLAM has many applications in robotics and autonomous systems, including self-driving cars, drones, mobile robots, and augmented reality, which has aroused research interest in mmWave radar sensing.

To map sparse mmWave signal reflections to an environment for constructing a dense grid map, milliMap [116] combines lidar and geometric priors with cross-modal supervision to train a reliable cGAN that can construct fine-grained and dense maps. With dense grid maps, it can identify and localize objects with spectral responses of mmWave signal reflections. Li et al. [193] propose a mmWave radar SLAM assisted by the radar cross section (RCS) feature of the target and inertial measurement unit (IMU). They combine IMU with continuous radar scanning point clouds into multi-scan to address the problem of small data volume. An improved correlative scan matching (CSM) method is proposed to match the radar point cloud with the local submap of the global grid map, realizing the tight coupling of localization and mapping. Another work [194] focuses on robots' ego-motion, especially the rotation angle and velocity. The rotation is estimated using the correlated distribution of detected points on a 2D plane at successive time instants, while the velocity is estimated by the trend line of the detected points on the 2D plane. Park et al. [195] composite two orthogonal mmWave radars for 3D ego-motion estimation. They introduce a radar instant velocity factor for pose-graph SLAM framework and solve for 3D ego-motion in the integration with IMU, which is effective in estimating general 3D motion indoors and outdoors under various visibility and structures. The multipath effect of mmWave signals can be exploited for positioning indoor electronic devices [196]. By establishing the correlation between multipath characteristics and the 3D position of

targets, the objects in an environment can be detected and localized. Besides, configuring the transmission mode of mmWave radars is another feasible way for accurate indoor mapping. For example, a dual-mode mmWave radar sensor is designed in [197], which alternately transmits two waveforms of different bandwidths to enable long-range and short-range detection respectively. With the range detection capability, the radar obtains surrounding information and the radar-equipped robot's motions to map the environment. Li et al. [199] aim to address radar false detections caused by multipath scattering in closed environments. They study radar multi-path scattering theory and propose a radar azimuth scattering angle signature. Different radar false detection revising methods based on correlative scan matching are designed to eliminate radar false detections. Aladsani et al. [200] design a merging scheme of mmWave imaging and communication. They propose to estimate the AoA and ToA of dominant channel paths, and project the estimated AoA and ToA information on the 3D mmWave images to achieve sub-centimeter SLAM. mmWave radar-based SLAM works are summarized in Table VI.

B. Smart Home Applications

mmWave radars now have stepped into home environments. Utilizing the radars to sense humans can facilitate the integration of users and smart homes, providing users with greater convenience, comfort, and security in daily life. Hence, they have become a promising enabler for smart homes and yielded a number of smart home applications, which can be further categorized as *activity recognition*, *pose estimation*, *gesture recognition*, *speech recognition*, *vital sign monitoring*, *user authentication*, and *indoor positioning*.

1) *Activity Recognition*: Human activity recognition (HAR) plays a critical role in supporting a wide range of smart home applications including human-computer interaction, elder care, security monitoring, etc. As a contactless sensing manner, mmWave radars can capture human behaviors

TABLE VI
COMPARISON OF MMWAVE RADAR-BASED SLAM WORKS

Work	Device	Key method	Scenario	Performance
milliMap [116]	TI AWR1443	Conditional GAN	Indoor	Map reconstruction error below 0.2m and object classification accuracy of 90%
Li et al. [193]	77GHz mmWave radar	Improved correlative scan matching	Automobile	N/A
Lim et al. [194]	62GHz radar	Matrix transformation	Indoor	Rotation estimation error of 3° and ego-velocity error of 0.073m/s
Park et al. [195]	TI IWR1443	Radar instant velocity factor	Indoor	3D translational error of 1.59m and rotational error of 17.66 deg
Hao et al. [196]	TI IWR1642	Multi-order reflection model	Indoor	3D positioning error within 15cm
Lee et al. [197]	62GHz radar	Dual-mode transmission	Indoor	Localization error of 5%
Yang et al. [198]	TI AWR1443	Inversely solving rotation-translation matrix	Indoor	N/A
Li et al. [199]	ARS408-21 radar	Azimuth scattering angle signature	Tunnel	improves the positioning accuracy by 20% compared with CSM
Aladsani et al. [200]	mmWave synthetic aperture radar	Synthetic aperture-based imaging & uplink pilot signaling	Outdoor	Resolve geometry of surroundings and localize with sub-centimeter accuracy

leveraging signal reflections from human body. By integrating signal processing techniques and machine learning techniques, sensing systems can predict the types of human activities.

A number of works utilize mmWave radar signals to train a learning model as a classifier for activity recognition, which does not rely on any other datasets from different data sources. The first step of a typical activity recognition system is to obtain the point clouds of mmWave radar data [71], [99], [128], [167], [201], [202], which are usually sparse and noisy. To process the point clouds and extract effective representations, RadHAR [71] designs sliding time windows to accumulate the sparse and non-uniform point clouds, and generate voxelized representation based on the point clouds. m-Activity [201] extracts human-oriented movements from the noisy point clouds by acquiring user location and voxelizing close ambient areas in complex environments. MMPPoint-GNN [128] processes sparse point clouds by a GNN-based deep learning model with dynamic edges. A modified voxelization approach is designed in [99] to process the spatial-temporal point clouds, and the symmetry property of radar rotations is utilized to enrich the sparse data. The fusion of point clouds and range-Doppler profiles are proposed in [167] to compensate for the sparsity and noise by multi-model deep learning. Besides point clouds, the spatial-temporal heatmaps [90], range-Doppler heatmaps [202], and range-angle-velocity heatmaps [203] generated by range, Doppler and angle are also utilized to represent human activities in mmWave signals.

With the processed data representations of signals, activity recognition systems further construct classifiers, which are usually deep neural networks. CNNs, RNNs, and their combinations are widely adopted for activity recognition due to their capability in processing spatial and temporal mmWave data. For example, CNN-LSTM deep learning model [71], CNN-GRU-based HARnet [201], Dual-view CNN [99], CNN-LSTM multi-model learning [167], deep CNN [90], [92], GRU [202], etc., are designed to extract the spatial body features from convolutional operation or temporal motion features from recurrent structure for activity recognition. In addition, MMPPoint-GNN [128] designs a GNN model with

bidirectional LSTM to leverage temporal information for activity recognition.

Some works propose to utilize existing labeled data in different data sources (e.g., vision or inertial measurement unit (IMU)) to aid the training process of deep neural networks, which aims to reduce the heavy training burden in activity recognition. For example, Vid2Doppler [100] synthesizes mmWave radar data from videos. By designing an encoder-decoder-based pipeline for synthetic Doppler data generation, Vid2Doppler reduces the burden of training with the help of massive video datasets. IMU2Doppler [204] combines IMU datasets of smartwatches and mmWave data to build an activity recognition model. It designs cross-modal domain adaptation where the IMU data acts as the source domain and Doppler data acts as the target domain. The cross-modal approach leads to a low-cost training process that only requires a small amount of mmWave data. mmWave radar-based activity recognition works are summarized in Table VII.

2) *Pose Estimation*: Human pose estimation refers to estimating the location of a person's skeleton joints to reconstruct the human pose. Pose estimation visually reveals a person's behaviors as the person stands, moves, walks, or sits, which supports numerous application scenarios involving human activities, such as athletic training, motion-sensing gaming, virtual reality (VR), etc. mmWave signals can capture human torso and limb movements. With deep learning techniques, the signals can be mapped into the coordinate of human skeleton joints, which realizes human pose estimation. An illustration of mmWave radar-based pose estimation is shown in Fig. 11.

Some studies aim to accurately estimate a single person's pose under a specific environment and location. The performance of pose estimation mainly depends on the design of neural network models. Hence, the researchers focus on constructing appropriate neural networks to accurately predict the coordinates of human skeleton joints. A widely employed neural network for mmWave radar-based pose estimation is CNN, which takes convolutional operations to extract spatial feature representation for human postures. For example, mm-Pose [205] designs a forked CNN to extract skeletal features from radar-to-image representations to estimate the

TABLE VII
COMPARISON OF MMWAVE RADAR-BASED ACTIVITY RECOGNITION WORKS

Work	Data domain	Device	Data representation	Key method	Performance
RadHAR [71]	mmWave	TI IWR1443	Point cloud	CNN-LSTM deep learning model	Accuracy of 90.74% for 5 daily activities.
m-Activity [201]	mmWave	TI IWR1443	Point cloud	CNN-GRU-based HARnet	Accuracy of 91.52% for 5 daily activities.
mmPoint-GNN [128]	mmWave	TI IWR1443	Point cloud	GNN with bidirectional LSTM	Accuracy of 96.97% for 5 daily activities.
Yu et al. [99]	mmWave	TI IWR1443	Point cloud	Dual-view CNN	Accuracy of 98% for 7 daily activities
Huang et al. [167]	mmWave	TI IWR1843	Point cloud& range-Doppler profiles	CNN-LSTM multi-model learning	Accuracy of 97.26% for 6 daily activities
Jin et al. [92]	mmWave	TI AWR1642	Point cloud	Deep CNN	Accuracy of 98.69% for 6 activities
mmEat [90]	mmWave	TI AWR1642	Spatial-temporal heatmap	Deep CNN	Accuracy of 97.5% for 5 eating behaviors
Abedi et al. [202]	mmWave	TI AWR1443	Range-Doppler heatmaps	GRU	Accuracy of 93% for in-home physical activities
Sheng et al. [203]	mmWave	TI IWR6843	Range-angle-Doppler heatmaps	Dynamic lightweight modules	Accuracy of 99.6% for 5 daily activities
Vid2Doppler [100]	mmWave&vision	TI AWR1642 & camera	Doppler profile	Encoder-decoder	Accuracy of 95.9% for 12 daily activities
IMU2Doppler [204]	mmWave&IMU	TI AWR1642 & smartwatch	Doppler profile	Cross-modal domain adaptation	Accuracy of 70% for 10 activities with 15s labeled Doppler data

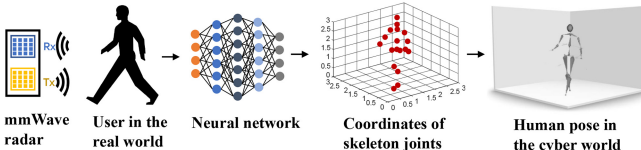


Fig. 11. A typical workflow of pose estimation using mmWave radars. The mmWave signals that sense a user's pose are fed into neural networks, and neural networks output the estimated coordinates of multiple skeleton joints to realize pose estimation.

coordinates of 17 skeleton joints. Mars [156] employs a CNN with 3D 5-channel stacked feature maps as the input, which can predict 19 skeleton joints in 3D spatial coordinates. Another CNN-based architecture [206] is designed with forward kinematics, which recalculates joint positions and improves stability in pose estimation for 25 joints. In addition to CNNs, another approach based on natural language processing (NLP) is proposed in mmPose-NLP [207] to enable pose estimation using mmWave signals. Through the analogy from key processing techniques in NLP, mmPose-NLP voxelizes radar point clouds and subjects multiple frames to a GRU-based encoder-decoder model, which extracts skeletal key points analogous to keywords in NLP. By converting the voxel indices back to real-world 3D space, mmPose-NLP achieves human pose estimation of 25 skeleton joints. Wei et al. [208] propose a human pose estimation method based on multi-angle mmWave data. They employ a transformer module between the encoder and decoder, and use a confidence refinement network to improve the position precision of human keypoints.

Other works pay more attention to addressing practical issues in complex usage scenarios, such as different indoor environments, different subjects, multi-user scenarios and body mesh construction. To enable pose estimation in complex environments with superimposed reflections, a two-branch

deep learning architecture is proposed in [209], where a global branch aims to reconstruct a global body pose and a local branch focuses on fining partial details of a human pose even under superimposed reflections. In this way, the local motion constraints of each part of a human body are incorporated into a global estimation of the whole human body, which describes more details of a human pose with 17 joints. mPose [210] focuses on mitigating the impact of environments and subjects in mmWave radar-based posture reconstruction. It dynamically localizes a user to remove environmental interference, and designs a domain adversary-based deep learning model to mitigate the impact of specific subjects, which can estimate 17 skeleton joints. In addition to single-user scenarios, multi-user pose estimation can also be achieved by mmWave radar sensing. m³Track [50] exploits range and angle information to separate multiple users on mmWave profiles, which extracts each user's spatial and temporal features. It then designs a forked-ConvLSTM to estimate skeleton joints and proposes a coordinate-corrected method to continuously track the position of each user. With the mapping between reconstructed skeletons and user positions, it realizes multi-user 3D human posture reconstruction and tracking with 17 skeleton joints. SynMotion [211] designs a vision-driven signal synthesis method to realize zero-shot learning activity recognition and few-shot learning skeleton tracking, achieving tracking body poses for multiple users with 19 skeleton joints. Besides the skeleton joint-based pose estimation, human mesh construction is also considered in the research community. mmMesh [159] designs a deep learning framework to estimate 3D human mesh using sparse mmWave point clouds. The proposed framework enables the alignment of the vertexes with corresponding body parts in complex scenarios and infers missing body parts through previous frames, which predicts a realistic and dynamic human mesh. A further work M⁴mesh [212] enables multi-user 3D mesh construction with a mmWave radar. To

TABLE VIII
COMPARISON OF MMWAVE RADAR-BASED POSE ESTIMATION WORKS

Work	Device	Key method	Scenario	Skeleton joints	Estimation error
mm-Pose [205]	TI AWR1642	Forked-CNN	Controlled settings & single-user pose	17 joints	3.2cm(X), 2.7cm(Z) and 7.5cm(Y)
Mars [156]	TI IWR1443	CNN	Controlled settings & single-user pose	19 joints	6.99cm(X), 6.54cm(Z) and 4.07cm(Y)
Hu et al. [206]	TI IWR6843	CNN	Controlled settings & single-user pose	25 joints	2.67cm(X), 4.65cm(Z) and 3.34cm(Y)
mmPose-NLP [207]	TI AWR1843	GRU-based encoder-decoder	Controlled settings & single-user pose	25 joints	2.68cm(X), 2.21cm(Z) and 2.37cm(Y)
Wei et al. [208]	TI IWR1843	Autoencoder & transformer module	Controlled settings & single-user pose	17 joints	Mean average precision of 59
Cao et al. [209]	TI AWR1843	Joint global-local network	Superimposed reflection & single-user pose	17 joints	2.433cm in average
mPose [210]	TI AWR1642	Deep regression with domain discriminator	Different environment and subject & single-user pose	17 joints	11.07cm(X), 1.68cm(Z) and 1.5cm(Y)
m ³ Track [50]	TI IWR1443	Multi-user separation & forked-ConvLSTM	Multi-user pose	17 joints	1.74cm(X), 3.25cm(Z) and 2.09cm(Y)
SynMotion [211]	TI IWR1443	Vision-driven signal synthesis & attention-based deep learning	Multi-user pose	19 joints	2.9cm(X), 3.2cm(Z), and 2.5cm(Y)
mmMesh [159]	TI AWR1843	Deep learning with anchor point module	Single-user mesh	N/A	2.47cm for human mesh
M ⁴ mesh [212]	TI AWR1843	Unet & ConvLSTM & deep learning	Multi-user mesh	N/A	3.72cm for human mesh
MI-Mesh [213]	TI AWR1443 & camera	Multi-modality fusion based deep learning	Single-user mesh	N/A	Mean average vertex error of 84.57mm

solve the occlusion problem, the work leverages information from previous frames to estimate users' meshes of current frame. In addition, fusing mmWave and image together for 3D human mesh construction is also studied [213] to work in dynamic motions and different conditions. The reviewed works in mmWave radar-based pose estimation are summarized in Table VIII.

3) *Gesture Recognition*: The human gesture is the basis to support human-computer interaction (HCI) applications including smart home control and mechanism operation. Using mmWave radars to sense human gestures provides a non-contact and non-intrusive human-computer interaction, which has attracted a great deal of research interest.

Due to the complexity and variability of actual HCI scenarios, mmWave radar-based hand gesture recognition faces a major challenge from various backgrounds, i.e., different environments, locations, orientations and subjects. This has prompted a large number of studies to focus on enhancing the capability of gesture recognition in various backgrounds. To enable gesture recognition in various backgrounds, some studies exploit the physical property of signals to build robust feature representations that stay consistent in different backgrounds. mHomeGes [86] designs a user discovery method to focus on the target human gestures, so that the feature representations could be robust to different locations, orientations and subjects. M-Gesture [160] proposes a pseudo representative model for mmWave signals, which can depict overall trajectory and structural skeleton changes to describe person-independent gestures. Another parameterized representation of the temporal space-velocity spectrogram is designed in [94] to represent hand gesture features of different data modalities. DI-Gesture [168] develops a mmWave data

augmentation framework based on correlations between signal patterns and gesture variations. With the framework, it can generate synthetic data to reduce data collecting burdens, enabling environment, locations and speed-independent gesture recognition. A GreBsMo algorithm is utilized in [214] to remove static backgrounds and clutters in signals, so that dynamic gestures can be described in an environment-independent way. The features in frequency ratio, motion range and detection coherence are utilized in [57] to eliminate the interference in unintended gestures. A robust intrinsic spectrogram is proposed in [215] to describe gesture motion patterns in variable locations, directions and speeds of gestures. It creates a virtual coordinate system and designs a coordinate transformation method to transform the signals into robust intrinsic spectrograms.

Others utilize the power of neural networks, especially deep learning techniques, to realize robust and reliable gesture recognition. A pioneer work [132] designs a deep CNN-LSTM model to enable fine-grained dynamic gesture recognition across users and sessions. Other CNN models, such as Deep CNN [91], 3D deep CNN [55], etc., are designed to learn embedded gesture features for gesture recognition. Besides CNNs, different deep learning models are also investigated in the research field for learning-based gesture recognition. For example, mmASL [216] takes advantage of the knowledge in the American sign language (ASL) domain and proposes a multi-task deep learning model to learn generalized feature representations, enabling environment-independent gesture recognition for ASL. Tesla-Rapture [217] develops a deep learning model consisting of temporal graph k-NN and self-attention message passing neural network (MPNN). The temporal graph

k-NN models the time-dimensional point clouds as temporal graphs, and the MPNN processes motion point clouds using graph convolution. Pantomime [162] utilizes sparse 3D point clouds to obtain high-resolution spatial and temporal information, and designs a deep learning model incorporating PointNet++ and LSTM to realize real-time gesture recognition. mTransSee [218] employs transfer learning techniques for training data adaptation, which can reduce training efforts of gesture recognition in adapting to new environments. mmGesture [219] focuses on semi-supervised learning for mmWave radar-based gesture recognition. It utilizes few labeled data in the source domain and large amounts of unlabeled data in the target domain, achieving domain-independent gesture recognition.

Different from gesture recognition which predicts the classification results of pre-defined gestures, the tracking for a hand or finger can quantitatively and visually describe hand motions. Hand tracking provides a more flexible capability to enable applications ranging from remote controlling, virtual keyboard, VR gaming, etc. Since a mmWave radar can spatially describe an object by revealing its relative range and angle, it becomes a feasible approach to track the movement of hands, fingers, or handheld objects. To track the movement of a hand, a mmWave radar needs to dynamically localize the position to form a moving trajectory of the hand, which is a small-scale localization problem. This can be solved by modeling the phase changes of mmWave signals to describe the displacement. Soli [220] leverages fine phase changes in mmWave signals to describe a moving hand, and combines instantaneous and dynamic information to enable location-robust hand tracking. mm4Arm [96] takes the phases of reflected mmWave signals from the forearm to estimate the movement of a hand. It observes that the muscles in the forearm activate the motion of the hand, so the reflections from the forearm can be used to estimate hand movement. Besides, deep learning-based approaches are also utilized in hand tracking. For example, a novel fully convolutional neural network (FCNN) [221] is designed to extract spatial and temporal features from mmWave signals to perform super-resolution localization of a hand, therefore realizing continuous hand motion tracking.

Similar to tracking a hand, tracking the movement of fingers or handheld objects also requires dynamic localization of spatial points to form moving trajectories. Some works rely on deep learning models to continuously track fingers' positions. For example, ThuMouse [58] designs a CNN-LSTM-based deep learning regressor to perform regressive tracking for fingers. Others exploit the phase of mmWave signals to build reliable tracking models. mTrack [222] models the phase changes caused by moving targets by removing background interference as well as counting and regenerating phases. With accurate phase changes, it can further track a writing pen precisely. Besides, using channel impulse response (CIR) to estimate the time of arrival (ToA) can also describe the location of targets. For example, mmWrite [223] utilizes ToAs in CIR and spatial information from digital beamforming to estimate spatial origin. With dynamic signal isolation, spatial refining and trajectory enhancement, it can passively track

a handwriting finger or pen. The summarization of gesture recognition works is presented in Table IX.

4) Speech Recognition: The recognition of human speech contents enables machines to receive and understand the requests from humans. As a fundamental function in artificial intelligence of things (AIoT), speech recognition facilitates many emerging AIoT applications, such as the voice-user interface (VUI) of smart devices. The voices generated by human or audio devices are usually accompanied by vibrations in the region where the voice is emitted. As shown in Fig. 12, human speeches cause movements in the mouth and throat region, which can be detected by mmWave signals. Through integrating machine learning techniques, the speech content can be recovered in mmWave signals. Hence, some studies exploit mmWave radars to aid the sensing of speech activities to enable robust and reliable speech recognition, i.e., human speech recognition. Others try to eavesdrop on voices from audio devices for voice attack, i.e., audio eavesdropping.

To recognize human speech, a feasible solution is to capture the vocal track's vibrations and exploit machine learning techniques to identify speech contents based on unique vibrations. For example, the vibrations of human throats can be utilized to recover human speech. WaveEar [101] localizes a speaker's throat to detect vibrations, and designs a Wave-voice Net composed of encoders and decoders to recover high-quality voices. Mouth movements [224] in speech activities can also be sensed by mmWave signals to enable silent speech recognition. The mouth movements cause phase changes in mmWave signals. By addressing phase ambiguity and linearly reconstructing the phase of speech, some specific speech contents are recovered [224]. The lip motion and vocal-cords vibration [225] could be combined together to enable multi-modal speech recognition. The researchers in mmMic propose cross-validation of lip motion and vocal-cords vibration, and utilize a multi-modal fusion framework for speech recognition. Wavoice [226] localizes a target speaker and detects the vocal vibrations and motions based on the fusion of mmWave and audio signals. With a fusion network to extract semantics, it realizes noise-resistant speech recognition. Another work mSilent [227] utilizes mmWave radars to realize silent speech recognition. The system extracts fine-grained articulatory features through a clustering-selection algorithm, which generates a multi-scale detrended spectrogram. A neural network model consisting of a multi-branch convolutional front-end and a Transformer-based back-end is designed to handle the complexity of the general corpus.

Furthermore, the surrounding objects vibrated by human speech activities can also be utilized to recover speech contents, which are robust to various user positions and postures. Since the surrounding objects are indirectly vibrated by human voice sources, challenges of low-SNR and distorted signals appear. To address the challenges, an incorporated design of common component extraction, signal superimposition and encoder-decoder network are proposed in AmbiEar [102] to guarantee the quality of signals for speech recognition. Besides, mmEcho [176] designs a phase calibration method to address these problems for obtaining high-quality signals reflected from surrounding objects. It can also release the

TABLE IX
COMPARISON OF MMWAVE RADAR-BASED GESTURE RECOGNITION WORKS

Work	Device	Data representation	Key method	Performance
mHomeGes [86]	TI IWR1443	Point cloud	User discovery & hidden Markov model	Accuracy over 95.3% for 10 multi-joint gestures
M-Gesture [160]	TI IWR1443	Range-Doppler image	Pseudo representation & EVL NN	Accuracy of 99% with 25ms latency for 5 gestures
Zhang et al. [94]	TI AWR1642	Temporal space-velocity spectrogram	CNN & ResNet	Accuracy of 93% for 6 gestures
DI-Gesture [168]	TI AWR1843	Dynamic range angle image	Data augmentation & CNN-LSTM	Accuracy of 99.18% for 6 gestures
Zhao et al. [214]	TI AWR1642	Range, Doppler, angle time map	GreBsmo & XGBoost classifier	Accuracy of 98.93% for 6 gestures
Liu et al. [57]	TI IWR 1642	Spectrums	Frequency ratio & decision tree	Accuracy over 90% for 6 gestures
Wu et al. [215]	TI AWR1443	Intrinsic spectrogram	Coordinate transformation & CNN	Accuracy of 88.4% for 10 gestures
Wang et al. [132]	Soli radar	Range-Doppler image	CNN-LSTM	Accuracy of 87% for 11 dynamic gestures
Smith et al. [91]	TI IWR1443	Range-angle profiles	DCNN	Accuracy of 93% for 3 gestures
Hazra et al. [55]	BGT60TR24 60-GHz radar	Range-Doppler image	k-NN & 3D DCNN	Accuracy of 94.5% for 6 gestures
mmASL [216]	60 GHz radio	Spatial spectrogram	CNN-based multi-task model	Accuracy of 87% for 50 ASL signs
Tesla-Rapture [217]	TI IWR1443	Point cloud	MPNN graph convolution	Accuracy of 98.71% for 5 gestures
Pantomime [162]	TI IWR1443	Point cloud	PointNet++ with LSTM	Accuracy of 95% for 21 gestures
mTransSee [218]	TI IWR1443	Point cloud	Transfer learning	Accuracy of 96.7% for 5 gestures
mmGesture [219]	IT mmWave radar	Range-angle-Doppler image	Semi-supervised leaning	Superior effectiveness for 6 gestures
Soli [220]	Soli radar	Range-Doppler image	Low level descriptor & RF	RMS displacement error of 0.43mm for moving velocities ranging from 20mm/s to 200mm/s
Liu et al. [96]	TI IWR6843	Phase	Encoder-decoder	Tracking error of 5.73° and 4.07mm
Smith et al. [221]	TI AWR1243	RMA image	FCNN	Tracking error of 8.5mm(Y) and 8.3mm(Z)
ThuMouse [58]	TI IWR 6843	Voxalized detected point	CRNN	Tracking MSE of 9.23 px ² (X), 23.6px ² (Y) and 64.4px ² (Z)
mTrack [222]	60GHz radio	RSS & Phase	Signal-phase model	Tracking error of 8mm for 90-percentile cases
mmWrite [223]	60GHz radio	CIR	CFAR & SPI & DCT	Tracking error of 2.8mm for 8m ² coverage

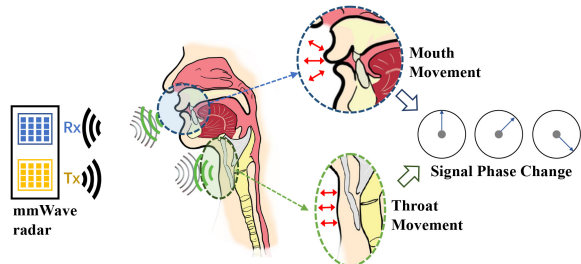


Fig. 12. The human speech causes movement in the mouth and throat region, which can be captured by mmWave signals in phase changes.

requirement of prior knowledge of audio signals and work under various sound-insulating materials.

Using mmWave signals can achieve voice eavesdropping of audio devices by detecting speakers' vibrations. A key enabler for audio eavesdropping is to accurately recover the audio contents using the signals. Hence, some studies exploit generative models to recover the audio or enhance the audio quality. For example, MILLIEAR [114], [115] detects fine-grained vibrations of a speaker by a virtual sub-chirp design, and proposes a conditional generative adversarial network (cGAN) to generate the audios from the vibrations. The generative model has no

vocabulary restrictions on the recovered audio. mmEve [117] addresses the motion interference problem in mmWave signals and utilizes GAN to improve the intelligibility in recovering speeches. mmPhone [228] proposes a multitarget adaptive fusion enhancement method to improve and guarantee the quality of recovered sounds. Besides, a problem in large-scale radar datasets is considered and addressed in mmSpy [98], by synthesizing large-scale mmWave data using a synthetic model. In addition to vibrations caused by audio devices, a new feature in mmWave signals, i.e., the piezoelectric film in mmWave band, is exploited in another mmPhone [229]. The property of piezoelectric films changes with sound pressure due to the piezoelectric effect, so it can be utilized to recover speeches from a loudspeaker. The reviewed speech recognition works are summarized in Table X.

5) *Vital Sign Monitoring*: Healthcare has gradually expanded from professional medical scenes to home environments. Vital sign monitoring is a key support to home healthcare services, which includes the detection of human breathing, heartbeat, blood pressure (BP), etc. Different from dedicated sensors attached to the human body, mmWave radars can monitor a person in a contactless and non-intrusive manner, becoming a promising solution for vital sign monitoring in daily scenarios. For example, human breathing

TABLE X
COMPARISON OF MMWAVE RADAR-BASED SPEECH RECOGNITION WORKS

Work	Device	Audio source	Key method	Performance
WaveEar [101]	24GHz mmWave probe	Human	Encoder-decoder-based Wave-voice Net	Speaking signal-to-noise ratio of 38.85dB for voice recovery
Wen et al. [224]	120GHz radar	Human	Trigonometric transform	N/A
mmMic [225]	TI IWR6843	Human	multi-modal fusion & cGAN	Accuracy is 92.8%
Wavoice [226]	TI IWR1642	Human	ResECA-based fusion network	Character recognition error below 1% in 7m range
mSilent [227]	TI IWR1843	Human	Clustering-selection & multi-branch convolutional & Transformer	Average word error rate of 9.5%
AmbiEar [102]	TI IWR1642	Surrounding object vibrated by human	Common component extraction& signal superimposition& Encoder-decoder	Word recognition accuracy of 87.21% in NLOS scenarios
mmEcho [176]	TI IWR1642	Surrounding object vibrated by human	Phase calibration & Multi-antenna noise removal	Mel-Cepstral distortion of 3.36 & word error rate of 18.1%
MILLIEAR [114], [115]	TI IWR1642	Audio device	Virtual sub-chirp & cGAN	Mel-Cepstral distortion of 3.68 and Likert user score of 6.38
mmEve [117]	TI AWR1843	Phone earpiece	Fitting function optimization & GAN	Peak signal-to-noise ratio of 20dB in a range of 8m
mmPhone (Li et al.) [228]	77-GHz FMCW probe	Loudspeaker	Multitarget adaptive fusion enhancement	N/A
mmSpy [98]	TI AWR1843 & TI IWR6843	Phone earpiece	Encoder-decoder& ResNet & CNN	Accuracy of 83% for classifying digits and keywords
mmPhone (Wang et al.) [229]	TI AWR1843	Loudspeaker	Denoising NN & enhancement	Accuracy over 93% for recognizing 10 digits

and heartbeat activities cause movements in the human chest, so a mmWave radar can measure the displacement and vibration of the human chest in phase changes to estimate the respiratory rate and heart rate for vital sign monitoring.

The studies in single-user vital sign monitoring mainly aim to enhance the accuracy of respiratory and heart rate estimation for providing reliable healthcare services. Key processing for vital sign monitoring is to obtain accurate phase of mmWave signals to precisely measure the fine-grained displacement of the human chest. To obtain an accurate phase from noisy mmWave signals, a novel phase unwrapping manipulation is proposed in [230]. It removes the direct current (DC) value in unwrapped phases and searches for the best range bin corresponding to the real vibration frequency of the target. A circle center dynamic tracking algorithm and extended differential and cross-multiply (DPCM) are applied in [231] for phase unwrapping. After obtaining the accurate phase of mmWave signals, the frequency components of breathing and heartbeat need to be further separated and estimated respectively for monitoring the two types of vital signs. This can be achieved by directly utilizing the frequency differences to separate breathing and heartbeat [230], or reconstructing the breathing and heartbeat signals based on compressive sensing and adaptive-threshold noise reduction [231]. Pi-ViMo [232] tries to address the limitation of users' fixed distance and static pose. It derives a multi-scattering point model of humans, enabling vital sign estimations at any location. A template matching method is then utilized to extract human vital signs. Besides, blood pressure can also be measured by sensing a subject's wrist and capturing skin or blood vessel displacement [233], [234], [235]. For example, mmBP [233] utilizes a mmWave radar to measure blood pressure by exploiting delay-Doppler domains for pulse waveform construction. It also

alleviates human tiny motions in measuring blood pressure by leveraging the characteristics of pulse waveform signals.

Monitoring multiple users' vital signs simultaneously is more challenging due to the uncertain interference of multiple users in sensing scenarios. To accurately detect each user's vital sign activities, monitoring systems should first localize a person to capture individual signals, or calibrate the signals to remove inference under complex multi-user scenarios. For example, mmVital [236], [237] designs a human finding technique to locate a target user using the reflection loss of the human body, which can accurately capture each user's chest movement for multi-user vital sign monitoring. A random body rejection algorithm is proposed in [238], which can track and detect the vital signs of target users in the presence of movement. Another work [239] leverages range-gating and beamforming techniques to extract target signal components and eliminate the influence of surroundings, enabling the detection of each user's vital sign in multi-user scenarios. ViMo [240], [244] designs an adaptive object detector to detect stationary or nonstationary users. It extracts respiratory components from the signal phase and utilizes dynamic programming (DP) to resist measurement noises for vital sign monitoring.

In addition, there have been studies on vital sign monitoring in dynamic environments (e.g., driving environments), which can keep tracking a person in changing backgrounds with body motions. To remove human motion artifacts in driving environments, a study [174] applies motion compensation for motion artifact removal, and utilizes periodicity checks to identify vital sign components. The respiration and heartbeat signals are reconstructed by an optimization method. To eliminate the impact of dynamic vehicle changes, mmECG [241] differentiates the phase changes caused by

TABLE XI
COMPARISON OF MMWAVE RADAR-BASED VITAL SIGN MONITORING WORKS

Work	Device	Key method	Scenario	Performance
Alizadeh et al. [230]	TI AWR1443	Phase unwrapping manipulation	Single-user	Correlation of 94% and 80% between reference and mmWave for breathing and heart rate
Wang et al. [231]	TI AWR1642	Autocorrelation estimation & compress sensing	Single-user	Accuracy of 93% for breathing and heartbeat rate
Pi-ViMo [232]	IT IWR6843	Multi-scattering point & coherent combining	Single-user	Respiration rate errors of 6%, heart rate errors of 11.9%
mmBP [233]	TI IWR1843	Delay-Doppler domain transformation & adaptive filter	Single-user BP	Mean error of 0.87mmHg and 1.55mmHg for SBP and DBP
Shi et al. [234]	TI IWR6843	Linear model regression analysis	Single-user BP	N/A
Kawasaki et al. [235]	mmWave sensor	Time-domain feature extraction in cardiac motion waveform	Single-user BP	N/A
mmVital [236], [237]	60GHz testbed	Human finding procedure	Multi-user	Mean error of 0.43bpm and 2.15bpm for breathe and heart rate
Mercuri et al. [238]	FMCW radar sensor	Random body motion rejection algorithm	Multi-user	Success rate of 99.5% and 90% for respiration and heart rate remained within 3bpm
Ahmad et al. [239]	TI IWR1443	Range-gating and beamforming	Multi-user	N/A
ViMo [240]	60GHz radio	Adaptive object detector & DP	Multi-user	Median error of 0.19rpm and 0.92bpm for breathing and hear rate
Wang et al. [174]	TI IWR1843	Motion artifacts removal & optimization	Dynamic environment	Median error of 0.16rpm and 0.82bpm for breathing and heartbeat
mmECG [241]	TI IWR1443 & cameras	VMD & template optimization	Dynamic environment	Error of 0.6bpm for heart rate
Wang et al. [242]	TI AWR1843	Beamforming & weighted multi-channel VMD	Dynamic environment	90% errors less than 0.5 RPM and 6 BPM
iSense [243]	TI AWR2243	Interference mitigation	Mutual device interference	99.2% and 98.6% for respiration and heartbeat estimation

different movements, and applies a hierarchy variational mode decomposition (VMD) approach to extract and estimate the essential heart movement in mmWave signals. The cardiac cycles are reconstructed based on a template optimization method. A recent work [242] proposes to deal with body movements and environmental changes by combining radars and cameras. They utilize a camera to assist a mmWave radar in accurately localizing the subjects of interest, and then exploit the calculated subject position to form transmitting and receiving beamformers. Afterward, they employ weighted multi-channel VMD to separate vital sign signals. iSense [243] aims to address vital sign monitoring in the presence of mutual device interference. It uses one-way propagation characteristic of device interference for suppressing the interference. The reviewed vital sign monitoring works are summarized in Table XI.

6) *User Authentication*: Nowadays, the concept of user authentication has been largely expanded from secure protection to the mapping between the human and IoT world. mmWave radars could sense and reveal a person's behaviors and biometrics. Through extracting behavioral or biometric features and constructing reliable classifiers, user authentication can be achieved in ubiquitous indoor environments for smart home control and privacy protection. A typical workflow of mmWave radar-based user authentication is shown in Fig. 13.

A person's gait exhibits unique patterns in step length, duration, instantaneous velocity and inter-lower distance of limb movement, making gait a reliable behavior for user authentication. In a behavioral feature-based manner, leveraging gaits for user authentication requires a strong capability in behavioral feature extraction. Hence, a crucial part of

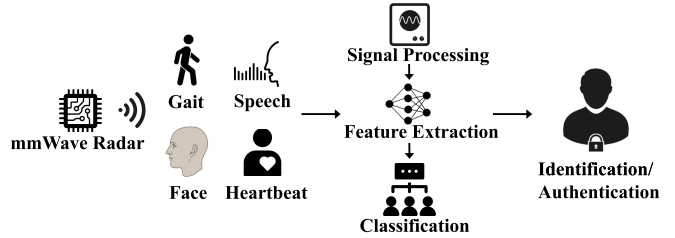


Fig. 13. A typical workflow of mmWave radar-based user authentication. A mmWave radar senses a user's activity, such as gait, speech, face, or heartbeat. The sensing signals are first processed by signal processing techniques. Then, behavioral features are extracted from the signals usually by neural networks. By classifying the user into a known user profile, the user's identity is identified and authenticated.

gait-based user authentication is to design reliable neural networks for feature extraction. To achieve this goal, some studies exploit the capability of CNNs to extract spatial features related to user behaviors. For example, a multi-channel three-dimensional CNN is designed in [245]. With motion speed and intensity of strong scattering points as the input, the CNN enables hierarchical extraction and fusion of multi-dimensional features of human gaits. Other studies construct new intermediate representations before feeding the signals to CNNs. A corrective velocity spectrogram is constructed in [169] by exploiting location and Doppler information, which reveals the actual velocity of users. With a CNN-based deep learning model, it can identify users walking on arbitrary paths. A GaitCube is constructed in [246] to reduce the training efforts in different environments for mmWave radar-based user authentication. GaitCube is a 3D joint-feature representation combining micro-Doppler and micro-range signatures.

With a CNN-based deep learning model, it achieves user authentication in unseen locations with less training data collection.

Other studies realize multi-user authentication by extracting individual features to describe each user in complex multi-user scenarios. To extract a user's behavioral features, MU-ID [247] leverages silhouette information to segment multi-user steps and combines a CNN to realize multi-user identification. A density-based classification algorithm is proposed in [105] to separate Doppler signatures of multiple users and combines autoencoder-based deep learning for user identification. mmGaitNet [97] incorporates ResNet and spatio-temporal convolutions kernels to extract each user's gait features for multi-user gait recognition. MGait [248] extracts gait features from range-Doppler profiles by a neural network with large-margin Gaussian mixture (L-GM) loss, where each component of Gaussian mixture distribution denotes a registered user. Another work named MCGait [249] leverages micro-Doppler calibration for multi-user authentication based on the gait. The highlight is to calibrate temporal gait micro-Doppler features of each user to eliminate the negative effect of gait direction dynamics. Besides the mmWave data sole method, another study [250] fuses vision and mmWave signals for multi-user gait-based authentication. It addresses the inter-modality discrepancy between vision and mmWave signals, and designs a cross-modal deep metric learning model to synchronize the two data, providing a cross-modal human re-identification (ReID) solution.

In addition to gait-based user authentication, there are other biometrics-based authentication approaches leveraging mmWave signals, such as face recognition [104], [251], [252], voice authentication [253], [254], and heartbeat authentication [255]. The biometrics features are embedded in human facial shapes, speech habits and heartbeat cycles. Hence, these studies put a lot of effort into designing customized deep neural networks for biometric feature extraction. For example, autoencoder-based deep learning models [104], [251] are designed to take the spatial facial information of each user as biometric features for user face recognition. Another facial-based study mmFace [252] designs a virtual registration process where photos are converted to mmWave profiles based on cross-modal transformation, which enables low training burdens based on mmWave signals. Besides, vocal vibrations of a user's throat are also exploited for voice authentication [175], [253], [254]. For example, a VocalPrint system [253], [254] proposes a resilience-aware clutter suppression approach to eliminate ambient noise and further extracts vocal tract and source features for authentication. Another system [175] uses mmWave radar to extract both vocal cord vibration (VCV) and lip motion (LM) as multimodal biometrics for speaker verification. In addition, there are vital sign-based user authentication approaches, which extract unique biometric features in heartbeat cycles for user authentication. For example, HeartPrint [255] uses the effect of skin surface vibrations caused by heartbeat on mmWave signals to extract fine-grained features in heartbeat traits. Its following work M-Auth [256] dynamically adjusts the radar orientation for isolating individual components

for multi-user authentication. Another work [257] utilizes environmental fingerprints caused by unique human outline profiles and vital signs for user detection and identification. The reviewed user authentication works are summarized in Table XII.

7) *Indoor Positioning*: Indoor positioning is a crucial function to enable location-based services for users in indoor environments. mmWave radars can estimate the range, angle and velocity of targets, which provides an accurate and dynamic estimation of users' position. A number of works focus on human positioning in indoor environments, providing device-free and non-intrusive location-based services for users.

Since mmWave signals are noisy in indoor environments, the FMCW-based range estimation and TDM-MIMO-based angle estimation could suffer from inaccuracy in tracking a moving person. Hence, the studies in human tracking pay attention to addressing noisy problems and improving estimation capabilities. For example, mmTrack [68] performs digital beamforming on mmWave signals to improve spatial estimation, and eliminates the near-far-effect and measurement noises as well. To localize and track users, it employs a clustering algorithm to detect multiple users and designs a weighted bipartite graph matching to track users' trajectories. Another work [258] designs a context-based algorithm for human detection and localization and utilizes a calibration algorithm leveraging radar irradiation to refine the positions. Li et al. [259] build a single-radar indoor positioning system, which determines the trajectory by estimating the velocity and heading of moving radar from sparse point clouds. Some works [47], [48], [49], [50], [260] make use of extended Kalman filters to continuously track users in indoor environments for indoor localization and tracking, yielding linear regression correction-based extended Kalman filter [47], nonlinear extended Kalman filter [48], recursive Kalman filter tracking with data association [49], and coordinate-corrected extended Kalman filter [50]. Besides these tracking algorithms, deep learning models [105] can also be utilized to dynamically estimate the position of users for human tracking. Another research [261] focuses on reconstructing accurate signal spectral peaks from the discrete samples for localization. Also, some studies explore the method to localize stationary human targets. For example, Li et al. [262] propose a fretting phase variation characteristics detection based on mmWave signals, which can achieve low detection time and high accuracy for stationary humans even if not directly in front of the radar. The indoor positioning works are summarized in Table XIII.

C. Industrial Applications

In addition to automotive applications and smart home applications, mmWave radars are also an alternative to sensors in industrial systems. The properties of low cost, small size and all-weather operation have prompted the integration of mmWave radars and the industry, leading to a huge development of industrial applications. These applications can be further classified as *industrial imaging*, *industrial measurement* and *environmental monitoring*.

TABLE XII
COMPARISON OF MMWAVE RADAR-BASED USER AUTHENTICATION WORKS

Work	Device	Key method	Scenarios	Performance
Jiang et al. [245]	TI IWR1443	Multi-channel CNN	Single-user gait	Accuracy of 92.5% under 8 trained users
Wu et al. [169]	TI AWR1443	Energy normalization & CNN	Single-user gait	Accuracy of 91% and 87% for non-radial straight path and curve path under 10 trained users
GaitCube [246]	TI IWR1443	Gait cube extraction&CNN	Single-user gait	Accuracy of 98.3% under 10 trained users
MU-ID [247]	TI AWR1642	Silhouette-based multi-user step segmentation&CNN	Multi-user gait	Accuracy of 97% for 1 user and 92% for 4 users under 10 trained users
Pegoraro et al. [105]	INRAS Radar-Log	Density-based classification &autoencoders	Multi-user gait	Accuracy of 98% for 2 users under 4 untrained users
mmGaitNet [97]	TI IWR1443 & IWR6843	ResNet& spatial-temporal convolutional kernel	Multi-user gait	Accuracy of 90% for 1 user and 86% for 2 users under 10 trained users
MGait [248]	TI IWR1443	Large-margin Gaussian mixture loss	Multi-user gait	Accuracy of 98.27% for 2 users under 10 trained users
MCGait [249]	TI IWR1443	Micro-Doppler calibration & CNN	Multi-user gait	Accuracy of 95.45% for multi-user
Cao et al. [250]	TI IWR6843& camera	Cross-modal deep metric learning model	Multi-user gait	Top-1 accuracy of 92.5% and top-5 of 97.5% under 56 trained users
Hof et al. [104]	60 GHz radar	Autoencoder	Single-user face	False negative rate below 2% under 200 trained users
Challa et al. [251]	60 GHz radar	Autoencoder	Single-user face	Accuracy of 98.45% under 186 trained users
mmFace [252]	TI IWR1642	Cross-modal Transformation	Single-user face	Accuracy of 96% under 30 trained users
VocalPrint [253], [254]	TI AWR1642	Resilience-aware clutter suppression	Single-user voice	Accuracy of 96% under 41 trained users
Dong et al. [175]	TI AWR1642	Multimodal biometrics extraction & CNN	Single-user voice	True accept rate of 95% at false accept rate of 5%
HeartPrint [255]	TI IWR1443	Wavelet packet transform& recursive feature elimination	Multi-user heartbeat	Accuracy of 95% under 54 trained users
M-Auth [256]	TI IWR1443	Isolating individual components & filter	Multi-user heartbeat	Accuracy over 96% for 37 users
Gu et al. [257]	60GHz radar	SVM & LSTM-based RNN	Multi-user vital sign	Accuracy of 93% under 5 trained users

TABLE XIII
COMPARISON OF MMWAVE RADAR-BASED INDOOR POSITIONING WORKS

Work	Device	Key method	Performance
mmTrack [68]	60GHz radio	Weighted bipartite graph matching	Localization error of 9.9cm and 19.7cm for dynamic and static users
Xu et al. [258]	TI IWR1443	Contextual information-based algorithm	Positioning errors of 8.7cm and 12.95cm for single and multiple users
Li et al. [259]	TI IWR6843	Cluster center association & normal distributions transform	Positioning accuracy within 1 m
Jiang et al. [47]	TI IWR6843	EKF	80% of tracking precision below 0.1m
Wang et al. [48]	mmWave radar	non-linear EKF	Minimum mean error of 0.6974m
Huang et al. [49]	TI IWR1642	Recursive KF	Root mean square error of 0.2992m
m ³ Track [50]	TI IWR1443	Coordinate-corrected EKF	Localization error of 2.15cm
Pegoraro et al. [260]	INRAS RadarLog	Encoder-decoder & EKF	Tracking accuracy of 97.96%
Pegoraro et al. [105]	INRAS RadarLog	Encoder-decoder with sequence-to-sequence network	Tracking error of 12 cm
Zhang et al. [261]	TI IWR1443	Spectral peak reconstruction & amplitude-based AoA	Median ranging accuracy of 5.5mm
Li et al. [262]	TI IWR6843	Fretting phase variation characteristics detection	Correct detection rate higher than 90% within ±10cm error

1) *Industrial Imaging*: Due to the sensing capability in azimuth and elevation angles, mmWave radars have gradually been able to realize industrial imaging. HawkEye [121] focuses on car imaging in fog scenarios. Based on the low-resolution mmWave radar point cloud, a cGAN is proposed to recover high-resolution images in the presence of dense fog, which overcomes the limitations of cameras and Lidar in car-imaging problems. A following work [263] design a back-to-back conditional GAN deep neural network. Two generators are integrated into the network, where the first one generates

2D depth images based on raw radar intensity data, and the second one outputs 3D point clouds based on the results of the first generator. The architecture exploits convolutional operation and the efficiency and detailed geometry capture capability of point clouds to generate accurate 3D images. Hansen et al. [148] utilize a self-designed mmWave radar for two industrial applications, i.e., tube extrusion for plastic materials and 3D radar imaging of fiber-composite materials. The work proves mmWave radar's high-resolution measurements in separating reflections and imaging targets of specific materials.

TABLE XIV
COMPARISON OF MMWAVE RADAR-BASED INDUSTRIAL IMAGING WORKS

Work	Device	Objective	Key method	Performance
HawkEye [121]	60 GHz radio	Imaging through fog	Conditional generative adversarial network	Error of 50cm, 83cm, 44cm, 11cm in ranging, length, width and height in fog
Sun et al. [263]	IT IWR6843	3D reconstruction and imaging	Conditional GAN	Length error of car is larger 29% and L-box is smaller 50% compared to HawkEye
Hansen et al. [148]	SiGe-Chip-Based D-Band FMCW-Radar Sensor	Tube extrusion & 3D imaging	D-Band transceiver MMIC	Separating two reflections at 0.25m & orientation measure of fiber layers of 7.03 mm
Brooker et al. [264]	77 and 94 GHz radar	Examining mine environment	Ranging and three-dimensional surface profiling	N/A
Osprey [265]	TI AWR1642	Tire wear sensing	Inverse synthetic aperture & spatial coding on tire	Median tread depth estimation error of 0.68mm and median error of 1.7cm in location of foreign object
Pan et al. [266]	100 and 122 GHz transceiver of silicon-radar GmbH	Radar reflectometry unit for sensing and imaging	FMCW combined with waveguides	N/A
Alvarez et al. [267]	Infineon radar-on-chip BGT60TR24B	Free hand scanning and imaging	Synthetic aperture based on movement & irregular sampling compensation	N/A
Gupta et al. [268]	TI AWR2243	Multiclass-target classification	Custom range-angle heatmaps and machine learning tools	Accuracy of 87.68% - 99.7%
Liu et al. [269]	Activate mmWave sensor	Object detection by imaging	Convolution and context embedding	Average precision of 85.61%

mmWave radars can also be utilized in mine environments [264], [270] including open cut and underground mines. Due to mmWave radars' superior penetration through adverse atmospheric conditions, they have become an alternative to laser and sonar implementations in mine environments. Osprey [265] is an on-automobile tire wear sensing and imaging system based on a mmWave radar. By placing a mmWave radar in the tire well of automobiles, Osprey observes reflected signals from the tire surface and grooves to measure tire wear and obtain an image showing the tire wear condition, even in the presence of debris. Pan et al. [266] develop an implementation of a guided FMCW radar reflectometry unit for sensing and imaging applications. The insight behind is the differentiation capability between reflected signals generated along the waveguide as parasitic signals or at its probing end as sensing information. Another freehand scanning system based on mmWave radar is proposed in [267]. The system exploits the free movements of a radar to create a synthetic aperture for scanning and imaging, and also reduces the artifacts in images by compensating for irregular sampling. Besides, Gupta et al. [268] utilize a YOLO model-based method and apply it to custom range-angle heatmaps, which realize multiclass target classification using mmWave signals. Liu et al. [269] investigate the deep learning-based object detection approaches for the mmWave images, and then develop a concealed object detector for the security system. The deep learning method is based on convolution and context embedding, which aims to capture both details and the context information for small object detection. The mmWave radar-based imaging application works are summarized in Table XIV.

2) *Industrial Measurement:* Other studies probe into the physical properties of mmWave signals to measure different physical parameters. mmVib [271] leverages a mmWave radar

to measure micrometer-level vibration. It identifies mmWave signal in the In-phase and quadrature (IQ) domain and proposes a multi-signal consolidation to describe the movement properties of signals. mmVib provides a vibration detection approach for industrial systems with a single COTS mmWave radar. Ahmad et al. [146] design a new mmWave radar sensor chipset working in 60GHz with FMCW techniques. The radar sensor can be utilized in ranging, vibration measuring, etc., in factories. Besides vibration of equipment, mmWave radars can also be exploited to measure wind turbine blade clearance [272]. In this work, the mmWave radars constantly measure the change in the distance between the tower and the blade, and then estimate the minimum clearance distance between the blade and the tower. Some researchers explore the feasibility of utilizing mmWave radars to launch various attacks. For example, WaveSpy [273] designs a side-channel attack for screen content leveraging mmWave signals. It utilizes the relation between screen content and the state of liquid crystal arrays in displays, and leverages an FMCW mmWave radar to estimate the liquid crystal nematic state, which aims to interfere with screen content for side-channel eavesdropping. Miura et al. [274] propose a distance-spoofing attack for automotive applications. They can manipulate distance measured at target radar by half-chirp modulation and two-step delay insertion, demonstrating the potential feasibility of low-cost malicious spoofing attacks in radar ranging.

The detection of various targets is another important application scenario in the industry. The targets that are detected by mmWave radars can be child [276], obstacles [277], drones [278], [279], etc. For instance, Caddemi and Cardillo [276] utilize a mmWave radar to detect the presence of a child in a car, which aims to avoid incidents where children being left inside a car die of heatstroke. A mmWave radar cane is designed in [277] to detect obstacles in the area

TABLE XV
COMPARISON OF MMWAVE RADAR-BASED INDUSTRIAL MEASUREMENT WORKS

Work	Device	Objective	Key method	Performance
mmVib [271]	TI IWR1642	Vibration detection for industrial systems	IQ phase & multi-signal consolidation	Median relative amplitude error of 8.2% and median relative frequency error of 0.5%
Ahmad et al. [146]	60GHz radar	Measuring vibration rates for factory machines	Doppler effect	Range resolution of 6cm and ranging precision of 0.1mm at 1m
Zhang et al. [272]	24 GHz Radar	Wind turbine blade clearance measuring	Least square curve regression fitting	Blade clearance value of 7.43m
WaveSpy [273]	24GHz FMCW probe	Screen content inference	Wavelet analysis & spectrogram feature augmentation	Accuracy of 99% in screen content type recognition and success rate of 87.77% in Top-3 sensitive information retrieval
Miura et al. [274]	EVRADAR-MMIC2	Distance-spoofing attack	Half-chirp modulation & two-step delay insertion	±10m ranging error in manipulating distance
Piotrowsky et al. [275]	UWB mmWave radar	Distance measurement	Signal processing chain of IFFT	Systematic error of ±1μm over 4.8m and random error at a minimum of 30 nm
Caddemi et al. [276]	79GHz radar	Child presence detection in cars	Maximum search algorithm	N/A
Cardillo et al. [277]	Silicon Radar	Obstacle detection	FFT	Range profiles up to the distance of 3.5m
Semkin et al. [278]	24-60GHz platform	Drone detection	Radar cross section signatures	N/A
Dogru et al. [279]	TI AWR1642	Drone tracking and pursuer	3D position estimation from 2D measurements	Root mean square errors of around 1m
Zhai et al. [280]	Delphi ESR 76GHz radar	Target tracking	Adaptive Sage-Husa Kalman filter	Longitudinal error of 0.051m and lateral error of 0.061m
Fernandez et al. [281]	TI IWR1443	Characterization of large raw material stockpiles	Processing adaptive-based scanned structure reconstruction	N/A
Wu et al. [282]	TI IWR6843	Package-height estimation and parcel-size classification	DBPC & DBCD	Classification accuracy of 96.4%
Leong et al. [283]	TI IWR1443	Obstructed material classification	Fully-connected neural network & convolution neural network	Perform under 16mm thick obstruction and classify less than 5mm thin material

scanned by a user and provide feedback about their distance for enhancing blind people's mobility. Semkin et al. [278] use radar cross-section signatures to detect drones with different materials. They prove that larger drones made of carbon fiber are easier to detect whereas drones made from plastic and styrofoam materials are less visible. Another similar work [279] proposes to track and pursue a target drone via the mmWave radars installed in another drone. Although the mmWave radar measurements are 2D, the work can estimate 3D position of the target drone. Zhai et al. [280] propose an adaptive Sage-Husa Kalman filter for target tracking, which can accurately estimate the position information of the lost target. It addresses the problems in the variety of targets on the road, the different scattering intensities of multiple parts, and the interference of the flicker noise. Besides, combining a mmWave radar array with an accurate positioning system can achieve characterization of large raw material (e.g., cereal grain, coal, etc.) stockpiles [281]. Wu et al. [282] design a package-height estimation and parcel-size classification using mmWave radars. They introduce three schemes using the range-profile data, i.e., the detection based on cumulative distribution, the detection based on peak-value clustering, and the DBCD-DBPC hybrid. The proposed schemes can accommodate parcels/packages in arbitrary orientations. Another work on material classification [283] utilizes mmWave radars' reflection to classify industrial materials. The classified materials are common

engineering materials which include metal, polymer, ceramic, composite and natural. This work exploits unique material properties and the physical structure of target object, with the assistance of deep neural networks. The works related to measurement applications are summarized in Table XV.

3) *Environmental Monitoring:* Environmental monitoring is a vital application for industrial production, agricultural production and social activities. The monitored objects include weather conditions, temperature, gases, liquid, humidity, soil, insects, etc. mmWave radars can be utilized as environmental monitoring sensors and many research works have been presented. A pioneering study [284] demonstrates clouds and precipitation sensing using mmWave radars with capturing reflectivity, Doppler, and polarimetric quantities. ThermoWave [285] exploits the thermal scattering effect on signals to monitor the temperature. The key insight of the system is that the cholesteryl materials have different molecular patterns at different temperatures, which can be modulated and sensed by mmWave signals. With a paper tag attached to the object, the temperature will modulate mmWave scattering and be demodulated by the system. mmWave signals can be utilized to monitor gases and aerosols [286]. The basic idea is to simulate the refractive index of arbitrary gases at mmWave frequencies using molecular spectroscopic data. The simulations then allow the identification of the respective gas or aerosols in the industry. Besides, using mmWave radars

can identify liquid. The researchers in [287] exploit signal attenuation, phase shift and propagation delay when penetrating liquid for identifying the type of liquid. Humidity sensing can be realized by mmWave radars. Reference [288] uses the impact of different levels of water vapor on mmWave signals and proposes an environmental humidity sensing method. To eliminate other environmental factors such as oxygen, it exploits a subspace projection technique to establish a linear relationship between humidity and mmWave signals. Rainfall monitoring [289] is achieved by studying rain attenuation characteristics of microwave backhaul techniques at different mmWave frequencies and link lengths. It shows great potential in estimating the path-averaged rain rates with different mmWave links. [290] explores the effects of different phases of water in atmosphere on the propagation of mmWave signals, and designs a modified mmWave propagation model to predict suspended water droplets and rain effects. Soil moisture sensing [291] can be realized by a single mmWave radar. The researchers exploit mmWave signals to obtain the soil moisture from the propagation time and AoA of the reflected signals. The above studies utilize mmWave radars to sense physical properties of the environment. Besides, mmWave radars can be utilized in another environmental monitoring scenario, i.e., detecting small living matter such as insects. Tahir and Brooker [292] utilize mmWave harmonic sensors and radar for observing and monitoring insects. Another work [293] explores mmWave imaging for insect motion sensing.

D. Summary and Insights

In this section, we provide a comprehensive review of the applications driven by mmWave radar sensing technologies. Through a systematic examination based on application taxonomy, we survey the applications and related studies across three primary categories.

In automotive scenarios, our focus lies in pivotal areas such as object detection, ego-motion estimation, and SLAM. Given the tendency of fusion of multiple sensors, we particularly explore fusion techniques and examine their synergistic contributions towards enhancing sensing capabilities in autonomous vehicles. Smart home applications represent human-centric services, aiming to augment the intelligence and convenience of daily life. Within this domain, recognition-related applications, including activity recognition, pose estimation, gesture recognition, and speech recognition, emerge as focal points. We comprehensively investigate research studies dedicated to each application, highlighting their unique attributes and contributions. Further, we explore other smart home applications such as vital sign monitoring, user authentication, and indoor positioning, each catering to specific usage scenarios with distinct judgment criteria. These applications exhibit a broad spectrum of functionalities, ranging from healthcare monitoring to security and navigation, demonstrating the adaptability of mmWave radar sensing technology. Industrial scenarios represent a traditional yet evolving landscape where mmWave radars find extensive utility in applications such as industrial imaging, measurement, and environmental monitoring. We review research works involving the objectives and

deployment scenarios of mmWave radar-based industrial applications. The inherent advantages of mmWave radar sensing, including privacy protection and cost-effectiveness, present high value in industrial environments. It enables continuous development and innovation in areas where traditional sensors may be insufficient or expensive. In general, the landscape of sensing applications continues to evolve dynamically in the foreseeable future. As technological advancements, mmWave radar sensing technology is poised to play an increasingly pivotal role across diverse domains.

VIII. CHALLENGES AND SOLUTIONS

mmWave radar sensing applications are developed rapidly with novel techniques and emerging usage scenarios in typical, mobile, and IoT environments. With the gradual integration of radar sensing systems and practical scenarios, some challenges arise in real-world deployment. In this section, we summarize existing technical challenges and discuss potential solutions.

A. ISAC

Integrated sensing and communication is drawing great attention from current research circles and industrial communities. The integration of sensing and communication drives the development of mobile crowdsensing, channel knowledge map construction, passive sensing network, vehicular communication, satellite imaging and broadcasting, etc. These applications have given full play to the advantages of ubiquitous communication in space as well as numerous sensors.

Together with the tendency of ISAC, existing research activities have paid attention to the integration of mmWave-based sensing and communications. Some studies [38], [294], [295] address integration issues of sensing and communication in mmWave MIMO systems to provide high-quality services. Intelligent reflecting surface [296] or reconfigurable intelligent surface [297] are another solution to reduce path loss for integration. Others aim to enable reliable data sharing and sensing for connected automated vehicles (CAVs) [298] or unmanned aerial vehicles (UAV) [299]. However, the mmWave-based ISAC for ubiquitous indoor environments, such as smart homes, smart offices, and smart manufacturing, is still an open issue that deserves future research efforts. For example, an indoor environment usually has few radars, making existing ISAC solutions of MIMO radars unsuitable in the indoor environment. However, the research community could further exploit the information embedded in chirp signals that are designed for sensing to help modulate communication data, which is another way to integrate sensing and communications.

B. LLM-Aided Sensing

The rapid development in large language models (LLMs) has demonstrated great success in recognizing and generating text. A revolutionary product is ChatGPT [300], which provides human-like conversations with extensive knowledge of the real world. When the concept of LLMs meets mmWave sensing, it is expected to merge and create huge potential among different sensing tasks.

TABLE XVI
COMPARISON OF MMWAVE RADAR-BASED ENVIRONMENTAL MONITORING WORKS

Work	Device	Objective	Key method	Performance
Mead et al. [284]	33GHz/95GHz polarimetric radar	Clouds and precipitation sensing	Calculating reflectivity, Doppler, and polarimetric quantities	N/A
ThermoWave [285]	24GHz FMCW radar	Temperature monitoring	mmWave scattering & GAN	Precision of $\pm 1.0^{\circ}\text{F}$ in the range of 30°F to 120°F
Hattenhorst et al. [286]	72 to 92GHz radar	Gases and aerosols monitoring	Simulation of refractive index of gases based on molecular spectroscopic data	Precision of 0.027ppm and linearity of 1.5 ppm
MmLiquid [287]	TI AWR1642	Liquid identification	Container position information filtering & deep complex model	Accuracy of 97.6% for 16 liquids at 24 different container positions
mm-Humidity [288]	QX60G system	Humidity sensing	Subspace projection & SVM	85 % measurement if the humidity interval is 3%
Han et al. [289]	32GHz/72GHz/82 radar	Rainfall monitoring	Microwave backhaul	Correlation between 0.8 and 0.9
Golovachev [290]	N/A	Weather monitoring	Analytical expressions of attenuation and group delay	N/A
Chen et al. [291]	TI IWR1443	Soil moisture sensing	propagation time and AoA	2.2% volumetric water content
Sheikh et al. [293]	72GHz-82GHz MIMO radar	Insect monitoring	Radar imaging	N/A

LLMs are mainly driven by generative AI technologies, which are an effective approach to synthesizing data. With pre-trained large models and generative capabilities, generative AI can create training or testing data by deeply understanding the data's underlying distribution. Data synthesis can release the heavy burden of collecting mmWave sensing data. Also, it can resist the effect of ambient noise and ensure data quality. Besides, the pre-trained large models with extensive training data provide the capability of generating data with different characteristics and forms, which increases the diversity of data. Hence, LLMs can help with the model construction of mmWave sensing by synthesizing data.

LLMs can bridge mmWave sensing and the comprehension of physical world. A major characteristic of LLMs is to learn common-sense knowledge and leverage the knowledge to give human-like comprehendings of the physical world. Hence, the integration of mmWave sensing and LLMs generates a new function, i.e., comprehending the physical world by mmWave sensing. Traditional mmWave sensing methods usually exploit the capability of neural networks to output predicted known labels, which can only generate imperceptible results. Differently, mmWave sensing integrated with LLMs is able to provide new insights into the sensing data. It can not only predict the known labels representing the data but also provide a further understanding of the sensing task and object. For example, with mmWave sensing data of a human target, LLMs can further analyze and judge the person's conditions, actions and intentions. If multiple sensors are accessible, a more comprehensive inference of the person can be realized by LLMs through integrating multi-modal data. Hence, LLM-aided mmWave sensing may provide a chance to further deeply understand user needs and personalize services for users.

Along with the tendency of LLMs' rapid development, the integration of LLMs with IoT sensing technologies, especially

mmWave sensing, has shown great potential and is expected to create a new application field.

C. Eliminating Environmental Noise

Environmental noises usually include background changes, dynamic interferences, NLOS blockages, etc. These environmental noises influence the propagation of mmWave signals, which limits the practical performance of sensing applications. For example, the change of background causes a change in signal propagation in the environment, which may result in different signal patterns of sensed objects. As many of the applications are driven by learning techniques, these varying signal patterns may suffer from performance degradation when relying on the model learned in one specific environment. Therefore, environmental noises have become one of the major impacts in mmWave radar sensing applications.

Existing research activities have proposed some approaches to address the problem and try to expand application scopes. These approaches can be divided into two categories, i.e., signal-based and learning-based. The signal-based approaches, such as voxelizing close area [201] and target localization [101], focus on utilizing physical properties to obtain signals of target and ignore the noises. The learning-based approaches, such as domain discriminator [210] and hierarchy VMD [241], incorporate special learning designs to mitigate or suppress the impact of noise components in signals. For future work, environmental noise is still a hot-spot issue due to the gradual integration of the research applications and real-world scenarios. The signal-based approaches can be developed with more physical properties of signals in noisy environments. For example, the mmWave signals reflected by background objects and humans could have different phase variation trends within a close ambient area, because background objects and humans usually have different surface

smoothness. This physical property could be used for noise elimination. For learning-based approaches, different from domain discriminator-based methods, the research community can leverage generators to compensate for missing parts caused by environmental noises, therefore achieving noise-resistant sensing.

D. Reducing Training Effort

Many machine learning-based applications usually have a training process where the labeled data is fed into the model to learn how to extract feature representations and give predictions. Generally, a better performance can be achieved by increasing the amount of training data. However, sensing applications gradually become more complex, diversified, and specialized. It is increasingly difficult to obtain appropriate and sufficient training data, and the inadequacy of large public datasets of mmWave signals also hinders the utilization of training data. At the same time, the training data and gradually deeper structures give rise to another issue of long training time, which is less considered by current research studies.

To release the heavy training burden of sensing applications, cross-modal transformation-based approaches [100], [204], [252] have been proposed, which take advantage of existing large datasets to generate data for training. The cross-modal approaches significantly reduce the requirement of large mmWave datasets and release the heavy workload of collecting signals in real-world environments. Others rely on more specialized deep learning models [210] or more efficient data representations [246] to enable few-shot learning. Although these approaches are successful, they may not be suitable for a variety of sensing applications with different intermediate representations and learning tasks. Hence, more generalized approaches are desirable to reduce training efforts for ubiquitous sensing applications. For further work, the research community could exploit methods like knowledge distillation [301] and transfer learning [302] to replace the traditional model construction process for reducing training efforts for more generalized sensing tasks. To release the time cost of training machine learning models in implementing sensing systems with deep learning technologies, fast machine learning technologies [303] are a promising solution. The researchers are encouraged to apply fast machine learning in multiple training processes. Moreover, using incremental learning technologies [304] to continuously train and improve the model by using new data rather than training with all data is another potential solution.

IX. CONCLUSION

Millimeter wave radars have gradually become a popular sensing solution in the face of emerging sensing scenarios. In this paper, we have provided a comprehensive review of mmWave radar-based techniques and applications in autonomous vehicles, smart homes and industry. To enable mmWave radar sensing, radar techniques have been first introduced from both dedicated radar and communication integration perspectives. Based on the preliminary signal acquisition, signal processing techniques have been further

elaborated on for extracting denoised and compressed data representations. To empower sensing signals for a variety of applications, machine learning especially deep learning techniques have been widely investigated for solving specific sensing tasks. The tools for implementing mmWave radar sensing, including radar devices, public datasets, and evaluation metrics, have been provided to assist replication. The applications driven by mmWave radars have advanced the convenience and intelligence in autonomous vehicles, smart homes and industry. To systematically access the emerging applications, an application taxonomy has been given to refine the applications in different scenarios. The automotive scenario includes object detection, ego-motion estimation and SLAM, in which mmWave radars play the role of environmental detection. The smart home scenario consists of activity recognition, pose estimation, gesture recognition, speech recognition, vital sign monitoring, user authentication and indoor positioning, in which the mmWave radars mainly act as monitors of human activity. The industrial scenario is divided into imaging, measurement and environmental monitoring, where physical parameters are acquired by mmWave radars. With the taxonomic applications, research studies have been introduced covering hardware, techniques and performance, providing comprehensive knowledge in the research actuality where new ideas spring up constantly. The analyses of practical challenges in ISAC, LLM-aided sensing, environmental noise, and training effort, have been given with current technical status and potential directions. We hope that this survey can inspire more pioneering research in the emerging area.

LIST OF ABBREVIATIONS

ADC	Analog-to-digital converter
AE	Autoencoder
AIoT	Artificial intelligence of thing
AoA	Angle of arrival
AOP	Antenna-on-package
CAV	Connected automated vehicle
CA	Cell average
CFAR	Constant false alarm rate
cGAN	Conditional generative adversarial network
CIR	Channel impulse response
CNN	Convolutional neural network
CRF-Net	CameraRadarFusionNet
CSM	Correlative scan matching
DACM	Differential and cross-multiply
DBSCAN	Density-based spatial clustering of applications with noise
dB	Decibel
DCNN	Deep convolutional neural network
DC	Direct current
DoF	Degree of freedom
DP	Dynamic programming
DRNN	Deep recurrent neural network
DSP	Digital signal processor
EKF	Extended Kalman filter
ESPRIT	Estimation of signal parameters via rotational invariant techniques

FAR	False accept rate	SVDD	Support vector domain description
FCNN	Fully convolutional neural network	SVM	Support vector machine
FFT	Fast Fourier transform	TDM	Time division multiplexing
FMCW	Frequency-modulated continuous-wave	TI	Texas instruments
FN	False negative	ToA	Time of arrival
FP	False positive	TP	True positive
FP	Feature propagation	TRX	Transceiver
FRR	False reject rate	UAV	Unmanned aerial vehicle
GAN	Generative adversarial network	UKF	Unscented Kalman filter
GCP	Ground control point	USV	Unmanned surface vehicle
GHz	Gigahertz	VCV	Vocal cord vibration
GMM	Gaussian mixture model	VMD	Variational mode decomposition
GNN	Graph neural network	VR	Virtual reality
GRU	Gated recurrent unit	VUI	Voice-user interface
HAR	Human activity recognition	YOLO	You only look once
HMM	Hidden Markov model		
IF	Intermediate frequency		
IMU	Inertial measurement unit		
IoT	Internet of thing		
IoU	Intersection over union		
IQ	In-phase and quadrature		
ISAC	Integrated sensing and communication		
JRC	Joint radar and communication		
k-NN	k-nearest neighbors		
KF	Kalman filter		
L-GM	Large-margin Gaussian mixture		
LFM	Linear frequency modulation		
LLM	Large language model		
LM	Lip motion		
LNA	Low-noise amplifier		
LSTM	Long short-term memory		
mAP	Mean average precision		
MCD	Mel-Cepstral distortion		
MIMO	Multi-input multi-output		
mmWave	Millimeter wave		
MPNN	Message passing neural network		
MSG	Multi-scale grouping module		
MUSIC	Multiple signal classification		
MVDR	Minimum variance distortionless response		
NLOS	none line of sight		
NLP	Natural language processing		
NOMA	Non-orthogonal multiple access		
OFDM	Orthogonal frequency division multiplexing		
PA	Power amplifier		
PCA	Principal component analysis		
PMCW	Phase modulated continuous wave		
PSK	Phase shift keying		
QAM	Quadrature amplitude modulation		
RCS	Radar cross section		
ResNet	Residual neural network		
RNN	Recurrent neural network		
SAF	Spatial attention fusion		
SAR	Synthetic aperture radar		
SiGe	Single-channel silicon-germanium		
SLAM	Simultaneous localization and mapping		
SNN	Spiking neural network		
SNR	Signal-to-noise-ratio		
SRNN	Spiking recurrent neural network		

REFERENCES

- [1] Q. Yu, C. Han, L. Bai, J. Choi, and X. Shen, "Low-complexity multiuser detection in millimeter-wave systems based on opportunistic hybrid beamforming," *IEEE Trans. Veh. Technol.*, vol. 67, no. 10, pp. 10129–10133, Oct. 2018.
- [2] J. Qiao, X. Shen, J. W. Mark, Q. Shen, Y. He, and L. Lei, "Enabling device-to-device communications in millimeter-wave 5G cellular networks," *IEEE Commun. Mag.*, vol. 53, no. 1, pp. 209–215, Jan. 2015.
- [3] S. He et al., "A survey of millimeter-wave communication: Physical-layer technology specifications and enabling transmission technologies," *Proc. IEEE*, vol. 109, no. 10, pp. 1666–1705, Oct. 2021.
- [4] (Texas Instrum., Dallas, TX, USA). *mmWave Radar Sensors*. Accessed: Apr. 20, 2024. [Online]. Available: <https://www.ti.com/sensors/mmwave-radar/overview.html>.
- [5] A. Davoli, G. Guerzoni, and G. M. Vitetta, "Machine learning and deep learning techniques for colocated MIMO radars: A tutorial overview," *IEEE Access*, vol. 9, pp. 33704–33755, 2021.
- [6] F. J. Abdu, Y. Zhang, M. Fu, Y. Li, and Z. Deng, "Application of deep learning on millimeter-wave radar signals: A review," *Sensors*, vol. 21, no. 6, p. 1951, 2021.
- [7] A. Shastri et al., "A review of millimeter wave device-based localization and device-free sensing technologies and applications," *IEEE Commun. Surveys Tuts.*, vol. 24, no. 3, pp. 1708–1749, 3rd Quart., 2022.
- [8] Z. Peng and C. Li, "Portable microwave radar systems for short-range localization and life tracking: A review," *Sensors*, vol. 19, no. 5, p. 1136, 2019.
- [9] A. Venon, Y. Dupuis, P. Vasseur, and P. Merriaux, "Millimeter wave FMCW RADARs for perception, recognition and localization in automotive applications: A survey," *IEEE Trans. Intell. Veh.*, vol. 7, no. 3, pp. 533–555, Sep. 2022.
- [10] L. Fan, J. Wang, Y. Chang, Y. Li, Y. Wang, and D. Cao, "4D mmWave radar for autonomous driving perception: A comprehensive survey," *IEEE Trans. Intell. Veh.*, vol. 9, no. 4, pp. 4606–4620, Apr. 2024.
- [11] Z. Wei, F. Zhang, S. Chang, Y. Liu, H. Wu, and Z. Feng, "MmWave radar and vision fusion for object detection in autonomous driving: A review," *Sensors*, vol. 22, no. 7, p. 2542, 2022.
- [12] A. Pearce, J. A. Zhang, R. Xu, and K. Wu, "Multi-object tracking with mmWave radar: A review," *Electronics*, vol. 12, no. 2, p. 308, 2023.
- [13] A. Coluccia, G. Parisi, and A. Fascista, "Detection and classification of multirotor drones in radar sensor networks: A review," *Sensors*, vol. 20, no. 15, p. 4172, 2020.
- [14] S. M. Patole, M. Torlak, D. Wang, and M. Ali, "Automotive radars: A review of signal processing techniques," *IEEE Signal Process. Mag.*, vol. 34, no. 2, pp. 22–35, Mar. 2017.
- [15] A. Singh, S. U. Rehman, S. Yongchareon, and P. H. J. Chong, "Multi-resident non-contact vital sign monitoring using radar: A review," *IEEE Sensors J.*, vol. 21, no. 4, pp. 4061–4084, Feb. 2021.
- [16] C. Gu, "Short-range noncontact sensors for healthcare and other emerging applications: A review," *Sensors*, vol. 16, no. 8, p. 1169, 2016.
- [17] Y. Wu, H. Ni, C. Mao, J. Han, and W. Xu, "Non-intrusive human vital sign detection using mmWave sensing technologies: A review," *ACM Trans. Sensor Netw.*, vol. 20, no. 1, pp. 1–36, 2023.

- [18] S. Ahmed, K. D. Kallu, S. Ahmed, and S. H. Cho, "Hand gestures recognition using radar sensors for human-computer-interaction: A review," *Remote Sens.*, vol. 13, no. 3, p. 527, 2021.
- [19] Z. Wang, F. Liu, X. Li, M. Ma, X. Feng, and Y. Guo, "A survey of hand gesture recognition based on FMCW radar," in *Proc. ACM ICPIP*, 2022, pp. 73–79.
- [20] X. Li, Y. He, and X. Jing, "A survey of deep learning-based human activity recognition in radar," *Remote Sens.*, vol. 11, no. 9, p. 1068, 2019.
- [21] B. van Berlo, A. Elkelany, T. Ozcelebi, and N. Meratnia, "Millimeter wave sensing: A review of application pipelines and building blocks," *IEEE Sensors J.*, vol. 21, no. 9, pp. 10332–10368, May 2021.
- [22] J. Zhang et al., "A survey of mmWave-based human sensing: Technology, platforms and applications," *IEEE Commun. Surveys Tuts.*, vol. 25, no. 4, pp. 2052–2087, 4th Quart., 2023.
- [23] C. Iovescu and S. Rao, *The Fundamentals of Millimeter Wave Sensors*, Texas Inst., Dallas, TX, USA, 2017, pp. 1–8.
- [24] A. Meta, P. Hoogeboom, and L. P. Ligthart, "Signal processing for FMCW SAR," *IEEE Trans. Geosci. Remote Sens.*, vol. 45, no. 11, pp. 3519–3532, Nov. 2007.
- [25] P. Duhamel and M. Vetterli, "Fast Fourier transforms: A tutorial review and a state of the art," *Signal Process.*, vol. 19, no. 4, pp. 259–299, 1990.
- [26] S. Rao, *Introduction to mmWave Sensing: FMCW Radars*, Texas Inst., Dallas, TX, USA, 2017, pp. 1–11.
- [27] R. Klukas and M. Fattouche, "Line-of-sight angle of arrival estimation in the outdoor multipath environment," *IEEE Trans. Veh. Technol.*, vol. 47, no. 1, pp. 342–351, Feb. 1998.
- [28] D. Bliss and K. Forsythe, "Multiple-input multiple-output (MIMO) radar and imaging: Degrees of freedom and resolution," in *Proc. IEEE ACSSC*, vol. 1, 2003, pp. 54–59.
- [29] T. Hwang, C. Yang, G. Wu, S. Li, and G. Y. Li, "OFDM and its wireless applications: A survey," *IEEE Trans. Veh. Technol.*, vol. 58, no. 4, pp. 1673–1694, May 2009.
- [30] W. Bai et al., "Millimeter-wave joint radar and communication system based on photonic frequency-multiplying constant envelope LFM-OFDM," *Opt. Exp.*, vol. 30, no. 15, pp. 26407–26425, 2022.
- [31] N. Zhong, P. Li, W. Bai, W. Pan, L. Yan, and X. Zou, "Spectral-efficient frequency-division photonic millimeter-wave integrated sensing and communication system using improved sparse LFM sub-bands fusion," *J. Lightw. Technol.*, vol. 41, no. 23, pp. 7105–7114, Dec. 1, 2023.
- [32] R. Song and J. He, "OFDM-NOMA combined with LFM signal for W-band communication and radar detection simultaneously," *Opt. Lett.*, vol. 47, no. 11, pp. 2931–2934, 2022.
- [33] X. Tian, T. Zhang, Q. Zhang, and Z. Song, "Waveform design and processing in OFDM based radar-communication integrated systems," in *Proc. IEEE/CIC ICCC*, 2017, pp. 1–6.
- [34] L. Qi, Y. Yao, B. Huang, and G. Wu, "A phase-coded OFDM signal for radar-communication integration," in *Proc. IEEE PAST*, 2019, pp. 1–4.
- [35] S. H. Dokhanchi, B. S. Mysore, K. V. Mishra, and B. Ottersten, "A mmWave automotive joint radar-communications system," *IEEE Trans. Aerosp. Electron. Syst.*, vol. 55, no. 3, pp. 1241–1260, Jun. 2019.
- [36] S. H. Dokhanchi, M. B. Shankar, K. V. Mishra, T. Stifter, and B. Ottersten, "Performance analysis of mmWave bi-static PMCWB-based automotive joint radar-communications system," in *Proc. IEEE RadarConf.*, 2019, pp. 1–6.
- [37] S. H. Dokhanchi, M. R. B. Shankar, T. Stifter, and B. Ottersten, "Multicarrier phase modulated continuous waveform for automotive joint radar-communication system," in *Proc. IEEE SPAWC*, 2018, pp. 1–5.
- [38] Z. Gao et al., "Integrated sensing and communication with mmWave massive MIMO: A compressed sampling perspective," *IEEE Trans. Wireless Commun.*, vol. 22, no. 3, pp. 1745–1762, Mar. 2023.
- [39] Z. Zhu et al., "Resource allocation for IRS assisted mmwave integrated sensing and communication systems," in *Proc. IEEE ICC*, 2022, pp. 2333–2338.
- [40] L. Fan, L. Xie, W. Zhou, C. Wang, Y. Bu, and S. Lu, "Beamforming for sensing: Hybrid beamforming based on transmitter-receiver collaboration for millimeter-wave sensing," *Proc. ACM Interact., Mobile, Wearable Ubiquitous Technol.*, vol. 8, no. 2, pp. 1–27, 2024.
- [41] P. P. Gandhi and S. A. Kassam, "Analysis of CFAR processors in nonhomogeneous background," *IEEE Trans. Aerosp. Electron. Syst.*, vol. 24, no. 4, pp. 427–445, Jul. 1988.
- [42] A. Jalil, H. Yousaf, and M. I. Baig, "Analysis of CFAR techniques," in *Proc. IEEE ICAST*, 2016, pp. 654–659.
- [43] M. Ester, H.-P. Kriegel, J. Sander, and X. Xu, "Density-based spatial clustering of applications with noise," in *Proc. Int. Conf. Knowl. Discov. Data Min.*, 1996.
- [44] K. Khan, S. U. Rehman, K. Aziz, S. Fong, and S. Sarasvady, "DBSCAN: Past, present and future," in *Proc. IEEE ICADIWT*, 2014, pp. 232–238.
- [45] Q. Li, R. Li, K. Ji, and W. Dai, "Kalman filter and its application," in *Proc. IEEE ICINIS*, 2015, pp. 74–77.
- [46] G. Welch and G. Bishop, "An introduction to the Kalman filter," Dept. Comput. Sci., Univ. North Carolina Chapel Hill, Chapel Hill, NC, USA, Rep. TR 95-041, 1995.
- [47] M. Jiang, S. Guo, H. Luo, and G. Cui, "Continuous tracking of indoor human targets based on millimeter wave radar," in *Proc. IEEE APSIPA ASC*, 2022, pp. 2071–2076.
- [48] X. Wang, Z. Zhang, N. Zhao, Y. Zhang, and D. Huang, "Indoor localization and trajectory tracking system based on Millimeter-wave radar sensor," in *Proc. IEEE DDCLS*, 2021, pp. 1141–1147.
- [49] X. Huang, H. Cheena, A. Thomas, and J. K. Tsai, "Indoor detection and tracking of people using mmwave sensor," *J. Sensors*, vol. 2021, no. 1, 2021, Art. no. 6657709.
- [50] H. Kong et al., "m3Track: Mmwave-based multi-user 3D posture tracking," in *Proc. ACM MobiSys*, 2022, pp. 491–503.
- [51] S. Bakhtiari et al., "Compact millimeter-wave sensor for remote monitoring of vital signs," *IEEE Trans. Instrum. Meas.*, vol. 61, no. 3, pp. 830–841, Mar. 2012.
- [52] M. Raja, Z. Vali, S. Palipana, D. G. Michelson, and S. Sigg, "3D head motion detection using millimeter-wave doppler radar," *IEEE Access*, vol. 8, pp. 32321–32331, 2020.
- [53] M. Z. Ikram, A. Ahmad, and D. Wang, "High-accuracy distance measurement using millimeter-wave radar," in *Proc. IEEE RadarConf*, 2018, pp. 1296–1300.
- [54] G. Mehdi and J. Miao, "Millimeter wave FMCW radar for foreign object debris (FOD) detection at airport runways," in *Proc. IEEE ICAST*, 2012, pp. 407–412.
- [55] S. Hazra and A. Santra, "Short-range radar-based gesture recognition system using 3D CNN with triplet loss," *IEEE Access*, vol. 7, pp. 125623–125633, 2019.
- [56] P. Feil, W. Menzel, T. Nguyen, C. Pichot, and C. Migliaccio, "Foreign objects debris detection (FOD) on airport runways using a broadband 78 GHz sensor," in *Proc. IEEE EuMC*, 2008, pp. 1608–1611.
- [57] C. Liu, Y. Li, D. Ao, and H. Tian, "Spectrum-based hand gesture recognition using millimeter-wave radar parameter measurements," *IEEE Access*, vol. 7, pp. 79147–79158, 2019.
- [58] Z. Li, Z. Lei, A. Yan, E. Solovey, and K. Pahlavan, "ThuMouse: A micro-gesture cursor input through mmWave radar-based interaction," in *Proc. IEEE ICCE*, 2020, pp. 1–9.
- [59] H. Abdi and L. J. Williams, "Principal component analysis," *Wiley Interdiscipl. Rev., Comput. Statist.*, vol. 2, no. 4, pp. 433–459, 2010.
- [60] P. Pal and P. P. Vaidyanathan, "Coprime sampling and the MUSIC algorithm," in *Proc. IEEE DSP/SPE*, 2011, pp. 289–294.
- [61] B. Li, S. Wang, J. Zhang, X. Cao, and C. Zhao, "Fast randomized-MUSIC for mm-wave massive MIMO radars," *IEEE Trans. Veh. Technol.*, vol. 70, no. 2, pp. 1952–1956, Feb. 2021.
- [62] B.-S. Kim, Y. Jin, J. Lee, and S. Kim, "Low-complexity MUSIC-based direction-of-arrival detection algorithm for frequency-modulated continuous-wave vital radar," *Sensors*, vol. 20, no. 15, p. 4295, 2020.
- [63] C. Ly, H. Dropkin, and A. Z. Manitis, "Extension of the music algorithm to millimeter-wave (mmw) real-beam radar scanning antennas," in *Proc. SPIE RSTDV*, 2002, pp. 96–107.
- [64] R. Roy and T. Kailath, "ESPRIT-estimation of signal parameters via rotational invariance techniques," *IEEE Trans. Acoust., speech, signal Process.*, vol. 37, no. 7, pp. 984–995, 1989.
- [65] F. Liu, X. Wang, M. Huang, L. Wan, H. Wang, and B. Zhang, "A novel unitary ESPRIT algorithm for monostatic FDA-MIMO radar," *Sensors*, vol. 20, no. 3, p. 827, 2020.
- [66] D. Wen, H. Yi, W. Zhang, and H. Xu, "2D-unitary ESPRIT based multi-target joint range and velocity estimation algorithm for FMCW radar," *Appl. Sci.*, vol. 13, no. 18, p. 10448, 2023.
- [67] J. Wu, H. Cui, and N. Dahnoun, "An improved angle estimation algorithm for millimeter-wave radar," in *Proc. IEEE MECO*, 2022, pp. 1–4.
- [68] C. Wu, F. Zhang, B. Wang, and K. R. Liu, "mmTrack: Passive multi-person localization using commodity millimeter wave radio," in *Proc. IEEE INFOCOM*, 2020, pp. 2400–2409.
- [69] G. Zhang, X. Geng, and Y.-J. Lin, "Comprehensive mPoint: A method for 3D point cloud generation of human bodies utilizing FMCW MIMO mm-wave radar," *Sensors*, vol. 21, no. 19, p. 6455, 2021.

- [70] M. A. Hearst, S. T. Dumais, E. Osuna, J. Platt, and B. Scholkopf, "Support vector machines," *IEEE Intell. Syst. Appl.*, vol. 13, no. 4, pp. 18–28, Jul./Aug. 1998.
- [71] A. D. Singh, S. S. Sandha, L. Garcia, and M. Srivastava, "Radhar: Human activity recognition from point clouds generated through a millimeter-wave radar," in *Proc. ACM mmNets@MobiCom*, 2019, pp. 51–56.
- [72] W. Baoshuai and Z. Wei, "FOD detection based on millimeter wave radar using higher order statistics," in *Proc. IEEE ICSPCC*, 2017, pp. 1–4.
- [73] A. J. Myles, R. N. Feudale, Y. Liu, N. A. Woody, and S. D. Brown, "An introduction to decision tree modeling," *J. Chemometr.*, vol. 18, no. 6, pp. 275–285, 2004.
- [74] L. Breiman, "Random forests," *Mach. Learn.*, vol. 45, no. 1, pp. 5–32, 2001.
- [75] J. M. Keller, M. R. Gray, and J. A. Givens, "A fuzzy k-nearest neighbor algorithm," *IEEE Trans. Syst., Man, Cybern.*, vol. SMC-15, no. 4, pp. 580–585, 1985.
- [76] C. Ding, Z. Ding, L. Wang, and Y. Jia, "A fall detection method based on K-nearest neighbor algorithm with MIMO millimeter-wave radar," in *Proc. IEEE ICSIP*, 2021, pp. 624–628.
- [77] S. A. Shah, S. Y. Shah, S. I. Shah, D. Haider, A. Tahir, and J. Ahmad, "Identifying elevated and shallow respiratory rate using mmWave radar leveraging machine learning algorithms," in *Proc. IEEE AECT*, 2020, pp. 1–4.
- [78] J. A. Hartigan and M. A. Wong, "Algorithm AS 136: A K-means clustering algorithm," *J. Roy. Statist. Soc. Ser. C (Appl. Statist.)*, vol. 28, no. 1, pp. 100–108, 1979.
- [79] A. Worasut, D. Worasawate, T. Pongthavornkamol, and K. Fukawa, "Improved human detection algorithm by indoor W-band FMCW RADAR using K-means technique," in *Proc. IEEE iEECON*, 2021, pp. 571–574.
- [80] C. K. Armeniakos, V. Nikolaidis, V. Tsekenis, K. Maliatatos, P. S. Bithas, and A. G. Kanatas, "Human fall detection using mmWave radars: A cluster-assisted experimental approach," *J. Ambient Intell. Human. Comput.*, vol. 14, pp. 1–13, Feb. 2022.
- [81] S. Matsuguma and A. Kajiwara, "Bathroom accident detection with 79GHz-band millimeter wave sensor," in *Proc. IEEE SAS*, 2019, pp. 1–5.
- [82] D. A. Reynolds, "Gaussian mixture models," *Encyclopedia of Biometrics*, vol. 741. Berlin, Germany: Springer, 2009.
- [83] F. Jin, A. Sengupta, S. Cao, and Y.-J. Wu, "Mmwave radar point cloud segmentation using GMM in multimodal traffic monitoring," in *Proc. IEEE RADAR*, 2020, pp. 732–737.
- [84] L. Zhu, X. Wei, Q. Zheng, and Y. Wang, "Research on adaptive target tracking method based on millimeter wave radar," in *Proc. ACM TURC*, 2021, pp. 261–265.
- [85] G. Malysa, D. Wang, L. Netsch, and M. Ali, "Hidden Markov model-based gesture recognition with FMCW radar," in *Proc. IEEE GlobalSIP*, 2016, pp. 1017–1021.
- [86] H. Liu et al., "Real-time arm gesture recognition in smart home scenarios via millimeter wave sensing," *Proc. ACM Inter., Mobile, Wearable Ubiquit. Technol.*, vol. 4, no. 4, pp. 1–28, 2020.
- [87] Z. Wang, G. Li, and L. Yang, "Dynamic hand gesture recognition based on micro-doppler radar signatures using hidden Gauss–Markov models," *IEEE Geosci. Remote Sens. Lett.*, vol. 18, no. 2, pp. 291–295, Feb. 2021.
- [88] K. Jimi, H. Seto, and A. Kajiwara, "Bathroom monitoring with fast-chirp modulation millimeter-wave UWB radar," in *Proc. IEEE RWS*, 2020, pp. 134–137.
- [89] K. O'Shea and R. Nash, "An introduction to convolutional neural networks," 2015, *arXiv:1511.08458*.
- [90] Y. Xie, R. Jiang, X. Guo, Y. Wang, J. Cheng, and Y. Chen, "mmEat: Millimeter wave-enabled environment-invariant eating behavior monitoring," *Smart Health*, vol. 23, Mar. 2022, Art. no. 100236.
- [91] J. W. Smith, S. Thiagarajan, R. Willis, Y. Makris, and M. Torlak, "Improved static hand gesture classification on deep convolutional neural networks using novel sterile training technique," *IEEE Access*, vol. 9, pp. 10893–10902, 2021.
- [92] F. Jin et al., "Multiple patients behavior detection in real-time using mmWave radar and deep CNNs," in *Proc. IEEE RadarConf.*, 2019, pp. 1–6.
- [93] Z. Ni and B. Huang, "Human identification based on natural gait micro-doppler signatures using deep transfer learning," *IET Radar, Sonar Navig.*, vol. 14, no. 10, pp. 1640–1646, 2020.
- [94] K. Zhang, S. Lan, and G. Zhang, "On the effect of training convolution neural network for millimeter-wave radar-based hand gesture recognition," *Sensors*, vol. 21, no. 1, p. 259, 2021.
- [95] G. Jaswal, S. Srirangarajan, and S. D. Roy, "Range-Doppler hand gesture recognition using deep residual-3DCNN with transformer network," in *Proc. Pattern Recognit. ICPR Int. Workshops Chall.*, 2021, pp. 759–772.
- [96] Y. Liu, S. Zhang, M. Gowda, and S. Nelakuditi, "Leveraging the properties of mmWave signals for 3D finger motion tracking for interactive IoT applications," *Proc. ACM Meas. Anal. Comput. Syst.*, vol. 6, no. 3, pp. 1–28, 2022.
- [97] Z. Meng et al., "Gait recognition for co-existing multiple people using millimeter wave sensing," in *Proc. AAAI*, vol. 34, 2020, pp. 849–856.
- [98] S. Basak and M. Gowda, "mmSpy: Spying phone calls using mmwave radars," in *Proc. IEEE SP*, 2022, pp. 1211–1228.
- [99] C. Yu, Z. Xu, K. Yan, Y.-R. Chien, S.-H. Fang, and H.-C. Wu, "Noninvasive human activity recognition using millimeter-wave radar," *IEEE Syst. J.*, vol. 16, no. 2, pp. 3036–3047, Jun. 2022.
- [100] K. Ahuja, Y. Jiang, M. Goel, and C. Harrison, "Vid2Doppler: Synthesizing doppler radar data from videos for training privacy-preserving activity recognition," in *Proc. ACM CHI*, 2021, pp. 1–10.
- [101] C. Xu et al., "WaveEar: Exploring a mmwave-based noise-resistant speech sensing for voice-user interface," in *Proc. ACM MobiSys*, 2019, pp. 14–26.
- [102] J. Zhang, Y. Zhou, R. Xi, S. Li, J. Guo, and Y. He, "AmbiEar: MmWave based voice recognition in NLoS scenarios," *Proc. ACM Interact., Mobile, Wearable Ubiquitous Technol.*, vol. 6, no. 3, pp. 1–25, 2022.
- [103] F. Jin, A. Sengupta, and S. Cao, "mmFall: Fall detection using 4-D mmwave radar and a hybrid variational RNN autoencoder," *IEEE Trans. Autom. Sci. Eng.*, vol. 19, no. 2, pp. 1245–1257, Apr. 2022.
- [104] E. Hof, A. Sanderovich, M. Salama, and E. Hemo, "Face verification using mmWave radar sensor," in *Proc. IEEE ICAIIC*, 2020, pp. 320–324.
- [105] J. Pegoraro, D. Solimini, F. Matteo, E. Bashirov, F. Meneghelli, and M. Rossi, "Deep learning for accurate indoor human tracking with a mm-wave radar," in *Proc. IEEE RadarConf.*, 2020, pp. 1–6.
- [106] M. Stephan, T. Stadelmayer, A. Santra, G. Fischer, R. Weigel, and F. Lurz, "Radar image reconstruction from raw ADC data using parametric variational autoencoder with domain adaptation," in *Proc. IEEE ICPR*, 2021, pp. 9529–9536.
- [107] H. Salehinejad, S. Sankar, J. Barfett, E. Colak, and S. Valaee, "Recent advances in recurrent neural networks," 2017, *arXiv:1801.01078*.
- [108] S. Hochreiter and J. Schmidhuber, "Long short-term memory," *Neural Comput.*, vol. 9, no. 8, pp. 1735–1780, 1997.
- [109] R. Dey and F. M. Salem, "Gate-variants of gated recurrent unit (GRU) neural networks," in *Proc. IEEE MWSCAS*, 2017, pp. 1597–1600.
- [110] B. Singh, T. K. Marks, M. Jones, O. Tuzel, and M. Shao, "A multi-stream bi-directional recurrent neural network for fine-grained action detection," in *Proc. IEEE CVPR*, 2016, pp. 1961–1970.
- [111] P. Zhao et al., "Human tracking and identification through a millimeter wave radar," *Ad Hoc Netw.*, vol. 116, May 2021, Art. no. 102475.
- [112] P. Zhao et al., "mID: Tracking and identifying people with millimeter wave radar," in *Proc. IEEE DCOS*, 2019, pp. 33–40.
- [113] I. J. Tsang, F. Corradi, M. Sifalakis, W. Van Leeuwijk, and S. Latré, "Radar-based hand gesture recognition using spiking neural networks," *Electronics*, vol. 10, no. 12, p. 1405, 2021.
- [114] P. Hu, Y. Ma, P. S. Santhalingam, P. H. Pathak, and X. Cheng, "MILLIEAR: Millimeter-wave acoustic eavesdropping with unconstrained vocabulary," in *Proc. IEEE INFOCOM*, 2022, pp. 11–20.
- [115] P. Hu et al., "Towards unconstrained vocabulary eavesdropping with Mmwave radar using GAN," *IEEE Trans. Mobile Comput.*, vol. 23, no. 1, pp. 941–954, Jan. 2024.
- [116] C. X. Lu et al., "See through smoke: Robust indoor mapping with low-cost mmwave radar," in *Proc. ACM MobiSys*, 2020, pp. 14–27.
- [117] C. Wang et al., "mmEve: Eavesdropping on smartphone's earpiece via COTS mmWave device," in *Proc. ACM MobiCom*, 2022, pp. 338–351.
- [118] I. Alnujaim, D. Oh, and Y. Kim, "Generative adversarial networks for classification of micro-Doppler signatures of human activity," *IEEE Geosci. Remote Sens. Lett.*, vol. 17, no. 3, pp. 396–400, Mar. 2020.
- [119] Y. Sun, Z. Huang, H. Zhang, and X. Liang, "3D reconstruction of multiple objects by mmWave radar on UAV," 2022, *arXiv:2211.02150*.
- [120] Y. Sun, H. Zhang, Z. Huang, and B. Liu, "DeepPoint: A deep learning model for 3D reconstruction in point clouds via mmWave radar," 2021, *arXiv:2109.09188*.
- [121] J. Guan, S. Madani, S. Jog, S. Gupta, and H. Hassanieh, "Through fog high-resolution imaging using millimeter wave radar," in *Proc. IEEE/CVF CVPR*, 2020, pp. 11464–11473.

- [122] C. R. Qi, H. Su, K. Mo, and L. J. Guibas, "PointNet: Deep learning on point sets for 3D classification and segmentation," in *Proc. IEEE CVPR*, 2017, pp. 652–660.
- [123] A. Danzer, T. Griebel, M. Bach, and K. Dietmayer, "2D car detection in radar data with pointNets," in *Proc. IEEE ITSC*, 2019, pp. 61–66.
- [124] T. Griebel, D. Authaler, M. Horn, M. Henning, M. Buchholz, and K. Dietmayer, "Anomaly detection in radar data using PointNets," in *Proc. IEEE ITSC*, 2021, pp. 2667–2673.
- [125] J. Bai, K. Long, S. Li, L. Huang, and L. Dong, "Multi-objective classification of three-dimensional imaging radar point clouds: Support vector machine and PointNet," *SAE Int. J. Connect. Autom. Veh.*, vol. 4, no. 4, pp. 371–382, 2021.
- [126] O. Schumann, M. Hahn, J. Dickmann, and C. Wöhler, "Semantic segmentation on radar point clouds," in *Proc. IEEE FUSION*, 2018, pp. 2179–2186.
- [127] F. Scarselli, M. Gori, A. C. Tsoi, M. Hagenbuchner, and G. Monfardini, "The graph neural network model," *IEEE Trans. neural Netw.*, vol. 20, no. 1, pp. 61–80, 2008.
- [128] P. Gong, C. Wang, and L. Zhang, "MMPPoint-GNN: Graph neural network with dynamic edges for human activity recognition through a millimeter-wave radar," in *Proc. IEEE IJCNN*, 2021, pp. 1–7.
- [129] C. Wang, P. Gong, and L. Zhang, "Stpointnet: Spatial temporal graph convolutional network for multiple people recognition using millimeter-wave radar," in *Proc. IEEE ICASSP*, 2022, pp. 3433–3437.
- [130] X. Liu et al., "General spiking neural network framework for the learning trajectory from a noisy mmWave radar," *Neuromorphic Comput. Eng.*, vol. 2, no. 3, 2022, Art. no. 034013.
- [131] Z. Zhang, Z. Tian, and M. Zhou, "Latern: Dynamic continuous hand gesture recognition using FMCW radar sensor," *IEEE Sensors J.*, vol. 18, no. 8, pp. 3278–3289, Apr. 2018.
- [132] S. Wang, J. Song, J. Lien, I. Poupyrev, and O. Hilliges, "Interacting with soli: Exploring fine-grained dynamic gesture recognition in the radio-frequency spectrum," in *Proc. ACM UIST*, 2016, pp. 851–860.
- [133] K. Alirezazad and L. Maurer, "FMCW radar-based hand gesture recognition using dual-stream CNN-GRU model," in *Proc. IEEE MIKON*, 2022, pp. 1–5.
- [134] B. Zhang, L. Zhang, M. Wu, and Y. Wang, "Dynamic gesture recognition based on RF sensor and AE-LSTM neural network," in *Proc. IEEE ISCAS*, 2021, pp. 1–5.
- [135] "Single-chip 76-GHz to 81-GHz automotive radar sensor integrating MCU and hardware accelerator," Data Sheet AWR 1443, Texas Instrum., Dallas, TX, USA, Jan. 2022. [Online]. Available: <https://www.ti.com/product/AWR1443>.
- [136] "Single-chip 76-GHz to 81-GHz automotive radar sensor integrating DSP and MCU," Data Sheet AWR 1642, Texas Instrum., Dallas, TX, USA, Jan. 2022. [Online]. Available: <https://www.ti.com/product/AWR1642>.
- [137] "Single-chip 76-GHz to 81-GHz automotive radar sensor integrating DSP, MCU and radar accelerator," Data Sheet AWR 1843, Texas Instrum., Dallas, TX, USA, Jan. 2022. [Online]. Available: <https://www.ti.com/product/AWR1843>.
- [138] "Single-chip 60-GHz to 64-GHz intelligent mmWave sensor with integrated antenna on package (AoP)," Data Sheet IWR6843AOP, Texas Instrum., Dallas, TX, USA, Jan. 2022. [Online]. Available: <https://www.ti.com/product/IWR6843AOP>.
- [139] Y. Song, Z. Xie, X. Wang, and Y. Zou, "MS-YOLO: Object detection based on YOLOv5 Optimized fusion millimeter-wave radar and machine vision," *IEEE Sensors J.*, vol. 22, no. 15, pp. 15435–15447, Aug. 2022.
- [140] "ARS 408-21 long range radar sensor 77 GHz," Data Sheet ARS 408, Continent. Eng. Serv., Frankfurt, Germany. Accessed: Mar. 1, 2023. [Online]. Available: <https://conti-engineering.com/components/ars-408/>.
- [141] (Navtech Radar, Oxfordshire, U.K.). *Nactech CTS350-X Technical Specifications*. Accessed: Oct. 2, 2023. [Online]. Available: <https://navtechradar.com/clearway-technical-specifications/>
- [142] S. H. Cen and P. Newman, "Precise ego-motion estimation with millimeter-wave radar under diverse and challenging conditions," in *Proc. IEEE ICRA*, 2018, pp. 6045–6052.
- [143] S. H. Cen and P. Newman, "Radar-only ego-motion estimation in difficult settings via graph matching," in *Proc. IEEE ICRA*, 2019, pp. 298–304.
- [144] "Soli technology." Google. Accessed: Apr. 20, 2023. [Online]. Available: <https://atap.google.com/soli/technology/>
- [145] (INRAS GmbH, Linz, Austria). *Radarlog*. Accessed: Oct. 2, 2023. [Online]. Available: <https://inras.at/en/radarlog>
- [146] W. A. Ahmad, J. Wessel, H. J. Ng, and D. Kissinger, "IoT-ready millimeter-wave radar sensors," in *Proc. IEEE GCIAIoT*, 2020, pp. 1–5.
- [147] N. Pohl, T. Jaeschke, S. Küppers, C. Bredendiek, and D. Nüßler, "A compact ultra-wideband mmWave radar sensor at 80 GHz based on a SiGe transceiver chip (focused session on highly-integrated millimeter-wave radar sensors in SiGe BiCMOS technologies)," in *Proc. IEEE MIKON*, 2018, pp. 345–347.
- [148] S. Hansen, C. Bredendiek, G. Briese, A. Froehly, R. Herschel, and N. Pohl, "A SiGe-chip-based D-band FMCW-radar sensor with 53-GHz tuning range for high resolution measurements in industrial applications," *IEEE Trans. Microw. Theory Tech.*, vol. 70, no. 1, pp. 719–731, Jan. 2022.
- [149] S. Kueppers, T. Jaeschke, N. Pohl, and J. Barowski, "Versatile 126–182 GHz UWB D-band FMCW radar for industrial and scientific applications," *IEEE Sensors Lett.*, vol. 6, no. 1, pp. 1–4, Jan. 2022.
- [150] H. Caesar et al., "nuscenes: A multimodal dataset for autonomous driving," in *Proc. IEEE/CVF CVPR*, 2020, pp. 11621–11631.
- [151] A. Kramer, K. Harlow, C. Williams, and C. Heckman, "ColoRadar: The direct 3D millimeter wave radar dataset," *Int. J. Robot. Res.*, vol. 41, no. 4, pp. 351–360, 2022.
- [152] J. Wang et al., "Realtime wide-area vehicle trajectory tracking using millimeter-wave radar sensors and the open TJRD TS dataset," *Int. J. Transp. Sci. Technol.*, vol. 12, no. 1, pp. 273–290, 2023.
- [153] S. Wei et al., "3DRIED: A high-resolution 3-D millimeter-wave radar dataset dedicated to imaging and evaluation," *Remote Sens.*, vol. 13, no. 17, p. 3366, 2021.
- [154] E. Gambi, G. Ciattaglia, A. De Santis, and L. Senigagliesi, "Millimeter wave radar data of people walking," *Data Brief*, vol. 31, Aug. 2020, Art. no. 105996.
- [155] S.-P. Lee, N. P. Kini, W.-H. Peng, C.-W. Ma, and J.-N. Hwang, "HuPR: A benchmark for human pose estimation using millimeter wave radar," in *Proc. IEEE/CVF WACV*, 2023, pp. 5715–5724.
- [156] S. An and U. Y. Ogras, "MARS: MmWave-based assistive rehabilitation system for smart healthcare," *ACM Trans. Embed. Comput. Syst.*, vol. 20, no. 5s, pp. 1–22, 2021.
- [157] S. An, Y. Li, and U. Ogras, "mRI: Multi-modal 3D human pose estimation dataset using mmwave, RGB-D, and inertial sensors," in *Proc. Adv. Neural Inf. Process. Syst.*, vol. 35, 2022, pp. 27414–27426.
- [158] A. Chen, X. Wang, S. Zhu, Y. Li, J. Chen, and Q. Ye, "mmBody benchmark: 3D body reconstruction dataset and analysis for millimeter wave radar," in *Proc. ACM MM*, 2022, pp. 3501–3510.
- [159] H. Xue et al., "mmMesh: Towards 3D real-time dynamic human mesh construction using millimeter-wave," in *Proc. ACM MobiSys*, 2021, pp. 269–282.
- [160] H. Liu et al., "M-gesture: Person-independent real-time in-air gesture recognition using commodity millimeter wave radar," *IEEE Internet Things J.*, vol. 9, no. 5, pp. 3397–3415, Mar. 2022.
- [161] Q. Chen, Nov. 2022, "MIMOGR:MIMO millimeter wave radar multi-feature dataset for gesture recognition," Dataset, IEEE DataPort. [Online]. Available: <https://dx.doi.org/10.21227/szqd-6772>
- [162] S. Palipana, D. Salami, L. A. Leiva, and S. Sigg, "Pantomime: Mid-air gesture recognition with sparse millimeter-wave radar point clouds," *Proc. ACM Interact., Mobile, Wearable Ubiquitous Technol.*, vol. 5, no. 1, pp. 1–27, 2021.
- [163] H. Cui, S. Zhong, J. Wu, Z. Shen, N. Dahnoun, and Y. Zhao, "MiliPoint: A point cloud dataset for mmWave radar," in *Proc. Adv. Neural Inf. Process. Syst.*, vol. 36, 2024, pp. 1–27.
- [164] F. Nobis, M. Geisslinger, M. Weber, J. Betz, and M. Lienkamp, "A deep learning-based radar and camera sensor fusion architecture for object detection," in *Proc. IEEE SDF*, 2019, pp. 1–7.
- [165] S. Chang et al., "Spatial attention fusion for obstacle detection using mmwave radar and vision sensor," *Sensors*, vol. 20, no. 4, p. 956, 2020.
- [166] R. Prophet, G. Li, C. Sturm, and M. Vossiek, "Semantic segmentation on automotive radar maps," in *Proc. IEEE IV*, 2019, pp. 756–763.
- [167] Y. Huang, W. Li, Z. Dou, W. Zou, A. Zhang, and Z. Li, "Activity recognition based on millimeter-wave radar by fusing point cloud and range-Doppler information," *Signals*, vol. 3, no. 2, pp. 266–283, 2022.
- [168] Y. Li et al., "Towards domain-independent and real-time gesture recognition using mmwave signal," *IEEE Trans. Mobile Comput.*, vol. 22, no. 12, pp. 7355–7369, Dec. 2023.
- [169] J. Wu, J. Wang, Q. Gao, M. Pan, and H. Zhang, "Path-independent device-free gait recognition using mmWave signals," *IEEE Trans. Veh. Technol.*, vol. 70, no. 11, pp. 11582–11592, Nov. 2021.

- [170] Y. Cheng, H. Xu, and Y. Liu, "Robust small object detection on the water surface through fusion of camera and millimeter wave radar," in *Proc. IEEE/CVF ICCV*, 2021, pp. 15263–15272.
- [171] K. Deng et al., "Geryon: Edge assisted real-time and robust object detection on drones via mmWave radar and camera fusion," *Proc. ACM Interact., Mobile, Wearable Ubiquitous Technol.*, vol. 6, no. 3, pp. 1–27, 2022.
- [172] X. Shuai, Y. Shen, Y. Tang, S. Shi, L. Ji, and G. Xing, "milliEye: A lightweight mmwave radar and camera fusion system for robust object detection," in *Proc. ACM IoTDI*, 2021, pp. 145–157.
- [173] C. X. Lu et al., "milliEgo: Single-chip mmWave radar aided egomotion estimation via deep sensor fusion," in *Proc. ACM SenSys*, 2020, pp. 109–122.
- [174] F. Wang, X. Zeng, C. Wu, B. Wang, and K. R. Liu, "Driver vital signs monitoring using millimeter wave radio," *IEEE Internet Things J.*, vol. 9, no. 13, pp. 11283–11298, Jul. 2022.
- [175] Y. Dong and Y.-D. Yao, "Secure mmWave-radar-based speaker verification for IoT smart home," *IEEE Internet Things J.*, vol. 8, no. 5, pp. 3500–3511, Mar. 2021.
- [176] P. Hu, W. Li, R. Spolaor, and X. Cheng, "mmEcho: A mmWave-based acoustic eavesdropping method," in *Proc. IEEE SP*, 2022, pp. 836–852.
- [177] J. Lombacher, K. Laudt, M. Hahn, J. Dickmann, and C. Wöhler, "Semantic radar grids," in *Proc. IEEE IV*, 2017, pp. 1170–1175.
- [178] N. Scheiner, N. Appenrodt, J. Dickmann, and B. Sick, "Radar-based road user classification and novelty detection with recurrent neural network ensembles," in *Proc. IEEE IV*, 2019, pp. 722–729.
- [179] X. Huang, J. K. Tsui, and N. Patel, "mmWave radar sensors fusion for indoor object detection and tracking," *Electronics*, vol. 11, no. 14, p. 2209, 2022.
- [180] B. Tan et al., "3-D object detection for multiframe 4-D automotive millimeter-wave radar point cloud," *IEEE Sensors J.*, vol. 23, no. 11, pp. 11125–11138, Jun. 2023.
- [181] X. Dong, B. Zhuang, Y. Mao, and L. Liu, "Radar camera fusion via representation learning in autonomous driving," in *Proc. IEEE/CVF CVPR*, 2021, pp. 1672–1681.
- [182] Y. Wang, Z. Jiang, Y. Li, J.-N. Hwang, G. Xing, and H. Liu, "RODNet: A real-time radar object detection network cross-supervised by camera-radar fused object 3D localization," *IEEE J. Sel. Topics Signal Process.*, vol. 15, no. 4, pp. 954–967, Jun. 2021.
- [183] A. Sengupta, L. Cheng, and S. Cao, "Robust multiobject tracking using mmwave radar-camera sensor fusion," *IEEE Sensors Lett.*, vol. 6, no. 10, pp. 1–4, Oct. 2022.
- [184] R. Zhang and S. Cao, "Extending reliability of mmwave radar tracking and detection via fusion with camera," *IEEE Access*, vol. 7, pp. 137065–137079, 2019.
- [185] M. Manzoni et al., "Motion estimation and compensation in automotive MIMO SAR," *IEEE Trans. Intell. Transp. Syst.*, vol. 24, no. 2, pp. 1756–1772, Feb. 2023.
- [186] K. Haggag, S. Lange, T. Pfeifer, and P. Protzel, "A credible and robust approach to ego-motion estimation using an automotive radar," *IEEE Robot. Autom. Lett.*, vol. 7, no. 3, pp. 6020–6027, Jul. 2022.
- [187] Z. Zeng, X. Liang, X. Dang, and Y. Li, "Joint velocity ambiguity resolution and ego-motion estimation method for mmWave radar," *IEEE Robot. Autom. Lett.*, vol. 8, no. 8, pp. 4753–4760, Aug. 2023.
- [188] X. Gao, S. Roy, and G. Xing, "MIMO-SAR: A hierarchical high-resolution imaging algorithm for mmWave FMCW radar in autonomous driving," *IEEE Trans. Veh. Technol.*, vol. 70, no. 8, pp. 7322–7334, Aug. 2021.
- [189] M. Steiner, T. Grebner, and C. Waldschmidt, "Millimeter-wave SAR-imaging with radar networks based on radar self-localization," *IEEE Trans. Microw. Theory Tech.*, vol. 68, no. 11, pp. 4652–4661, Nov. 2020.
- [190] Y. Almalioglu, M. Turan, C. X. Lu, N. Trigoni, and A. Markham, "Milli-RIO: Ego-motion estimation with low-cost millimetre-wave radar," *IEEE Sensors J.*, vol. 21, no. 3, pp. 3314–3323, Feb. 2021.
- [191] P. Meiresone, D. Van Hamme, W. Philips, and T. Verbelen, "Ego-motion estimation with a lowpower millimeterwave radar on a UAV," in *Proc. IET RADAR*, 2022, pp. 371–376.
- [192] H.-W. Cho, S. Choi, Y.-R. Cho, and J. Kim, "Deep complex-valued network for ego-velocity estimation with millimeter-wave radar," in *Proc. IEEE SENSORS*, 2020, pp. 1–4.
- [193] Y. Li, Y. Liu, Y. Wang, Y. Lin, and W. Shen, "The millimeter-wave radar SLAM assisted by the RCS feature of the target and IMU," *Sensors*, vol. 20, no. 18, p. 5421, 2020.
- [194] S. Lim, J. Jung, S.-C. Kim, and S. Lee, "Radar-based ego-motion estimation of autonomous robot for simultaneous localization and mapping," *IEEE Sensors J.*, vol. 21, no. 19, pp. 21791–21797, Oct. 2021.
- [195] Y. S. Park, Y.-S. Shin, J. Kim, and A. Kim, "3D ego-motion estimation using low-cost mmWave radars via radar velocity factor for pose-graph SLAM," *IEEE Robot. Autom. Lett.*, vol. 6, no. 4, pp. 7691–7698, Oct. 2021.
- [196] Z. Hao, H. Yan, X. Dang, Z. Ma, P. Jin, and W. Ke, "Millimeter-wave radar localization using indoor multipath effect," *Sensors*, vol. 22, no. 15, p. 5671, 2022.
- [197] S. Lee, S.-Y. Kwon, B.-J. Kim, H.-S. Lim, and J.-E. Lee, "Dual-mode radar sensor for indoor environment mapping," *Sensors*, vol. 21, no. 7, p. 2469, 2021.
- [198] Z. Yang and Z. Zhu, "An ego-motion estimation method using millimeter-wave radar in 3D scene reconstruction," in *Proc. IEEE IHMSC*, 2022, pp. 18–21.
- [199] Y. Li, Y. Wei, Y. Wang, Y. Lin, W. Shen, and W. Jiang, "False detections revising algorithm for millimeter wave radar SLAM in tunnel," *Remote Sens.*, vol. 15, no. 1, p. 277, 2023.
- [200] M. Aladsani, A. Alkhateeb, and G. C. Trichopoulos, "Leveraging mmWave imaging and communications for simultaneous localization and mapping," in *Proc. IEEE ICASSP*, 2019, pp. 4539–4543.
- [201] Y. Wang, H. Liu, K. Cui, A. Zhou, W. Li, and H. Ma, "m-Activity: Accurate and real-time human activity recognition via millimeter wave radar," in *Proc. IEEE ICASSP*, 2021, pp. 8298–8302.
- [202] H. Abedi, A. Ansariyan, P. P. Morita, A. Wong, J. Boger, and G. Shaker, "AI-powered non-contact in-home gait monitoring and activity recognition system based on mm-wave FMCW radar and cloud computing," *IEEE Internet Things J.*, vol. 10, no. 11, pp. 9465–9481, Jun. 2023.
- [203] B. Sheng, Y. Bao, F. Xiao, and L. Gui, "DyLiteRADHAR: Dynamic lightweight Slowfast network for human activity recognition using MMWAVE radar," in *Proc. IEEE ICASSP*, 2023, pp. 1–5.
- [204] S. Bhalla, M. Goel, and R. Khurana, "IMU2Doppler: Cross-modal domain adaptation for doppler-based activity recognition using IMU data," *Proc. ACM Interact., Mobile, Wearable Ubiquitous Technol.*, vol. 5, no. 4, pp. 1–20, 2021.
- [205] A. Sengupta, F. Jin, R. Zhang, and S. Cao, "mm-pose: Real-time human skeletal posture estimation using mmWave radars and CNNs," *IEEE Sensors J.*, vol. 20, no. 17, pp. 10032–10044, Sep. 2020.
- [206] S. Hu, A. Sengupta, and S. Cao, "Stabilizing skeletal pose estimation using mmWave radar via dynamic model and filtering," in *Proc. IEEE BHI*, 2022, pp. 1–6.
- [207] A. Sengupta and S. Cao, "mmPose-NLP: A natural language processing approach to precise skeletal pose estimation using mmWave radars," *IEEE Trans. Neural Netw. Learn. Syst.*, vol. 34, no. 11, pp. 8418–8429, Nov. 2023.
- [208] G. Wei, C. Cui, and X. Dong, "A transformer-based network for human pose estimation using millimeter wave radar data," in *Proc. IEEE ACES-China*, 2023, pp. 1–4.
- [209] Z. Cao, W. Ding, R. Chen, J. Zhang, X. Guo, and G. Wang, "A joint global-local network for human pose estimation with millimeter wave radar," *IEEE Internet Things J.*, vol. 10, no. 1, pp. 434–446, Jan. 2023.
- [210] C. Shi, L. Lu, J. Liu, Y. Wang, Y. Chen, and J. Yu, "mPose: Environment-and subject-agnostic 3D skeleton posture reconstruction leveraging a single mmWave device," *Smart Health*, vol. 23, Mar. 2022, Art. no. 100228.
- [211] X. Zhang, Z. Li, and J. Zhang, "Synthesized Millimeter-waves for human motion sensing," in *Proc. 20th ACM Conf. Embed. Netw. Sens. Syst.*, 2022, pp. 377–390.
- [212] H. Xue et al., "M4esh: MmWave-based 3D human mesh construction for multiple subjects," in *Proc. 20th ACM Conf. Embed. Netw. Sens. Syst.*, 2022, pp. 391–406.
- [213] H. Ding et al., "MI-mesh: 3D human mesh construction by fusing image and millimeter wave," *Proc. ACM Interact., Mobile, Wearable Ubiquitous Technol.*, vol. 7, no. 1, pp. 1–24, 2023.
- [214] Y. Zhao, V. Sark, M. Krstic, and E. Grass, "Novel approach for gesture recognition using mmWave FMCW RADAR," in *Proc. IEEE 95th VTC*, 2022, pp. 1–6.
- [215] J. Wu, J. Wang, Q. Gao, M. Cheng, M. Pan, and H. Zhang, "Toward robust device-free gesture recognition based on intrinsic spectrogram of mmWave signals," *IEEE Internet Things J.*, vol. 9, no. 19, pp. 19318–19329, Oct. 2022.
- [216] P. S. Santhalingam, A. A. Hosain, D. Zhang, P. Pathak, H. Rangwala, and R. Kushalnagar, "mmaSL: Environment-independent ASL gesture recognition using 60 GHz millimeter-wave signals," *Proc. ACM Interact., Mobile, Wearable Ubiquitous Technol.*, vol. 4, no. 1, pp. 1–30, 2020.

- [217] D. Salami, R. Hasibi, S. Palipana, P. Popovski, T. Michoel, and S. Sigg, "Tesla-rapture: A lightweight gesture recognition system from mmWave radar sparse point clouds," *IEEE Trans. Mobile Comput.*, vol. 22, no. 8, pp. 4946–4960, Aug. 2023.
- [218] H. Liu et al., "mTransSee: Enabling environment-independent mmWave sensing based gesture recognition via transfer learning," *Proc. ACM Interact., Mobile, Wearable Ubiquitous Technol.*, vol. 6, no. 1, pp. 1–28, 2022.
- [219] B. Yan, P. Wang, L. Du, X. Chen, Z. Fang, and Y. Wu, "mmGesture: Semi-supervised gesture recognition system using mmWave radar," *Expert Syst. Appl.*, vol. 213, Mar. 2023, Art. no. 119042.
- [220] J. Lien et al., "Soli: Ubiquitous gesture sensing with millimeter wave radar," *ACM Trans. Graph.*, vol. 35, no. 4, pp. 1–19, 2016.
- [221] J. W. Smith, O. Furxhi, and M. Torlak, "An FCNN-based super-resolution mmWave radar framework for contactless musical instrument interface," *IEEE Trans. Multimedia*, vol. 24, pp. 2315–2328, Jun. 2022.
- [222] T. Wei and X. Zhang, "mTrack: High-precision passive tracking using millimeter wave radios," in *Proc. ACM 21st Annu. Int. Conf. Mobile Comput. Netw.*, 2015, pp. 117–129.
- [223] S. D. Regani, C. Wu, B. Wang, M. Wu, and K. R. Liu, "mmWrite: Passive handwriting tracking using a single millimeter-wave radio," *IEEE Internet Things J.*, vol. 8, no. 17, pp. 13291–13305, Sep. 2021.
- [224] L. Wen, C. Gu, and J.-F. Mao, "Silent speech recognition based on short-range millimeter-wave sensing," in *Proc. IEEE IMS*, 2020, pp. 779–782.
- [225] L. Fan, L. Xie, X. Lu, Y. Li, C. Wang, and S. Lu, "mmMIC: Multi-modal speech recognition based on mmWave radar," in *Proc. IEEE Conf. Comput. Commun. (INFOCOM)*, 2023, pp. 1–10.
- [226] T. Liu et al., "Wavoice: A noise-resistant multi-modal speech recognition system fusing mmwave and audio signals," in *Proc. 19th ACM Conf. Embed. Netw. Sens. Syst.*, 2021, pp. 97–110.
- [227] S. Zeng, H. Wan, S. Shi, and W. Wang, "mSilent: Towards general corpus silent speech recognition using COTS mmWave radar," *Proc. ACM Interact., Mobile, Wearable Ubiquitous Technol.*, vol. 7, no. 1, pp. 1–28, 2023.
- [228] S. Li, Y. Xiong, P. Zhou, Z. Ren, and Z. Peng, "mmPhone: Sound recovery using millimeter-wave radios with adaptive fusion enhanced vibration sensing," *IEEE Trans. Microw. Theory Tech.*, vol. 70, no. 8, pp. 4045–4055, Aug. 2022.
- [229] C. Wang et al., "mmPhone: Acoustic eavesdropping on loudspeakers via mmWave-characterized piezoelectric effect," in *Proc. IEEE Conf. Comput. Commun. (INFOCOM)*, 2022, pp. 820–829.
- [230] M. Alizadeh, G. Shaker, J. C. M. De Almeida, P. P. Morita, and S. Safavi-Naeini, "Remote monitoring of human vital signs using mm-wave FMCW radar," *IEEE Access*, vol. 7, pp. 54958–54968, 2019.
- [231] Y. Wang, W. Wang, M. Zhou, A. Ren, and Z. Tian, "Remote monitoring of human vital signs based on 77-GHz mm-wave FMCW radar," *Sensors*, vol. 20, no. 10, p. 2999, 2020.
- [232] B. Zhang, B. Jiang, R. Zheng, X. Zhang, J. Li, and Q. Xu, "Pi-ViMo: Physiology-inspired robust vital sign monitoring using mmWave radars," *ACM Trans. Internet Things*, vol. 4, no. 2, pp. 1–27, 2023.
- [233] Z. Shi, T. Gu, Y. Zhang, and X. Zhang, "mmBP: Contact-free Millimetre-wave radar based approach to blood pressure measurement," in *Proc. 20th ACM Conf. Embed. Netw. Sens. Syst.*, 2022, pp. 667–681.
- [234] J. Shi and K. Lee, "Systolic blood pressure measurement algorithm with mmWave radar sensor," *KSII Trans. Internet Inf. Syst.*, vol. 16, no. 4, pp. 1209–1223, 2022.
- [235] R. Kawasaki and A. Kajiwara, "Continuous blood pressure estimation using millimeter wave radar," in *Proc. IEEE RWS*, 2022, pp. 135–137.
- [236] Z. Yang, P. H. Pathak, Y. Zeng, X. Liran, and P. Mohapatra, "Vital sign and sleep monitoring using millimeter wave," *ACM Trans. Sens. Netw.*, vol. 13, no. 2, pp. 1–32, 2017.
- [237] Z. Yang, P. Pathak, Y. Zeng, X. Liran, and P. Mohapatra, "Monitoring vital signs using millimeter wave," in *Proc. 17th ACM Int. Symp. Mobile Ad Hoc Netw. Comput.*, 2016, pp. 211–220.
- [238] M. Mercuri, I. R. Lorato, Y.-H. Liu, F. Wieringa, C. V. Hoof, and T. Torfs, "Vital-sign monitoring and spatial tracking of multiple people using a contactless radar-based sensor," *Nature Electron.*, vol. 2, no. 6, pp. 252–262, 2019.
- [239] A. Ahmad, J. C. Roh, D. Wang, and A. Dubey, "Vital signs monitoring of multiple people using a FMCW millimeter-wave sensor," in *Proc. IEEE Radar Conf. (RadarConf)*, 2018, pp. 1450–1455.
- [240] F. Wang, F. Zhang, C. Wu, B. Wang, and K. J. R. Liu, "ViMo: Multiperson vital sign monitoring using commodity millimeter-wave radio," *IEEE Internet Things J.*, vol. 8, no. 3, pp. 1294–1307, Feb. 2021.
- [241] X. Xu et al., "mmECG: Monitoring human cardiac cycle in driving environments leveraging millimeter wave," in *Proc. IEEE Conf. Comput. Commun. (INFOCOM)*, 2022, pp. 90–99.
- [242] Y. Wang, Z. Wang, J. A. Zhang, H. Zhang, and M. Xu, "Vital sign monitoring in dynamic environment via mmWave radar and camera fusion," *IEEE Trans. Mobile Comput.*, vol. 23, no. 5, pp. 4163–4180, May 2024.
- [243] S. Yang, D. Zhang, Y. Li, Y. Hu, Q. Sun, and Y. Chen, "iSense: Enabling radar sensing under mutual device interference," *IEEE Trans. Mobile Comput.*, early access, Mar. 20, 2024, doi: 10.1109/TMC.2024.3379570.
- [244] F. Wang, F. Zhang, C. Wu, B. Wang, and K. R. Liu, "ViMo: Vital sign monitoring using commodity millimeter wave radio," in *Proc. IEEE ICASSP*, 2020, pp. 8304–8308.
- [245] X. Jiang, Y. Zhang, Q. Yang, B. Deng, and H. Wang, "Millimeter-wave array radar-based human gait recognition using multi-channel three-dimensional convolutional neural network," *Sensors*, vol. 20, no. 19, p. 5466, 2020.
- [246] M. Z. Ozturk, C. Wu, B. Wang, and K. R. Liu, "GaitCube: Deep data cube learning for human recognition with millimeter-wave radio," *IEEE Internet Things J.*, vol. 9, no. 1, pp. 546–557, Jan. 2022.
- [247] X. Yang, J. Liu, Y. Chen, X. Guo, and Y. Xie, "MU-ID: Multi-user identification through gaits using millimeter wave radios," in *Proc. IEEE Conf. Comput. Commun. (INFOCOM)*, 2020, pp. 2589–2598.
- [248] Z. Ni and B. Huang, "Gait-based person identification and intruder detection using mm-wave sensing in multi-person scenario," *IEEE Sensors J.*, vol. 22, no. 10, pp. 9713–9723, May 2022.
- [249] J. Li, B. Li, L. Wang, and W. Liu, "Passive multi-user gait identification through micro-doppler calibration using mmWave radar," *IEEE Internet Things J.*, vol. 11, no. 4, pp. 6868–6877, Feb. 2024.
- [250] D. Cao, R. Liu, H. Li, S. Wang, W. Jiang, and C. X. Lu, "Cross vision-RF gait re-identification with low-cost RGB-D cameras and mmWave radars," *Proc. ACM Interact., Mobile, Wearable Ubiquitous Technol.*, vol. 6, no. 3, pp. 1–25, 2022.
- [251] M. R. Challa, A. Kumar, and L. R. Cenkeramaddi, "Face recognition using mmWave RADAR imaging," in *Proc. IEEE iSES*, 2021, pp. 319–322.
- [252] W. Xu et al., "Mask does not matter: Anti-spoofing face authentication using mmWave without on-site registration," in *Proc. 28th Annu. Int. Conf. Mobile Comput. Netw.*, 2022, pp. 310–323.
- [253] H. Li et al., "VocalPrint: Exploring a resilient and secure voice authentication via mmWave biometric interrogation," in *Proc. ACM 18th Conf. Embed. Netw. Sens. Syst.*, 2020, pp. 312–325.
- [254] H. Li et al., "VocalPrint: A mmWave-based unmediated vocal sensing system for secure authentication," *IEEE Trans. Mobile Comput.*, vol. 22, no. 1, pp. 589–606, Jan. 2023.
- [255] Y. Wang, T. Gu, T. H. Luan, M. Lyu, and Y. Li, "HeartPrint: Exploring a heartbeat-based multiuser authentication with single mmWave radar," *IEEE Internet Things J.*, vol. 9, no. 24, pp. 25324–25336, Dec. 2022.
- [256] Y. Wang, T. Gu, and H. Zhang, "Simultaneous authentication of multiple users using a single mmWave radar," *IEEE Internet Things J.*, vol. 11, no. 10, pp. 17797–17811, May 2024.
- [257] T. Gu, Z. Fang, Z. Yang, P. Hu, and P. Mohapatra, "MmSense: Multi-person detection and identification via mmWave sensing," in *Proc. 3rd ACM Workshop Millim.-wave Netw. Sens. Syst.*, 2019, pp. 45–50.
- [258] Z. Xu, Z. Wu, D. Li, L. Chen, S. Zhang, and Z. D. Chen, "Position estimation and calibration for high precision human positioning and tracking using millimeter-wave radar," *Meas. Sci. Technol.*, vol. 34, no. 2, 2022, Art. no. 025108.
- [259] W. Li, R. Chen, Y. Wu, and H. Zhou, "Indoor positioning system using a single-chip millimeter wave radar," *IEEE Sensors J.*, vol. 23, no. 5, pp. 5232–5242, Mar. 2023.
- [260] J. Pegoraro, F. Meneghelli, and M. Rossi, "Multiperson continuous tracking and identification from mm-wave micro-doppler signatures," *IEEE Trans. Geosci. Remote Sens.*, vol. 59, no. 4, pp. 2994–3009, Apr. 2020.
- [261] G. Zhang, G. Chi, Y. Zhang, X. Ding, and Z. Yang, "Push the limit of millimeter-wave radar localization," *ACM Trans. Sens. Netw.*, vol. 19, no. 3, pp. 1–21, 2022.
- [262] Q. Li, M. Yang, Z. Wang, and H. Chen, "Stationary human target detection based on Millimeter wave radar in complex scenarios," in *Proc. IEEE ICONAT*, 2023, pp. 1–5.

- [263] Y. Sun, Z. Huang, H. Zhang, Z. Cao, and D. Xu, “3DRIMR: 3D reconstruction and imaging via mmWave radar based on deep learning,” in *Proc. IEEE IPCCC*, 2021, pp. 1–8.
- [264] G. Brooker, R. Hennessey, C. Lobsey, M. Bishop, and E. Widzyk-Capehart, “Seeing through dust and water vapor: Millimeter wave radar sensors for mining applications,” *J. Field Robot.*, vol. 24, no. 7, pp. 527–557, 2007.
- [265] A. Prabhakara, V. Singh, S. Kumar, and A. Rowe, “Osprey: A mmWave approach to tire wear sensing,” in *Proc. 18th Int. Conf. Mobile Syst., Appl., Serv.*, 2020, pp. 28–41.
- [266] M. Pan, A. Chopard, F. Fauquet, P. Mounaix, and J.-P. Guillet, “Guided reflectometry imaging unit using millimeter wave FMCW radars,” *IEEE Trans. Terahertz Sci. Technol.*, vol. 10, no. 6, pp. 647–655, Nov. 2020.
- [267] G. Alvarez-Narciandi, M. López-Portugués, F. Las-Heras, and J. Laviada, “Freehand, agile, and high-resolution imaging with compact mm-wave radar,” *IEEE Access*, vol. 7, pp. 95516–95526, 2019.
- [268] S. Gupta, P. K. Rai, A. Kumar, P. K. Yalavarthy, and L. R. Cenkeramaddi, “Target classification by mmWave FMCW radars using machine learning on range-angle images,” *IEEE Sensors J.*, vol. 21, no. 18, pp. 19993–20001, Sep. 2021.
- [269] T. Liu, Y. Zhao, Y. Wei, Y. Zhao, and S. Wei, “Concealed object detection for activate millimeter wave image,” *IEEE Trans. Ind. Electron.*, vol. 66, no. 12, pp. 9909–9917, Dec. 2019.
- [270] G. M. Brooker, S. Scheding, M. V. Bishop, and R. C. Hennessy, “Development and application of millimeter wave radar sensors for underground mining,” *IEEE Sensors J.*, vol. 5, no. 6, pp. 1270–1280, Dec. 2005.
- [271] C. Jiang, J. Guo, Y. He, M. Jin, S. Li, and Y. Liu, “mmVib: Micrometer-level vibration measurement with mmWave radar,” in *Proc. 26th Annu. Int. Conf. Mobile Comput. Netw.*, 2020, pp. 1–13.
- [272] L. Zhang and J. Wei, “Measurement and control method of clearance between wind turbine tower and blade-tip based on millimeter-wave radar sensor,” *Mech. Syst. Signal Process.*, vol. 149, Feb. 2021, Art. no. 107319.
- [273] Z. Li et al., “WaveSpy: Remote and through-wall screen attack via mmWave sensing,” in *Proc. IEEE Symp. Security Privacy (SP)*, 2020, pp. 217–232.
- [274] N. Miura, T. Machida, K. Matsuda, M. Nagata, S. Nashimoto, and D. Suzuki, “A low-cost replica-based distance-spoofing attack on mmWave FMCW radar,” in *Proc. 3rd ACM ASHES*, 2019, pp. 95–100.
- [275] L. Piotrowsky, S. Kueppers, T. Jaeschke, and N. Pohl, “Distance measurement using mmWave radar: Micron accuracy at medium range,” *IEEE Trans. Microw. Theory Tech.*, vol. 70, no. 11, pp. 5259–5270, Nov. 2022.
- [276] A. Cademi and E. Cardillo, “Automotive anti-abandon systems: A millimeter-wave radar sensor for the detection of child presence,” in *Proc. IEEE 14th TELSIKS*, 2019, pp. 94–97.
- [277] E. Cardillo, C. Li, and A. Cademi, “Empowering blind people mobility: A millimeter-wave radar cane,” in *Proc. IEEE MetroInd IoT*, 2020, pp. 213–217.
- [278] V. Semkin et al., “Analyzing radar cross section signatures of diverse drone models at mmWave frequencies,” *IEEE Access*, vol. 8, pp. 48958–48969, 2020.
- [279] S. Dogru and L. Marques, “Pursuing drones with drones using millimeter wave radar,” *IEEE Robot. Autom. Lett.*, vol. 5, no. 3, pp. 4156–4163, Jul. 2020.
- [280] G. Zhai, C. Wu, and Y. Wang, “Millimeter wave radar target tracking based on adaptive Kalman filter,” in *Proc. IEEE IV*, 2018, pp. 453–458.
- [281] H. F. Álvarez, G. Álvarez-Narciandi, M. García-Fernández, J. Laviada, Y. Álvarez López, and F. L. Andrés, “A portable electromagnetic system based on mm-wave radars and GNSS-RTK solutions for 3d scanning of large material piles,” *Sensors*, vol. 21, no. 3, p. 757, 2021.
- [282] B.-H. Wu, S.-H. Fang, and H.-C. Wu, “Novel robust parcel-size classification using mmWave radar,” *IEEE Trans. Ind. Informat.*, vol. 20, no. 2, pp. 2873–2883, Feb. 2024.
- [283] Y. S. Leong, S. Roy, and K. H. Lim, “Obstructed material classification using mmWave radar with deep neural network for industrial applications,” in *Advances in Smart Energy Systems*. Singapore: Springer, 2022, pp. 147–162.
- [284] J. B. Mead, A. L. Pazmany, S. M. Sekelsky, and R. E. McIntosh, “Millimeter-wave radars for remotely sensing clouds and precipitation,” *Proc. IEEE*, vol. 82, no. 12, pp. 1891–1906, Dec. 1994.
- [285] B. Chen, H. Li, Z. Li, X. Chen, C. Xu, and W. Xu, “ThermoWave: A new paradigm of wireless passive temperature monitoring via mmWave sensing,” in *Proc. 26th Annu. Int. Conf. Mobile Comput. Netw.*, 2020, pp. 1–14.
- [286] B. Hattenhorst, L. Piotrowsky, N. Pohl, and T. Musch, “An mmWave sensor for real-time monitoring of gases based on real refractive index,” *IEEE Trans. Microw. Theory Tech.*, vol. 69, no. 11, pp. 5033–5044, Nov. 2021.
- [287] D. Cao, Y. Lin, G. Ren, Y. Gao, and W. Dong, “MmLiquid: Liquid identification using mmWave,” in *Proc. 16th China Conf. CWSN*, 2022, pp. 1–18.
- [288] Q. Dai, Y. Huang, L. Wang, R. Ruby, and K. Wu, “mm-humidity: Fine-grained humidity sensing with millimeter wave signals,” in *Proc. IEEE ICPADS*, 2018, pp. 204–211.
- [289] C. Han, J. Huo, Q. Gao, G. Su, and H. Wang, “Rainfall monitoring based on next-generation millimeter-wave backhaul technologies in a dense urban environment,” *Remote Sens.*, vol. 12, no. 6, p. 1045, 2020.
- [290] Y. Golovachev, A. Etinger, G. Pinhasi, and Y. Pinhasi, “The effect of weather conditions on millimeter wave propagation,” *Int. J. Circuits, Syst., Signal Process.*, vol. 13, pp. 690–695, Dec. 2019.
- [291] W. Chen et al., “Soil moisture sensing with mmWave radar,” in *Proc. 6th ACM Workshop Millim.-Wave Terahertz Netw. Sens. Syst.*, 2022, pp. 19–24.
- [292] N. Tahir and G. Brooker, “Toward the development of millimeter wave harmonic sensors for tracking small insects,” *IEEE Sensors J.*, vol. 15, no. 10, pp. 5669–5676, Oct. 2015.
- [293] F. Sheikh et al., “Towards continuous real-time plant and insect monitoring by miniaturized THz systems,” *IEEE J. Microw.*, vol. 3, no. 3, pp. 913–937, Jul. 2023.
- [294] M. A. Islam, G. C. Alexandropoulos, and B. Smida, “Integrated sensing and communication with millimeter wave full duplex hybrid beamforming,” 2022, *arXiv:2201.05240*.
- [295] C. Qi, W. Ci, J. Zhang, and X. You, “Hybrid beamforming for Millimeter wave MIMO integrated sensing and communications,” *IEEE Commun. Lett.*, vol. 26, no. 5, pp. 1136–1140, May 2022.
- [296] Z. Chen, M.-M. Zhao, M. Li, F. Xu, Q. Wu, and M.-J. Zhao, “Joint location sensing and channel estimation for IRS-aided mmWave ISAC systems,” *IEEE Trans. Wireless Commun.*, early access, Apr. 17, 2024, doi: [10.1109/TWC.2024.3387021](https://doi.org/10.1109/TWC.2024.3387021).
- [297] W. Lyu et al., “CRB minimization for RIS-aided mmWave integrated sensing and communications,” *IEEE Internet Things J.*, vol. 11, no. 10, pp. 18381–18393, May 2024.
- [298] Q. Zhang, X. Wang, Z. Li, and Z. Wei, “Design and performance evaluation of joint sensing and communication integrated system for 5G mmWave enabled CAVs,” *IEEE J. Sel. Topics Signal Process.*, vol. 15, no. 6, pp. 1500–1514, Nov. 2021.
- [299] B. Chang, W. Tang, X. Yan, X. Tong, and Z. Chen, “Integrated scheduling of sensing, communication, and control for mmWave/THz communications in cellular connected UAV networks,” *IEEE J. Sel. Areas Commun.*, vol. 40, no. 7, pp. 2103–2113, Jul. 2022.
- [300] J. Achiam et al., “GPT-4 technical report,” 2024, *arXiv:2303.08774*.
- [301] G. Hinton, O. Vinyals, and J. Dean, “Distilling the knowledge in a neural network,” 2015, *arXiv:1503.02531*.
- [302] S. J. Pan and Q. Yang, “A survey on transfer learning,” *IEEE Trans. Knowl. Data Eng.*, vol. 22, no. 10, pp. 1345–1359, Oct. 2010.
- [303] A. M. Deiana et al., “Applications and techniques for fast machine learning in science,” *Front. Big Data*, vol. 5, Apr. 2022, Art. no. 787421.
- [304] Y. Wu et al., “Large scale incremental learning,” in *Proc. IEEE/CVF CVPR*, 2019, pp. 374–382.



Hao Kong (Member, IEEE) received the B.E. degree in computer science and technology from Ocean University of China and the Ph.D. degree in computer science and technology from Shanghai Jiao Tong University. He is currently an Assistant Professor with the School of Computer Engineering and Science, Shanghai University. He was also a visiting research student with the Broadband Communications Research Lab and the Department of Electrical and Computer Engineering, University of Waterloo, Canada. He has published over ten papers in prestigious journals and conferences, including *IEEE TRANSACTIONS ON MOBILE COMPUTING*, *IEEE/ACM TRANSACTIONS ON NETWORKING*, *IEEE INFOCOM*, *ACM MobiSys*, *ACM MobiHoc*, and *IEEE ICDCS*. His research interests include mobile sensing, wireless sensing, and ubiquitous computing. He is the recipient of the ACM China SIGAPP Chapter Doctoral Dissertation Award.



Cheng Huang (Member, IEEE) received the B.Eng. and M.S. degrees in information security from Xidian University, China, in 2013 and 2016, respectively, and the Ph.D. degree in electrical and computer engineering from the University of Waterloo, ON, Canada, in 2020. He is currently an Associate Professor with the School of Computer Science, Fudan University. Before joining Fudan University, he was a Research Fellow with the Department of Electrical and Computer Engineering, University of Waterloo from 2020 to 2023. He has

published over 60 papers in prestigious journals and conferences, including IEEE TRANSACTIONS ON DEPENDABLE AND SECURE COMPUTING, IEEE JOURNAL ON SELECTED AREAS IN COMMUNICATIONS, IEEE TRANSACTIONS ON VEHICULAR TECHNOLOGY, and IEEE TRANSACTIONS ON INDUSTRIAL INFORMATICS. His research interests lie in the areas of security and privacy in vehicular networks, data security, and secure computation. He has received Best Paper Awards from ICCC '15, ICC '18, GLOBECOM '22, and ICCC '23. He serves as an Associate Editor for *Peer-to-Peer Networking and Applications* (Springer) and the Symposium Chair of IEEE GLOBECOM '24. He has served as the Publicity Chair of ICA3PP '22, PST '23, and SustainCom '23, and as a TPC member of many international conferences.



Xuemin (Sherman) Shen (Fellow, IEEE) received the Ph.D. degree in electrical engineering from Rutgers University, New Brunswick, NJ, USA, in 1990. He is a University Professor with the Department of Electrical and Computer Engineering, University of Waterloo, Canada. His research focuses on network resource management, wireless network security, Internet of Things, 5G and beyond, and vehicular ad hoc and sensor networks. He received the Canadian Award for Telecommunications Research from the Canadian

Society of Information Theory in 2021, the R.A. Fessenden Award from IEEE, Canada, in 2019, the Award of Merit from the Federation of Chinese Canadian Professionals, Ontario, in 2019, the James Evans Avant Garde Award from the IEEE Vehicular Technology Society in 2018, the Joseph LoCicero Award in 2015, the Education Award from the IEEE Communications Society in 2017, the Technical Recognition Award from Wireless Communications Technical Committee in 2019, and the AHSN Technical Committee in 2013. He has also received the Excellent Graduate Supervision Award from the University of Waterloo in 2006, and the Premier's Research Excellence Award from the Province of Ontario, Canada, in 2003. He served as the Technical Program Committee Chair/Co-Chair for IEEE Globecom' 16, IEEE Infocom'14, IEEE VTC'10 Fall, and IEEE Globecom'07, and the Chair for the IEEE Communications Society Technical Committee on Wireless Communications. He served as the Editor-in-Chief for the IEEE INTERNET OF THINGS JOURNAL, IEEE NETWORK, and *IET Communications*. He is the President of the IEEE Communications Society. He was the Vice President for Technical and Educational Activities, the Vice President for Publications, a Member-at-Large on the Board of Governors, the Chair of the Distinguished Lecturer Selection Committee, and a member of IEEE Fellow Selection Committee of the ComSoc. He is a registered Professional Engineer of Ontario, Canada, an Engineering Institute of Canada Fellow, a Canadian Academy of Engineering Fellow, a Royal Society of Canada Fellow, a Chinese Academy of Engineering Foreign Member, and a Distinguished Lecturer of the IEEE Vehicular Technology Society and Communications Society.



Jiadi Yu (Senior Member, IEEE) received the Ph.D. degree in computer science from Shanghai Jiao Tong University, China, in 2007. He is currently an Associate Professor with the Department of Computer Science and Engineering, Shanghai Jiao Tong University, Shanghai, China. Prior to joining Shanghai Jiao Tong University, he was with the Stevens Institute of Technology, USA, as a Postdoctoral Fellow. He has published more than 100 refereed papers in international leading journals and key conferences in the areas of wireless communications and networking, mobile computing, and security and privacy.

His current research interests include mobile computing and sensing, cyber security and privacy, Internet of Things, smart healthcare. He is a Senior Member of the IEEE Communication Society.